AD-A084 447 UNIVERSITY COLL OF NORTH WALES BANGOR SCHOOL OF PHYS--ETC F/G 20/3
PREPARATION AND PROPERTIES OF A STABLE METALLIC FERROFLUID.(U)
FEB 80 S R HOON, S W CHARLES, J POPPLEWELL DA-ERO-77-G-037
UNCLASSIFIED NL

1 OF 2
AD
A084447

(12) LEVEL II

(6) PREPARATION AND PROPERTIES OF A STABLE METALLIC FERROFLUID.

(9) Final Technical Report,

by

(10) MR S R HOON
DR S W CHARLES
DR J POPPLEWELL

(12) 101

(11) FEB 80

European Research Office
United States Army
London W 1 England

(15) Agreement Numbered DAERO-77-G-037

(16) 1T161102BH57 (17) 04

School of Physical and Molecular Sciences
University College of North Wales
Bangor, Gwynedd, UK

Approved for public release; distribution unlimited

409165

Unclassified

SECURITY CLASSIFICATION OF THIS PAGE (When Data Entered)

R&D 2341-MS

REPORT DOCUMENTATION PAGE	READ INSTRUCTIONS BEFORE COMPLETING FORM
1. REPORT NUMBER	2. GOVT ACCESSION NO. AD-A084 447	3. RECIPIENT'S CATALOG NUMBER
4. TITLE (and Subtitle) Preparation and Properties of a stable Metallic Ferrofluid	5. TYPE OF REPORT & PERIOD COVERED Final Technical
	6. PERFORMING ORG. REPORT NUMBER
7. AUTHOR(s) Mr. S. Hoon Dr. S. W. Charles Dr. J. Popplewell	8. CONTRACT OR GRANT NUMBER(s) DAERO 77-G-037
9. PERFORMING ORGANIZATION NAME AND ADDRESS University College of North Wales School of Molecular & Physical Sciences Bangor, Wales LL57 2UW	10. PROGRAM ELEMENT, PROJECT, TASK AREA & WORK UNIT NUMBERS 6.11.02A IT161102BH57-04
11. CONTROLLING OFFICE NAME AND ADDRESS USARSG (EUR) Box 65 FPO NY 09510	12. REPORT DATE February 1980 13. NUMBER OF PAGES 93
14. MONITORING AGENCY NAME & ADDRESS(if different from Controlling Office)	15. SECURITY CLASS. (of this report) Unclassified 15a. DECLASSIFICATION/DOWNGRADING SCHEDULE

16. DISTRIBUTION STATEMENT (of this Report)

Approved for Public Release: distribution unlimited

17. DISTRIBUTION STATEMENT (of the abstract entered in Block 20, if different from Report)

18. SUPPLEMENTARY NOTES

19. KEY WORDS (Continue on reverse side if necessary and identify by block number)

(u) Ferromagnetic Fluids
(u) Liquid Metal Systems
(u) Suspensions of Particles in Fluids
(u) Mercury Alloys

20. ABSTRACT (Continue on reverse side if necessary and identify by block number)

The aim of this research work has been to characterise the properties of suspensions of small single domain iron particles in mercury. These ferromagnetic liquids have been stabilised against diffusional growth by tin, antimony and sodium additives. That the tin, antimony and sodium associate themselves with the iron particles to form coatings is strikingly shown in this report by resistivity and latent heat of melting experiments.

DD FORM 1 JAN 73 1473 EDITION OF 1 NOV 65 IS OBSOLETE

Unclassified

SECURITY CLASSIFICATION OF THIS PAGE (When Data Entered)

Settling experiments in a gravitational field indicate that the iron particles aggregate to form clusters or loose flocs. These aggregates can contain as many as 10^5 iron particles. It appears, however, that the particles within the aggregates do not grow by diffusion if they are stabilised by tin and sodium coatings. This is demonstrated by magnetic data which shows that the particles retain their discrete single domain magnetic properties. Magnetic data is presented which demonstrates the importance of nearest neighbour magnetic interactions. The previously unexplained magnetic field gradient instability is also ascribed to the existence of large aggregates.

The existence of aggregates is further corroborated by viscosity, and time dependent magnetisation measurements at room temperature. A transition from a liquid to a paste-like viscosity is observed when the fluids are magnetically concentrated. The concentrated fluids behave as 'Bingham bodies'. This viscosity behaviour is also consistent with the existence of aggregates. The high, paste-like viscosity of concentrated fluids is almost wholly attributable to large quantities of mercury trapped within the aggregate structure.

That particle aggregation in fluids occurs at room temperature demonstrates that there exists in the total particle-particle interaction energy, a minimum of greater depth than kT at some finite particle separation. The total particle-particle interaction energy include magnetic, van der Waals' and electronic charge layer terms. The magnitude of these various terms has also been investigated theoretically.

The results in this report indicate that although stability of mercury based ferromagnetic liquids can be much improved by tin, antimony and sodium additives, van der Waals and magnetic dipole forces are still responsible for the aggregation which gives rise to the undesirable high viscosities.

However it has also been observed that metal additives can reduce the viscosity of these fluids significantly. It is believed that this viscosity reduction is principally attributable to a reduction in the magnetic dipole interaction between particles. It is thus believed that the fluid viscosity may be further reduced by making the median magnetic particle diameter even smaller.

TABLE OF CONTENTS

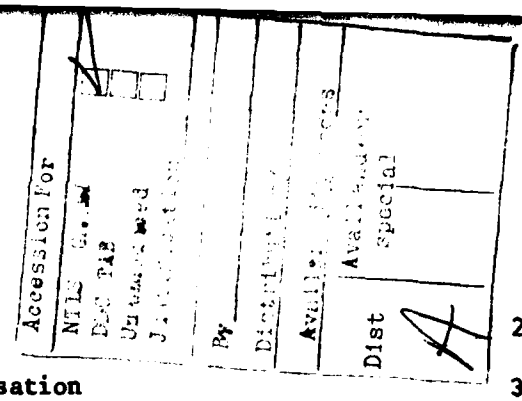

LIST OF FIGURES

Summary

The aim of this research work has been to characterise the properties of suspensions of small single domain iron particles in mercury. These ferromagnetic liquids have been stabilised against diffusional growth by tin, antimony and sodium additives. That the tin, antimony and sodium associate themselves with the iron particles to form coatings is strikingly shown in this report by resistivity and latent heat of melting experiments.

Settling experiments in a gravitational field indicate that the iron particles aggregate to form clusters or loose flocs. These aggregates can contain as many as 10^5 iron particles. It appears, however, that the particles within the aggregates do not grow by diffusion if they are stabilised by tin and sodium coatings. This is demonstrated by magnetic data which shows that the particles retain their discrete single domain magnetic properties. Magnetic data is presented which demonstrates the importance of nearest neighbour magnetic interactions. The previously unexplained magnetic field gradient instability is also ascribed to the existence of large aggregates.

The existence of aggregates is further corroborated by viscosity, and time dependent magnetisation measurements at room temperature. A transition from a liquid to a paste-like viscosity is observed when the fluids are magnetically concentrated. The concentrated fluids behave as 'Bingham bodies'. This viscosity behaviour is also consistent with the existence of aggregates. The high, paste-like viscosity of concentrated fluids is almost wholly attributable to large quantities of mercury trapped within the aggregate structure.

That particle aggregation in fluids occurs at room temperature demonstrates that there exists in the total particle-particle interaction energy, a minimum of greater depth than kT at some finite particle separation. The total particle-particle interaction energy include magnetic, van der Waals' and electronic charge layer terms. The magnitude of these various terms has also been investigated theoretically.

The results in this report indicate that although stability of mercury based ferromagnetic liquids can be much improved by tin, antimony and sodium additives, van der Waals and magnetic dipole forces are still responsible for the aggregation which gives rise to the undesirable high viscosities.

However it has also been observed that metal additives can reduce the viscosity of these fluids significantly. It is believed that this viscosity reduction is principally attributable to a reduction in the magnetic dipole interaction between particles. It is thus believed that the fluid viscosity may be further reduced by making the median magnetic particle diameter even smaller.

1. Introduction

Ferromagnetic liquids consist of suspensions of small, single domain ferromagnetic particles dispersed in a liquid carrier. The particles are made small to reduce magnetic interactions and are coated with a dispersant to prevent aggregation through van der Waals' forces. It is also a necessary requirement for most applications that the particles remain in suspension in both magnetic and gravitational field gradients. This criterion for stability is readily met by those ferromagnetic liquids, identified by the term ferrofluids, produced commercially by Ferrofluidics Corp. Such ferrofluids consist of Fe_3O_4 particles of 100–200 A diameter, dispersed in a hydrocarbon or diester carrier. Ferrofluids using water or silicone oil as the carrier fluid are more difficult to prepare and their stability is often unpredictable.

Ferromagnetic liquids containing ferromagnetic metal particles of iron or cobalt would be magnetically stronger than ferrofluids containing ferrite particles since the saturation magnetisation of these elements is appreciably greater ($I_s(Fe_3O_4)$ = 480 emu/cc. $I_s(Fe)$ = 1707 emu/cc). Their use in devices would, therefore be expected to be more extensive. Moreover, if the carrier is a liquid metal such as mercury the high thermal and electrical conductivity makes possible other uses of the fluids in switches and in energy conversion systems. Ferromagnetic liquids of this type containing iron particles in mercury are the subject of this final report.

2. Applications of Metallic Ferromagnetic Liquids

The application of metallic ferromagnetic liquids for energy conversion has been described in previous U.S. Army reports and by Popplewell et al[1] (1976). Essentially, a reliable energy conversion system with an efficiency of approximately 30% could be developed using a circulating metallic ferromagnetic liquid in a device shown diagrammatically in figure (2.1). This application requires the ferromagnetic liquid to be stable in large magnetic field gradients and at high temperatures. Moreover, since an attractive feature of this energy conversion system is its reliability the fluid must remain stable over the long term. The problem of stability has been studied in some detail and will be discussed later in this report.

A further application of the metallic ferromagnetic liquid would be in rotating shaft seals. Normally the sealing ferrofluid recommended for this application would be a 400G diester based fluid. Although seals currently available may operate continuously at 60,000 rpm further increase in speed is limited because heat generated in the seal produces evaporation of the carrier. A metallic carrier, however, would be expected to dissipate the heat generated more effectively and thus higher rotational speeds should be possible. It is the application in rotating shaft seals where metallic ferromagnetic liquids will first find application since the demands on the liquids are less for this application.

The work on metallic systems, as outlined in this report, is also relevant to other situations where metallic liquids are used. It has been found that the liquid metal coolant in a nuclear reactor acquires ferromagnetic particles from the stainless steel tubes along which it flows. These particles, which may pass through large magnetic field gradients and be at high temperatures, increase in size by diffusional growth and eventually aggregate, thereby restricting the fluid flow. An appreciation of the kinetics of growth and aggregation in these circumstances is invaluable.

It is shown in this report that aggregation can also be reduced by adding certain metals such as antimony in excess. This causes a reduction in the particle magnetisation and hence the contribution of the dipole-dipole interaction to aggregation.

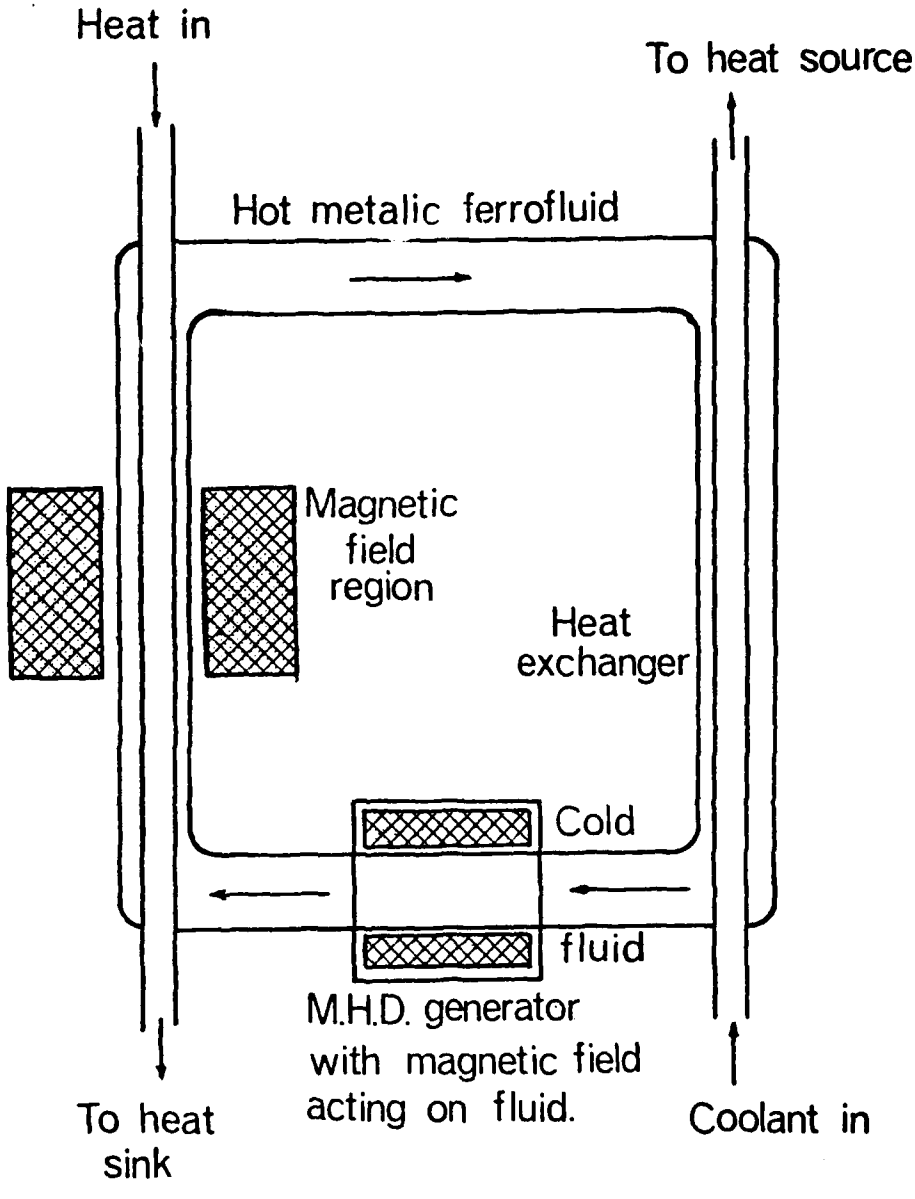

Figure(2.1). Schematic energy conversion system

3. Essential Properties of a Metallic Ferromagnetic Liquid

(a) Magnetic Properties

It is desirable to produce ferromagnetic liquids with a high saturation magnetisation and a large initial susceptibility. This is best achieved by selecting iron or cobalt (I_s (Fe) = 1707 emu/cc, I_s (Co) = 1400 emu/cc) as the ferromagnetic particle component. The particles must be made small, <45A diameter, in order to prevent aggregation due to magnetostatic interactions. The particle concentration in the carrier must also be large if the saturation magnetisation of the liquid is to be large. Commercial ferrofluids containing Fe_3O_4 particles normally have a magnetisation ($M_s = 4\pi I_s$) of 100 - 400 G. Such magnetisations correspond to particle concentrations of $\sim 10^{17}$/cc or some 10 volume %. The maximum particle concentration and hence the maximum magnetisation is limited by the final viscosity of the ferrofluid. This is a particularly important consideration in the preparation of strong metallic ferromagnetic liquids. Previous to this report low viscosity metallic systems have only been prepared with $M_s \sim$ 400G where the magnetic particle concentration is only 2-3% by volume. Above this value the ferromagnetic liquids acquired a high and unacceptable viscosity. Some reduction in the viscosity has now been achieved by the further use of additives, such that M_s is 1000G before the liquid becomes a paste. This represents an important step forward in producing a metallic magnetic sealing fluid.

(b) Ferromagnetic Liquid Viscosity

Commercial ferrofluids of 100 - 200 G saturation magnetisation have viscosities of a few centipoise. A concentrated fluid of 600 G may have a viscosity of 200 cp.

The Einstein equation for the ferrofluid viscosity η_f

$$\eta_f/\eta_o = 1 + 2.5\,\phi \qquad (1)$$

where η_o is the carrier viscosity and ϕ the solid fraction, may be expected to apply for low concentrations where the particle radius is small compared with the particle separation. For more concentrated systems the relation

$$\frac{\eta_f - \eta_o}{\eta_f} = 2.5\,\phi \left[\frac{2.5\phi_c - 1}{\phi_c^2} \right] \phi^2 \qquad (2)$$

due to De Bruyn[2] is more appropriate, ϕ_c represents a critical concentration at which the fluid becomes solid. A value of $\phi_c = 0.74$ corresponding to hexagonal close packed spheres would seem to be a reasonable value to take for the ferrofluid system (Rosensweig et al[3] 1965). ϕ is related to the particle volume fraction ϕ_p and particle coating δ by the expression

$$\phi = \phi_p \left[1 + \delta/r\right]^3 \qquad (3)$$

It is clear from expressions (2) and (3) that the viscosity of ferrofluids depends on the size of the surfactant coating since the physical diameter rather than the magnetic diameter is important.

As has been previously noted, iron mercury systems tend to have higher viscosities than might be expected from equations (1), (2) and (3). It is believed that this is primarily due to the existence of aggregates in the fluid, as discussed in the experimental section. However, it is also possible that bound mercury layers may contribute to the liquid viscosity. These layers (of thickness δ of 3 to 6A) would increase the physical size of the particle, in a manner similar to the dispersant coatings in non-metallic systems.

(c) Short term stability and aggregation in metallic systems

The short term stability of a ferromagnetic liquid is determined by particle interactions and the presence of magnetic or gravitational field gradients. In the simplest situation particles may aggregate under magnetic or van der Waals' forces and then settle under gravitational forces. Agglomeration through magnetic interactions may be prevented if the magnetic energy of particles in contact is less than the thermal energy transmitted to the particles through the carrier liquid. In general however aggregation occurs when particle collisions are perfectly inelastic. Such collisions occur when for some finite particle separation, there exists in the total inter-particle potential, $E_T(r)$ a well of greater depth than kT. Thus the condition for non-aggregation may be written

$$E_T(r) + kT > 0 \qquad (4)$$

The terms that contribute to $E_T(r)$ in a ferromagnetic liquid will be the attractive magnetic and van der Waals' forces, $E_m(r)$ and $E_V(r)$ respectively, and the repulsive electrostatic and steric forces, $E_E(r)$ and $E_S(r)$. These terms are investigated more fully for iron particles in mercury in the results section of this report.

The rate of aggregation (co-agulation) for a colloid system not satisfying the stability criterion of equation (4), was first investigated by Smoluchowski (4). He considered the particles to have no long range attraction for one another and to stick together when their centres came within a critical interaction distance 2R. The total number of aggregates/cm^3 at time t was shown to be given by

$$n = n_o\left[1 + 4\pi \mathfrak{D} R\, n_o\, t\right]^{-1} \qquad (5)$$

where n_o is the number of aggregates (or particles) per cm^3 at $t = 0$ and $\mathfrak{D}$ is the diffusion coefficient. Since $\mathfrak{D}$ is inversely proportional to R, n is independent of particle size.

If $\mathfrak{D}$ is given by the Stokes-Einstein relation equation (5) may be rewritten

$$n = n_o\left[1 + {}^{t}/_{\theta}\right]^{-1} \qquad (6)$$

$$\text{where} \quad \theta = \frac{1}{4\pi D R n_o} = \frac{3\eta}{4 k T n_o} \qquad (7)$$

For a 1 wt % iron in mercury fluid with 40 A diameter particles $n_o \sim 10^{17}$/cc. With $\eta = 1$ p, as observed for a 1 wt % fluid, $\theta \sim 10^{-4}$ secs at room temperature, i.e. the number of aggregates is reduced by a half in 10^{-4} secs. θ is a measure of the coagulation time in the absence of long range interactions. In the presence of interactions an effective coagulation time $\theta^* = q\,\theta$ may be defined where

$$q = 2R \int_{2R}^{\infty} \bar{r}^{2} \exp\left[{}^{W}/_{kT}\right] dr \qquad (8)$$

where W denotes the interaction energy which may be positive or negative depending on whether the interaction is repulsive or attractive. A value of q equal to 0.66 has been calculated by Hoon (5) for a van der Waals' attractive interaction in the iron - mercury system. The magnetostatic interaction results in $q \sim 0.95$ and $q \sim 0.72$ for 30A and 80A diameter iron particles. From these values of q it is seen that the iron particle coagulation time is close to ideal. Since $\theta \sim \theta^*$ aggregation of iron particles in

mercury fluids would take place quickly in the absence of any repulsive interaction. Furthermore, this aggregation causes settlement to take place. The time for this to take place can be readily calculated by equating the gravitational potential energy of an aggregate at a height h cm in the fluid with the thermal energy kT necessary to keep the aggregate dispersed. Thus, $m^* gh \ll kT$ is the condition for stability in a gravitational field where

$$m^* = 4/3\ \pi a^3\ \rho^* \tag{9}$$

and $$\rho^* = \rho_{Hg} - \rho_{Fe}$$

is the effective density of the particles in mercury.

For an aggregate containing x spherical iron particles of radius (a) a distance of 1 cm below the mercury surface, the condition for sedimentation is given by

$$m^* gh \sim \frac{4}{3}\ \pi a^3\ \rho^* \times gh > kT \tag{10}$$

Setting (a) to 20 A predicts $x > 10^2$ particles.

Equation (6) shows that this aggregation takes place in a time $t \sim 10^{-2}$ secs. Thus settling takes place rapidly in the absence of repulsive particle/particle interactions. Moreover, since settling increases the local particle density, aggregation may be expected to increase more rapidly as settling takes place.

The prevention of aggregation whether due to magnetic or van der Waals' interactions is difficult since a particle size distribution must always be considered and large particles which seed the aggregation will always be present. In commercial ferrofluids the problem is minimised by removing the large particles by centrifuging. This improves the stability significantly. In metallic systems the larger particles may be removed by magnetic separation provided the particle concentration and size distribution is such that aggregation does not occur before or during separation. These conditions are difficult to achieve in metallic systems. Aggregation due to van der Waals' forces (in metallic systems) cannot be prevented using entropic repulsion at present since there are no known metal-compatible dispersants equivalent to oleic acid. This is the main obstacle to the preparation of stable metallic ferromagnetic liquids.

The use of particle coatings to reduce particle interactions has been considered by Hoon et al (6). In this case the possibility of coatings forming charged surface layers through charge transfer at the interface between the particle surface and the carrier is considered. The situation thus existing at the particle surface is analogous to the charged double layers in colloids in non-metallic systems. Hoon et al (6) were able to show that the spacial extent of the charge depended on the difference in Fermi energy between carrier and particle and the magnitude of the charge transfer on the difference of the work functions of the two metals. Thus sodium with a work function very different from that of iron or mercury would be an appropriate coating material for the particles. Calculations show that though charge transfer should indeed take place the assumptions in the theory make it uncertain whether it would be sufficient to provide the necessary repulsion between particles to make the system stable.

(d) Diffusional Growth

In metallic systems ferromagnetic liquids may become unstable if particle growth takes place. This arises in a metallic carrier if the particles are not of one size. The larger particles will grow at the expense of the smaller particles through diffusion of atoms from the surfaces of small particles where the surface energy is large to the surfaces of large particles where the surface energy is low. The surface of the iron particles may be protected with coatings of tin, sodium, or antimony and in this way diffusional growth may be prevented. Data for these systems is presented in the results section of this report. Other experiments relating to diffusional growth have been described by Windle et al (7) and Hoon et al (6). Their results are consistent with the theory of Greenwood (8) who predicts that the particle growth rate is a maximum for particles with a radius (a_{2m}) twice that of the mean and that $a_{2m}^3 \alpha t$.

(e) Stability in Magnetic Fields

The stability of a ferromagnetic liquid depends on the magnitude of the magnetic field gradient acting on it. The liquid would be considered unstable if the ferromagnetic particles separated out from the carrier. Since the ferromagnetic particles experience a force

$$F_m = \frac{(\underline{M} \cdot \underline{\nabla}) \underline{H}}{4\pi} \cdot \frac{\pi D^3}{6} \qquad (11)$$

in a field gradient $\nabla \cdot \underline{H}$ the particles reach a terminal velocity

$\underline{u}$ when the magnetic F_m and viscous F_s forces are equal. F_s is given in terms of $\underline{u}$ and the viscosity η_o by

$$\underline{F_s} = 3 \pi D \eta_o \underline{u} \tag{12}$$

Hence the terminal velocity $$\underline{u} = -\frac{D^2}{18\eta_o} \quad \frac{\underline{M}.\underline{\nabla}.\underline{H}}{4\pi} \tag{13}$$

Equating the particle flux $n\underline{u}$ (n = the number of particles/cc) with the flux due to diffusion $\nabla nKT/3\pi \eta_o D$ (as given by the Einstein relation), gives a steady state condition when

$$D^3 = 24 \frac{\nabla n}{n} \frac{kT}{\underline{M}.\underline{\nabla}.\underline{M}} \tag{14}$$

A criterion of stability, $\frac{\nabla n}{n} = 1 \text{ cm}^{-1}$ is usually adopted.

This represents a 100% change in concentration for each centimetre. Hence iron particles of $D \sim 15$ A dispersed in mercury would be expected to be 'stable' in a field gradient $\underline{\nabla} H \sim 10^4$ Oe/cm.

An overriding consideration, however, would be the time τ to reach the steady state condition. Indeed it can be shown that in a field gradient of 10^4 Oe/cm it would take one hour to reach steady state conditions. When this time is large compared with the time spent by the fluid in the field, as might be the case for the energy conversion system described in figure 1, the fluid can be described as 'stable' for all practical purposes. Stability as defined in this way thus depends on the calculations of u in equation (13).

It is observed that the iron-mercury fluids separate out much more quickly than might be expected from equations (13) and (14). However, these equations assume that the particles have not aggregated. The observed values of u may be expected if aggregates, of the size inferred from gravitational and viscosity measurements, occur in the fluid.

4. Experimental

(a) Sample Preparation

Ferromagnetic liquids containing iron particles were prepared by electrodepositing iron on to a mercury-tin amalgam cathode. The anode was made of platinum and the electrolyte was an aqueous solution of ferrous chloride. Magnetic agitation by an alternating field of 200 G was found to be necessary in addition to mechanical stirring of the mercury amalgam surface in order to prevent particle dendrites forming on the surface of the cathode. Ferromagnetic liquids with a saturation magnetisation of up to 400 G, corresponding to $\sim$ 1 wt % iron were prepared by this method.

The iron particles were coated with tin to prevent diffusional growth as outlined in section 1(d) by adding 0.7 wt % tin to the mercury prior to deposition. However, sodium which was found to enhance stability by forming a second coating could only be added after the preparation because of the reaction of sodium with the aqueous electrolyte. About 2 wt % of sodium was added by mixing stock sodium amalgam of known composition with the iron-mercury amalgam.

(b) Magnetic Measurements

The magnetisation $M = 4 \pi I$ was measured in fields up to 9K Oe at room temperature and 77K with a vibrating sample magnetometer. Measurements were thus made in both liquid and solid samples.

In general, the samples were superparamagnetic in the liquid state but possessed a remanence and coercivity in the solid. These measurements were useful in evaluating particle sizes and the size distribution.

(c) Resistivity Measurements

The resistivity of a number of metallic samples was measured at room temperature and temperatures down to 77K using a standard four probe method with current reversal. Only in those fluids containing sodium was difficulty encountered. These measurements are less reliable because of the reactivity of sodium with atmospheric water which caused the formation of bubbles in the cell. Resistances could be measured accurately to $\pm 10^{-6}$ Ω.

(d) Viscosity Measurements

The viscosity was measured at room temperature for different shear stresses and shear rates using a specially designed Poiseuille flow viscometer. The quantity of ferromagnetic liquid required for this experiment was of the order of 8 cm^3. The use of various other methods of measuring the viscosity were attempted but the high surface tension and density of mercury precluded the use of most of these methods. Viscosity measurements were made in the range 10^{-2} p < η < 10^{-5} p, i.e. a range reflecting the transition from the viscosity of pure mercury to that of a self supporting paste.

(e) Latent heats of fusion

Latent heats of fusion were obtained using a commercial Perkin-Elmer differential scanning calorimeter with a sensitivity of ∿ 5 m cals K^{-1} s^{-1} using scan rates of 0.5 K min^{-1} to 8 K min^{-1} in the range 180K to 300K. A sample volume of ∿ 15 x 10^{-3} cm^3 was required and yielded latent heats of fusion to a reproducibility of ∿ 5%. Because of the limitation of the dewar it was necessary to slow quench the samples from room temperature to below 230 K (their approximate freezing point) at a rate of ∿ 5 K min^{-1}. It was possible to detect the presence of ∿0.01 wt % Sn in solution by examining the line-shape which was important when determining the spatial location of tin.

(f) Electron microscopy

The physical diameter of iron particles in mercury have been determined by the 'direct' observation of particles in transmission electron micrographs. Collodian coated copper grids were used to support the iron particle samples and special care was taken during the preparation of the grids to take samples (with a pipette) from the bulk of the fluid rather than its surface. The principal problem in determining the sizes of iron particles in mercury by electron microscopy is the difficulty in distinguishing between iron, mercury and mercury coated iron.

(g) Stability in a gravitational field

The change in inductance that occurs when a ferromagnetic liquid is placed in a coil is proportional to the initial susceptibility and concentration of the iron particles. The settling of iron particles within a fluid contained in a glass tube positioned vertically in a gravitational field has been monitored by measuring the change in inductance with time of a search coil wound around the glass tube. The coil was scanned vertically along the tube enabling the time dependent concentration profile of iron particles to be determined.

5. Results and Discussion

5.1 The magnetisation curve

The magnetisation curves for ferromagnetic liquids containing iron particles in mercury have been determined at 77K and room temperature. Typical examples are shown in figure (5.1). From these the ferromagnetic iron concentration may be determined by plotting the magnetisation as saturation is approached versus 1/H and extrapolating to infinite field, as shown in figure (5.2). The absence of a remanence and coercivity in figure (5.1a) clearly shows that the fluid is superparamagnetic at room temperature. However, it is not possible from this curve alone to determine whether the superparamagnetism occurs via the Brownian relaxation and rotation of the bulk particles, the Néel relaxation of the magnetic movement of the particle or a mixture of the two processes.

It is found that the experimental points of the room temperature magnetisation curves cannot be fitted by a simple single particle volume Langevin curve. This is indicative of the existence of a particle size distribution. The form of the particle size distribution is investigated further in the following section.

Figure (5.1b) demonstrates that when the fluid is frozen at 77K, it exhibits hysteresis due to the solid mercury matrix freezing out the Brownian relaxation mechanism, which is only possible in the liquid state. The value of the sample's coercivity at 77K may be related to the iron particle size, after Luborsky (11), as shown in figure (5.3).

5.2 Some comparative methods of particle size determination

(a) Particle size determination from magnetic data

The relationship between particle volume and coercivity (H_c) at 77K of frozen iron-mercury samples is shown in figure (5.3), after Luborsky (11). This offers a simple method of determining particle sizes from magnetic measurements by simple comparison of the observed sample's coercivity with figure (5.3). Thus the coercivity of 106 Oe observed in figure (5.1b) implies an average particle diameter D_{H_c} of (35 ± 5)A. It is clear that many particles must have a diameter greater than 35A as the condition for superparamagnetism, $D < Dp$ where Dp is defined by

$$\frac{\pi}{6} K Dp^3/kT = 25 \quad , \qquad (15)$$

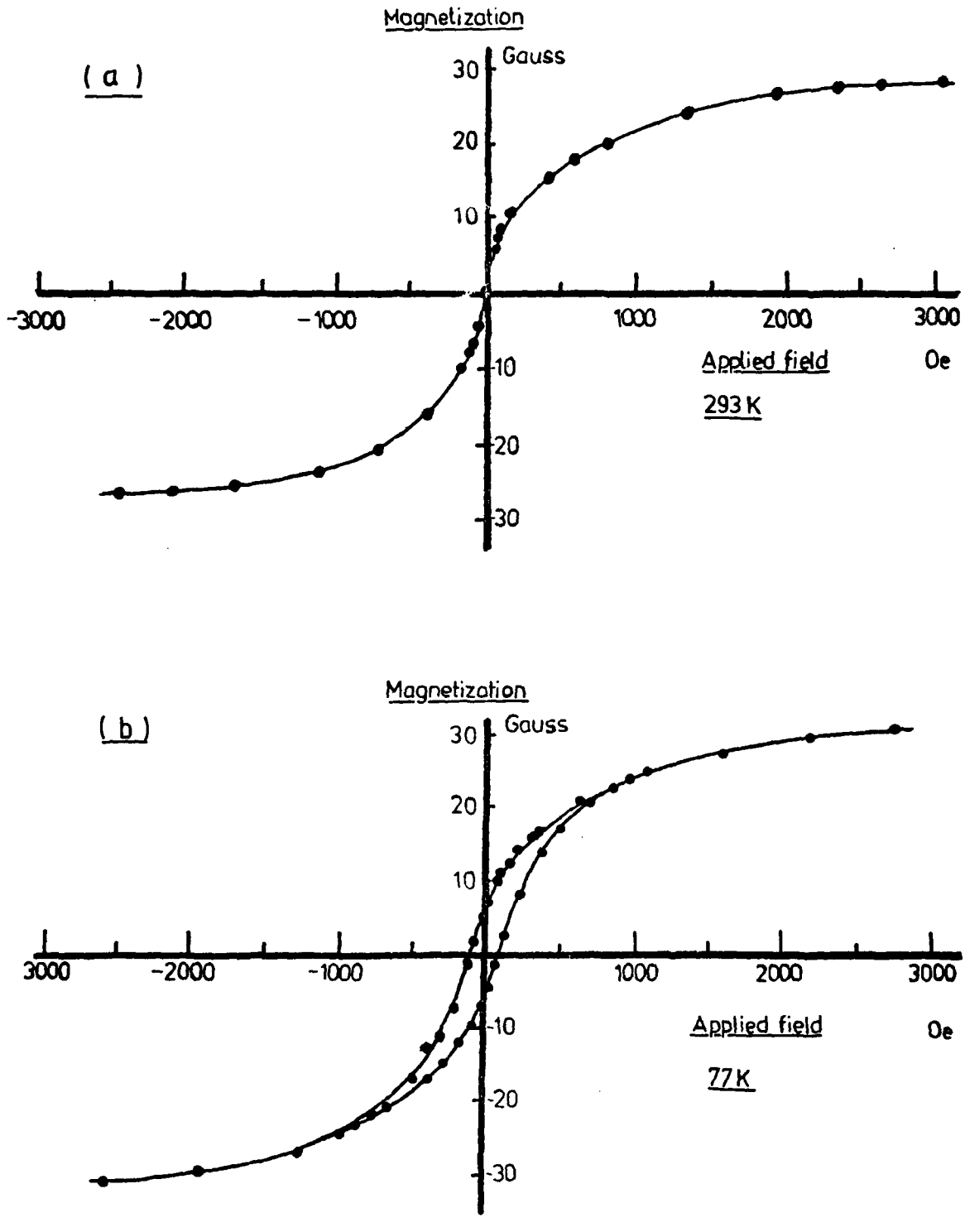

Figure (5.1) Magnetisation curves at 293K and 77K for iron particles in mercury.

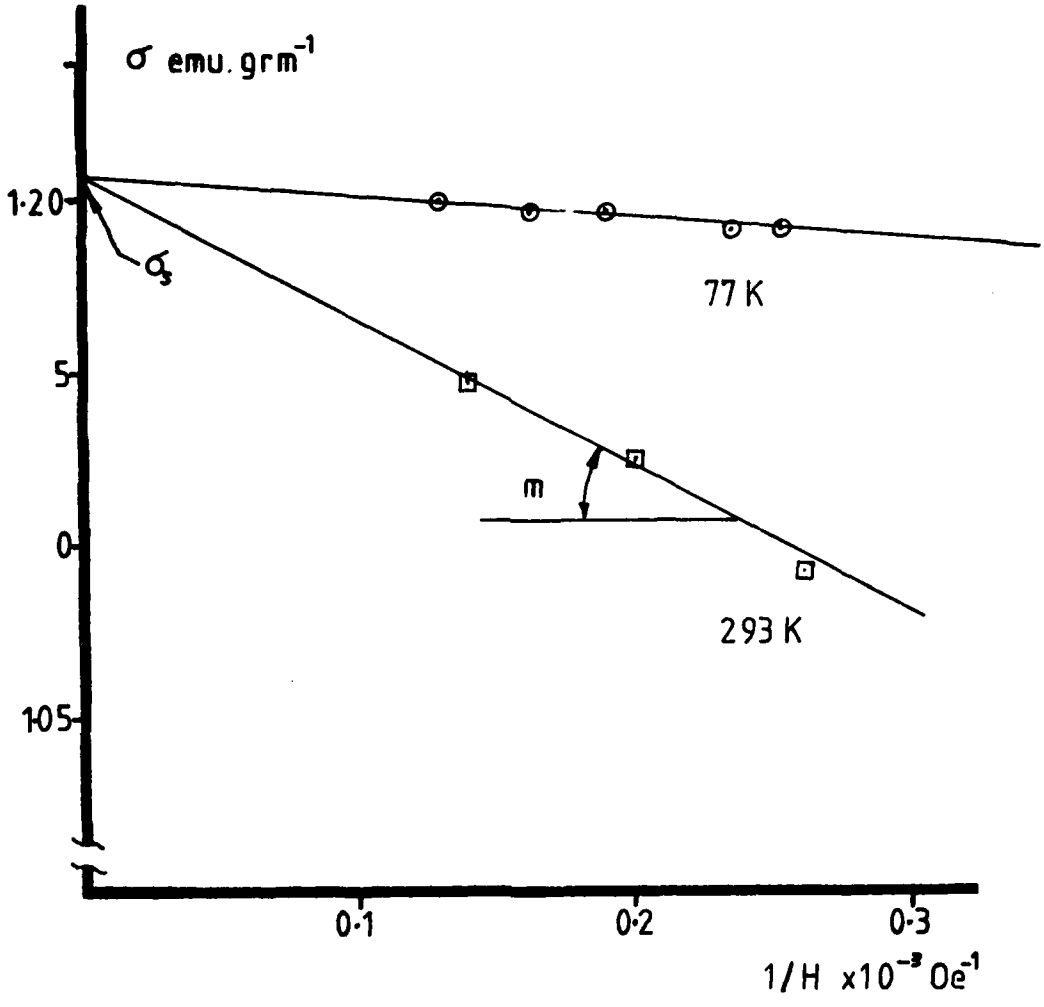

Figure(5.2) Plot of fluid magnetisation versus 1/H at 293 and 77 K for iron particles in mercury.

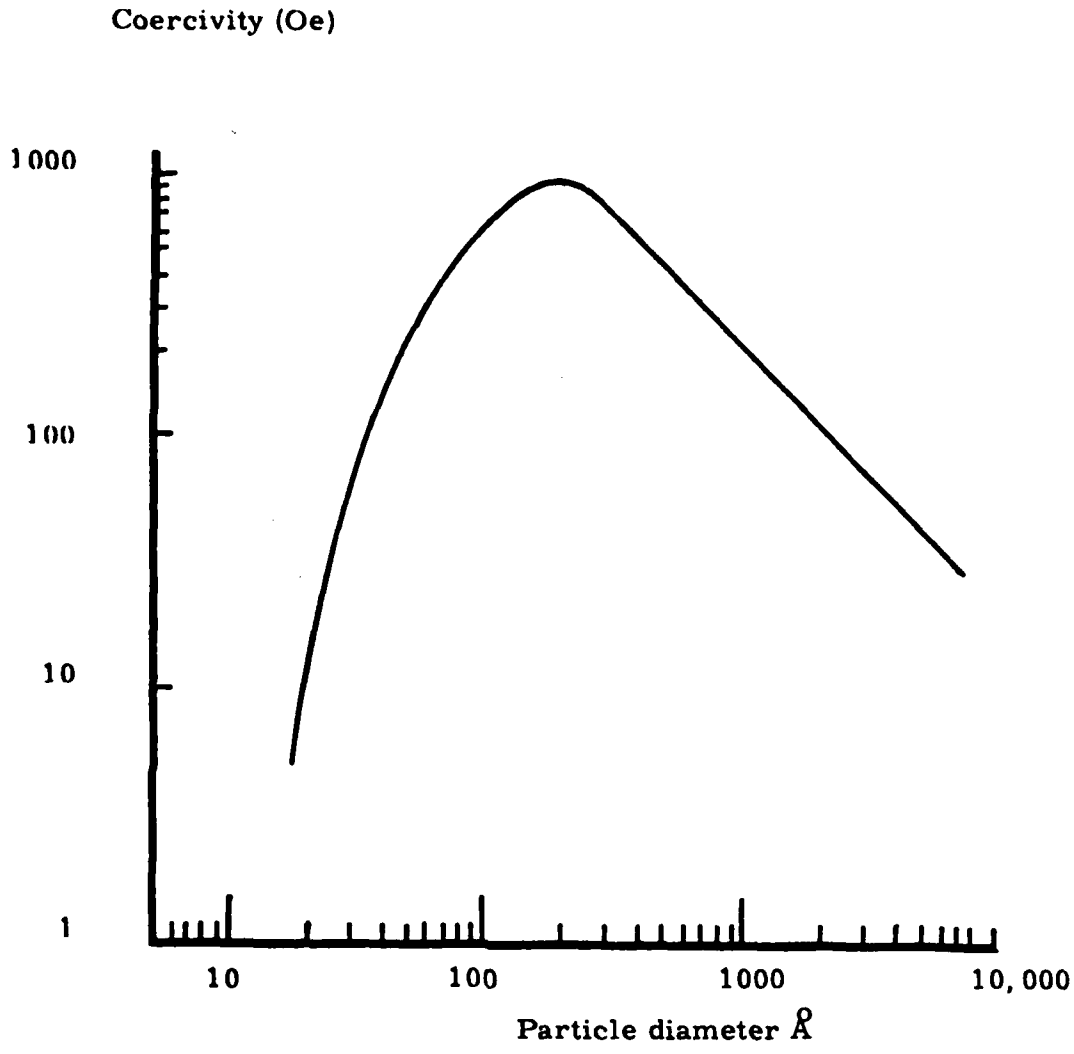

Fig. (5.3) Change in coercive force with particle diameter of spherical iron particles as measured at 77°K, after Luborsky[11].

predicts that Dp has the value 100A or 70A for K, the anisotropy constant, equal to 0.52×10^6 erg cm^{-3} (cubic crystalline anisotropy) or 1.32×10^6 erg cm^{-3} (10% uniaxial elongation) respectively. Thus particles of 35A diameter would be expected to be superparamagnetic. As the remanence is caused by particles for which D > Dp then there must be a number of particles in excess of 100A diameter.

Particle sizes inferred in this way from figure (5.3) must be treated with caution. This is because it must be assumed that both the maximum anisotropy field $H_K \sim 2K/I_s$ and the particle size distribution of the fluid are similar to those in the samples of Luborsky from which figure (5.3) was constructed. Chantrell et al (35) have shown that for an assembly of particles the dependence of H_c/H_K upon D_v/D_p is sensitive to the particle size standard deviation σ. This dependence is shown in figure (5.4). However, the average particle sizes determined from H_c are not inconsistent with those inferred from tin adsorption measurements (Hoon et al (6)).

Bean and Livingstone (22,23) have used the low and high field forms of the Langevin equation to determine characteristic particle sizes. They make the assumption that the contribution to the initial susceptibility χ_i is determined principally by large particles of diameter D_L and the high field susceptibility by smaller particles of diameter D_s, namely

$$D_L = \chi_i^{1/3} \cdot \frac{18kT}{\pi I_s^2} \qquad (16)$$

and

$$D_s = \left(\frac{\sigma_s}{m}\right)^{1/3} \left(\frac{6kT}{\pi I_s}\right)^{1/3} \qquad (17)$$

where χ_i is experimentally determined and m represents the negative gradient of the magnetisation σ_s emu grm^{-1} versus 1/H graph as shown in figure (5.2). Applying equations (16) and (17) to figure (5.1) and (5.2) yields $D_L = 64 \pm 7$A and $D_s = 51 \pm 1$A, in comparison with $D_{Hc} = 35 \pm 5$A. In practise Bean's technique yields a 'best fit' in terms of the low and high field Langevin function rather than two physically meaningful particle diameters.

A better technique for determining particle sizes from superparamagnetic magnetisation curves is to employ a theory, such as that of Asinow (24) or Chantrell et al (25), which incorporate a particle size distribution function. Chantrell et al (25) use, with some justification, the log normal distribution function to describe the particle volume distribution in a fluid. They derive the following equations for the median particle diameter D_v and the standard deviation σ_{SD}, namely,

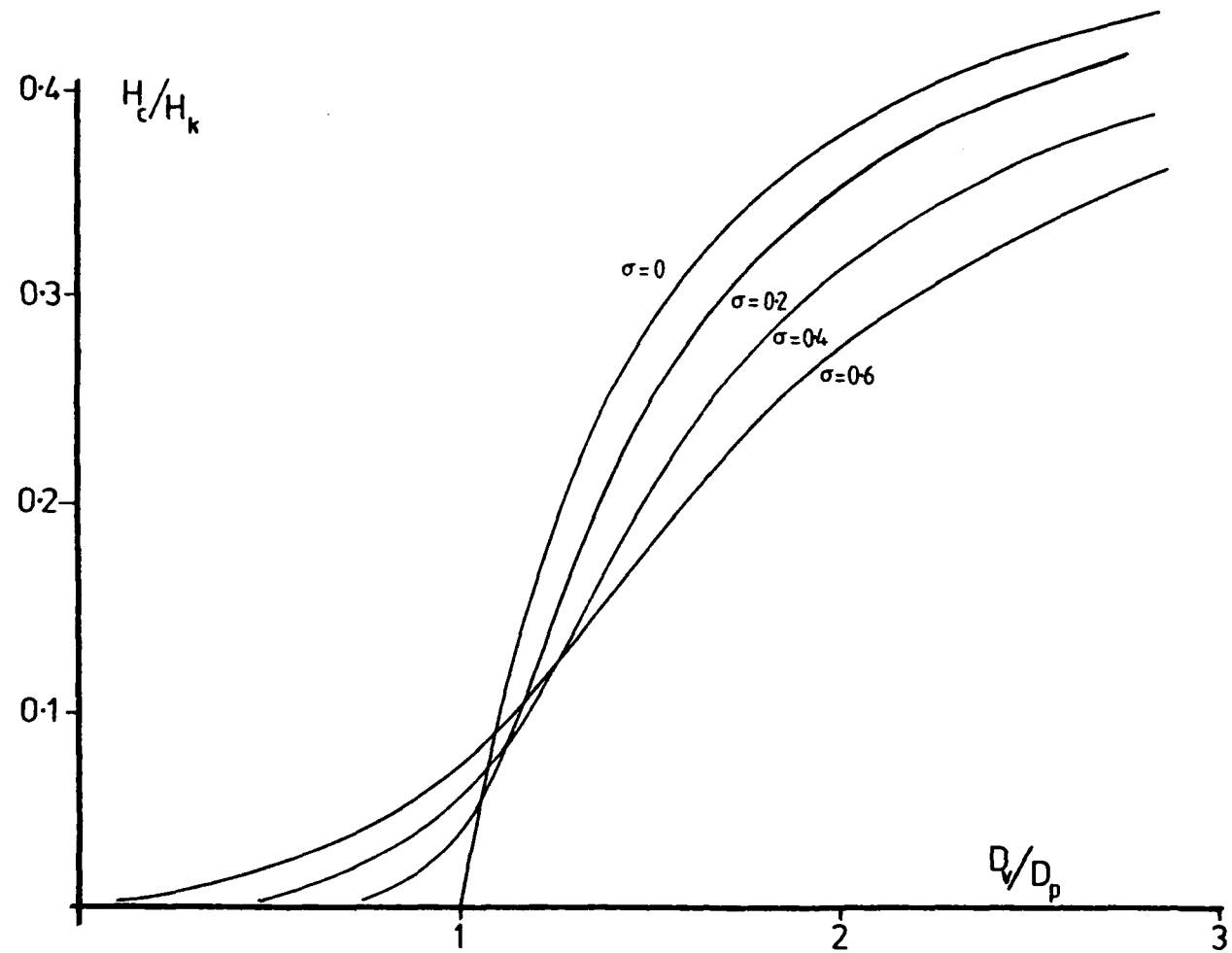

Figure (5.4) The interdepenence of $H_c.H_k^{-1}$, $D_v.D_p^{-1}$ and σ.

Fluid	F14Sn		F5Na		F13	
Parameter	293K	77K	293K	77K	293K	77K
D_{Hc} (A)		30±5		35±5		44±5
D_v (A)	50±2		60±3		56±0.1	
$\sigma_{S.D.}$	0.5 ±0.04		0.28 ±0.01		0.24 ±0.01	
D_L (A)	75±0.1		64±7		79±1	
D_s (A)	35±2		51±1		55±3	

TABLE 5.1

Particle sizes as determined by the Luborsky, Chantrell and Bean methods for three iron-mercury fluids

$$D_v = \frac{18kT}{\pi I_s} \left(\frac{\chi_i}{3I_s} \cdot \frac{1}{H_o} \right)^{\frac{1}{2}}{}^{13} \qquad (18)$$

$$\sigma_{SD} = \frac{1}{3} \ln(3\,\chi_i/I_s \cdot 1/H_o)^{\frac{1}{2}} \qquad (19)$$

where $1/H_o$ is the value of the intercept at $I_s = 0$ of the tangent 'xy' defined in figure (5.2) and I_s the saturation magnetisation of the fluid (emu cm^{-3}). Applying equations (18) and (19) to figures (5.1) and (5.2) yields $\sigma_{SD} = 0.28$ and $D_v = (60 \pm 3)$A. This value of D_v lies between D_L and D_S as may be expected.

Table (5.1) summarises the results of applying the above three analyses to three different fluids. It is seen that in each case D_{H_c} lies approximately one standard deviation below D_v. This is consistent with the fact that the median particle diameter D_v of a log-normal distribution function always lies to the right of the modal volume, whereas D_{H_c} tends to reflect the modal particle volume. If due consideration is given to the dependence of H_c upon σ_{SD} as shown in figure (5.4), then the disagreement between D_{H_c} and D_v is yet further reduced.

(b) Particle size determination from electron microscopy data

The physical and magnetic diameters of particles are expected to differ, the former being larger due to the presence of non-magnetic surface layers and the particle stabilising coatings such as tin. It is the physical diameter that is observed in the electron microscope. However, because of the opacity of mercury to an electron beam and its tendency to adhere to iron particles it can be difficult or even impossible to distinguish between mercury coated and uncoated particles. Thus the diameter observed from electron microscopy is consistently higher than that determined magnetically, as also discussed in a previous report by Windle et al (26).

Figure (5.5) shows a high definition electron micrograph of particles from an iron-mercury fluid stable to heating by a high intensity electron beam, which suggests that the sample is composed principally of iron particles. Most of the particles show elongations of a few percent. The average diameter of every apparently individual particle in this figure was measured using a Zeiss particle size analyser. The number distribution that was observed is plotted in figure (5.6). It is clearly bimodal of mean and standard deviation 115A and 1.25 and 300A and 0.85 respectively. Each component is clearly log normal as the distributions as plotted on the log abscissae may be shown, to a good approximation, to be Gausian. The origin of the bimodal distribution in this fluid is unknown and may be due to either a genuine growth process during the fluids preparation and subsequent aggregation or due to an experimental artefact a consequence of the microscope grid preparation technique.

1200 A

Figure (5 5) Electron micrograph of as prepared iron particles in mercury

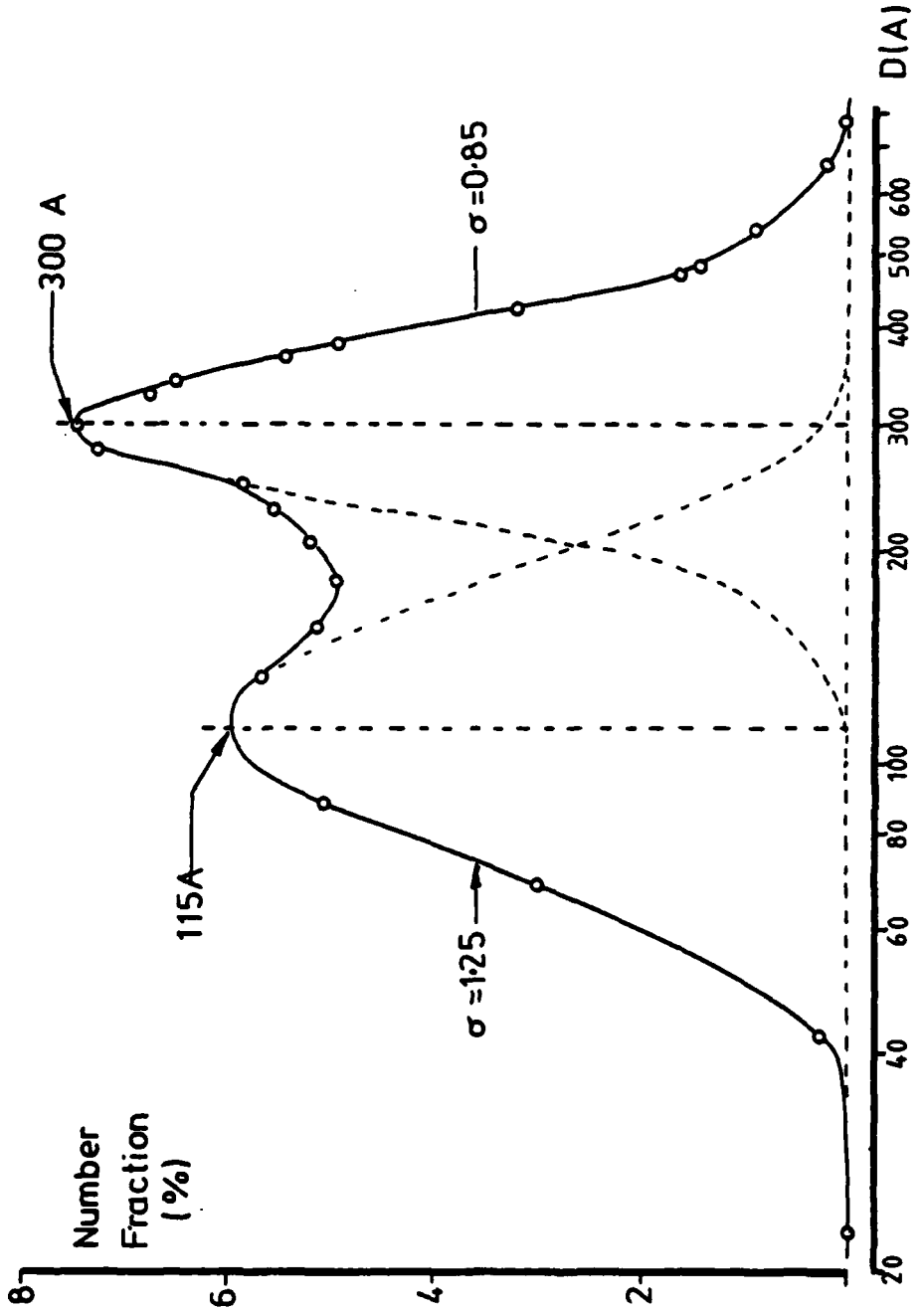

Figure(5.6) Paticle size distribution, derived from figure(5.5).

D_1 = 115A ..... σ_1 = 1.25 (54% of particles)

D_2 = 300A ..... σ_2 = 0.85 (46% " ")

D_L = 500A

D_s = 40A

D_v = 146A ..... σ_{SD} = 0.94

D_{Hc} = 50A

TABLE 5.2

Summary of the electromicrograph particle size data derived from figures (5.5) and (5.6) in comparison with the Bean, Chantrell and Luborsky methods.

The above microscopy particle size data determined from figure (5.6) has been compared with particle size data determined magnetically. The results of this comparison are summarised in table (5.2). The data is broadly self consistent, especially when it is recalled that the physical and magnetic diameters are expected to differ.

The Bean values of D_L and D_S appear in this instance to define the extent of the (diameter) number distribution. The value of D_V compares favourably with the centre of the bimodal distribution whilst σ_{SD} compares with the individual bimodal values of 1.25 and 0.85. It is perhaps not surprising that the magnetic value of σ_{SD} underestimates the observed value of σ_{SD} for the bimodal distribution as the magnetic theory from which it is derived assumes only a mono-modal distribution with a single value of D_V.

Agreement between the magnetic estimates of D_V and σ_{SD} and those produced from electron microscopy could be improved if it were supposed that the right hand peak of figure (5.6) corresponded to aggregates of particles and the left hand peak to individual particles. For as D_V is determined from χ_i, which is expected to be fairly sensitive to particle interactions, D_V and σ_{SD} (magnetic) should reflect the size distribution of the individual particles, and thus also the particles within the aggregates, rather than the aggregate's size.

The poor agreement of D_{Hc} ($\sim$ 40A) with the other data may be understood in terms of the sensitivity of H_c to changes in D_V for large values of σ_{SD}, in this case $\sim$ 3.5 for the whole distribution, as shown in figure (5.4).

5.3 Magnetic Interactions

A knowledge of the effect of particle interactions upon the magnetisation curve is important as this will affect the analysis of magnetisation measurements. If the particles form chains, rings or clusters then χ_i, H_c and the remanence I_R may be expected to differ from those of a fluid in which the particles remain isolated. Further, the parameters may be expected to be particle concentration dependent. In addition it may be necessary to apply a demagnetising field correction to the applied field to account for sample container shape effects.

Figure (5.7) shows magnetic measurements made on a fluid containing tin-coated 45A diameter particles in mercury at room temperature. The fluid is superparamagnetic and there is no remanence or coercivity. The measurements are shown to be independent of the sample shape and the inclusion of a demagnetising factor would not, therefore, appear to be necessary. Since Kondorskii (10) also rules out the inclusion of a Lorentz field correction on theoretical grounds, particle interactions from nearest neighbours would seem most important in determining the form of the magnetisation curve, particularly in concentrated samples.

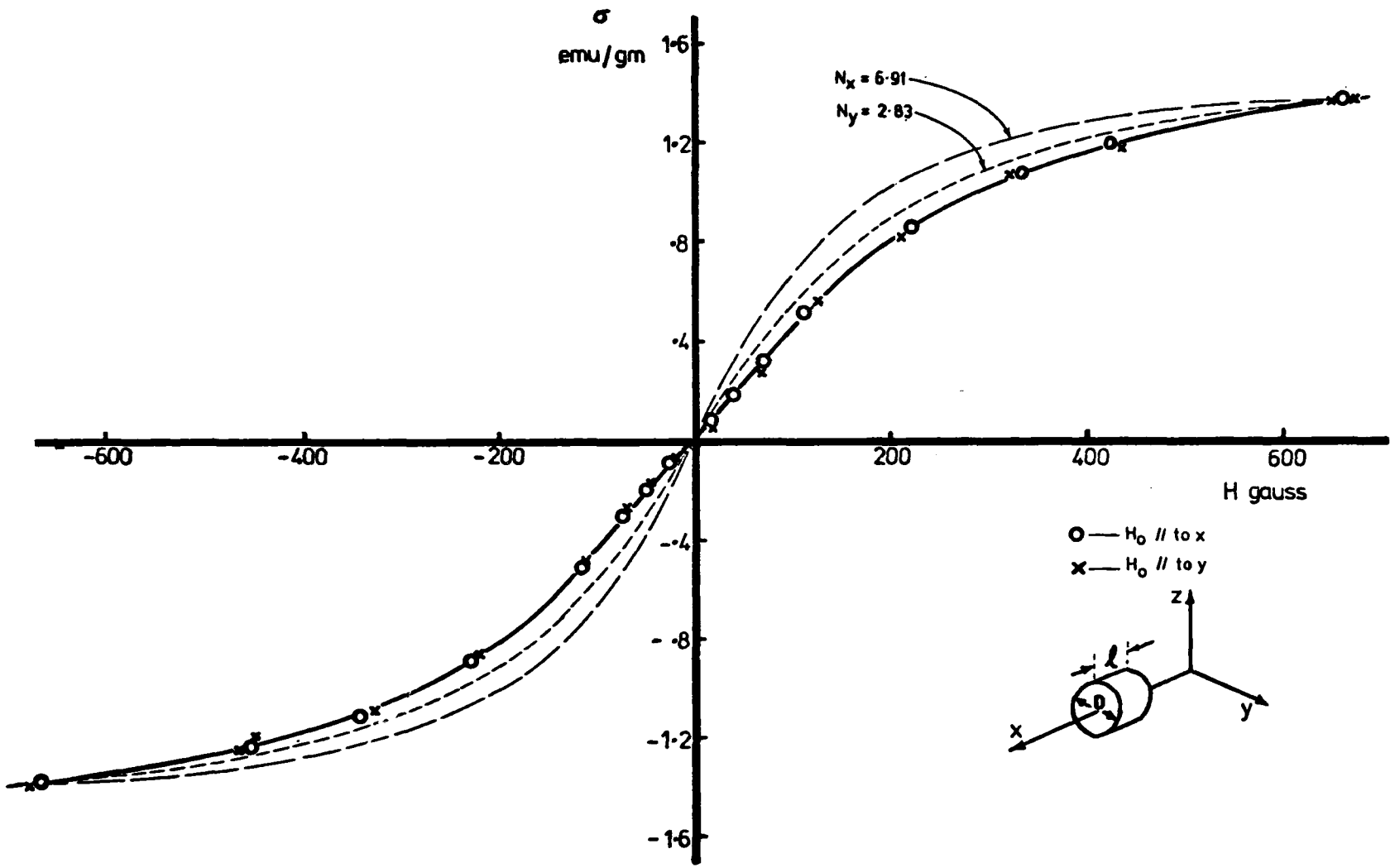

Figue (5.7) The superposition of the experimental points for $H_\perp$ and $H_{//}$ to the samples x direction without the need for a demagnetising field correction.

Figure (5.8) shows the reduced magnetisation curves of two samples of fluid F 11 Na at 77K. One sample corresponds to the fluid in its as prepared state and the other to the fluid after magnetic concentration in a 1.45 k Oe cm^{-1} field gradient. The concentrations of these two samples were determined as 1.27 or 2.70 emu grm^{-1} respectively.

It is immediately apparent from figure (5.8) that the act of concentration in a magnetic field gradient has altered the (reduced) magnetic properties of the fluid. These changes are summarised in Table (5.3). Whilst χ_i remains unchanged, H_c has fallen by 20% and I_R/I_s risen by 8%. A decrease in H_c as the particle concentration increases is to be expected from the interaction theory of Kondorski (11), to be discussed presently.

However, it is not possible from this data alone to distinguish between changes in magnetic parameters due to the increase in particle concentration, and changes that arise as a direct result of the fluids exposure to the field gradient, for example irreversible changes in aggregate structure.

Figure (5.9) and (5.10) show respectively a series of low and high field magnetisation curves at 77K for samples containing 70A diameter particles in the concentration range 3.6 emu grm^{-1} to 8×10^{-2} emu grm^{-1}. This concentration range corresponds to $\sim 10^{17}$ and 10^{15} particles cm^{-3} or volume fractions (ϕ_m) of ~ 0.03 and 6×10^{-4} respectively.

The samples were prepared by first magnetically concentrating the as prepared fluid (F18) and then diluting it with pure mercury. This ensured that the magnetic history of the samples was identical. The sample concentrations were determined from the extrapolation to infinite field of the plot of magnetisation versus 1/H. It is seen from figure (5.9) that the low field behaviour of the reduced magnetisation for the samples containing 3.32, 2.19 and 1.74 emu grm^{-1} iron is identical within experimental error, but that the sample of 0.54 emu grm^{-1} shows a slight increase in coercivity and reduction in χ_i. The 7.9×10^{-2} emu grm^{-1} sample exhibits both a smaller value of χ_i and I_R/I_s and a larger value of H_c. This data is summarised in Table (5.4).

Kondorskii (10) has considered the dependence of H_c upon particle volume fraction by considering how the local effective field changes with particle concentration, and derives a relationship predicting that H_c should decrease linearly with increasing particle concentration. This linear dependence is not observed. However Wohlfarth[47], using a different approach whereby the magnetostatic particle energy is minimised, has demonstrated that the variation of H_c upon ϕ_m is highly structure sensitive and that depending upon structure H_c may either increase or decrease with ϕ_m.

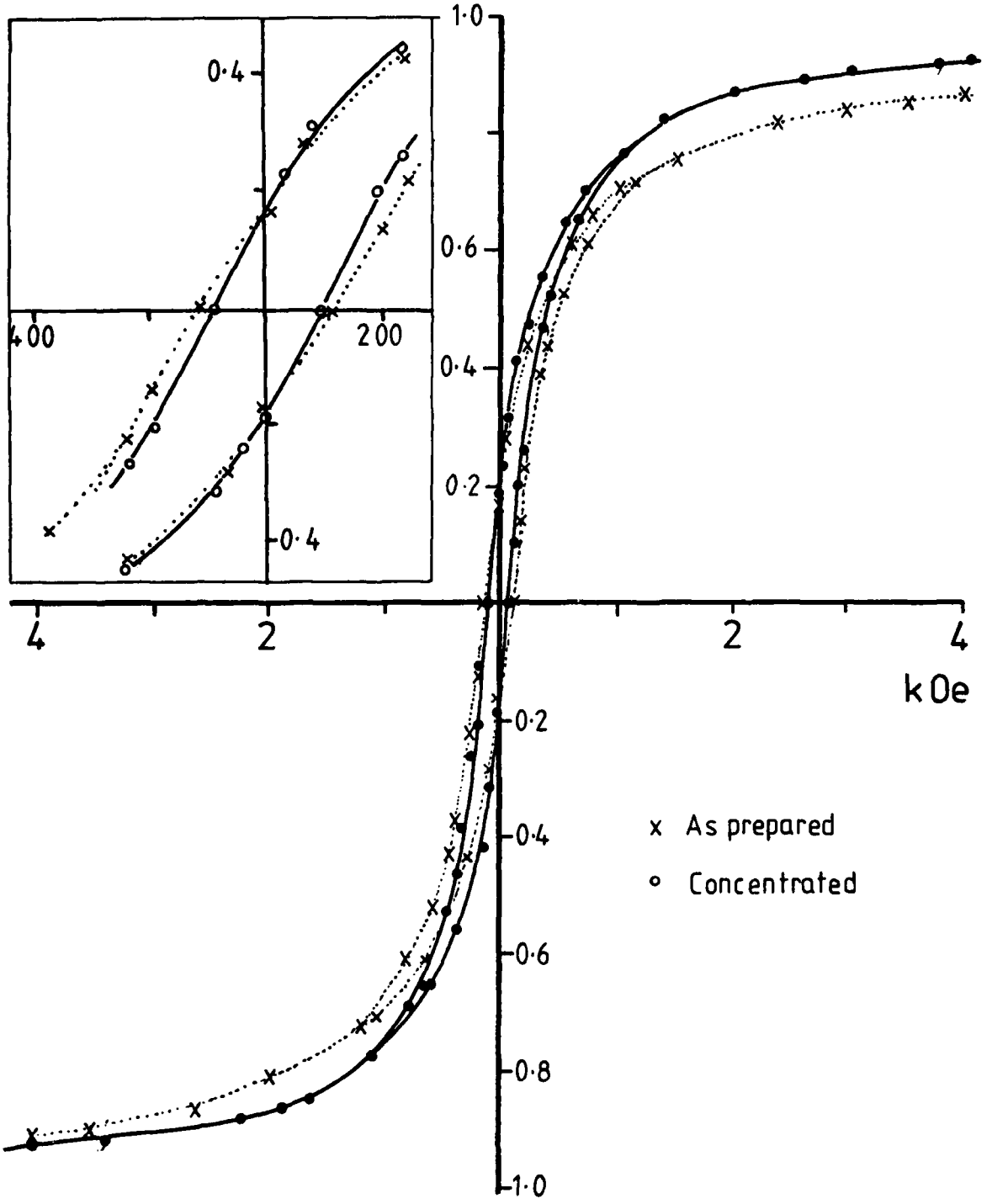

Figure (5.8) The reduced magnetisation at 77K before and after magnetic concentration.

	As Prepared	After magnetic concentration	Change in parameter
σ_s (emu/grm)	1.27	2.70	110%
I_R/I_s (at 77K)	0.168	0.181	8%
H_c (Oe)	118	94.6	-20%
D_{Hc}	40±3	34±5	-15%
χ_i	1.6×10^{-3}	1.6×10^{-3}	0

TABLE 5.3

Summary of the magnetic data shown in figure (5.8) for a fluid before and after magnetic concentration

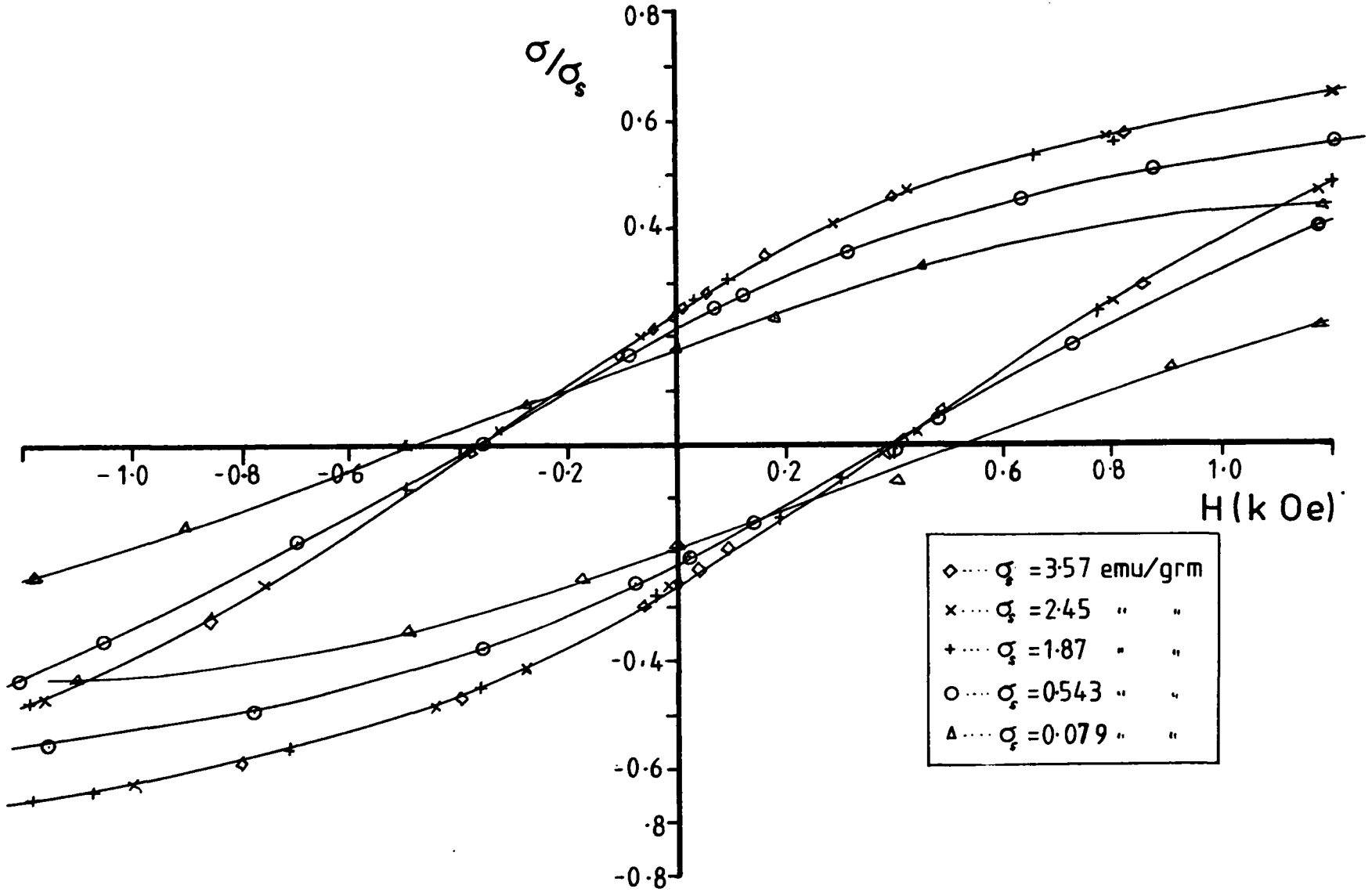

Figure (5.9) The effect of dilution, subsequent to concentration, upon the magnetisation, at 77K, in low magnetic fields.

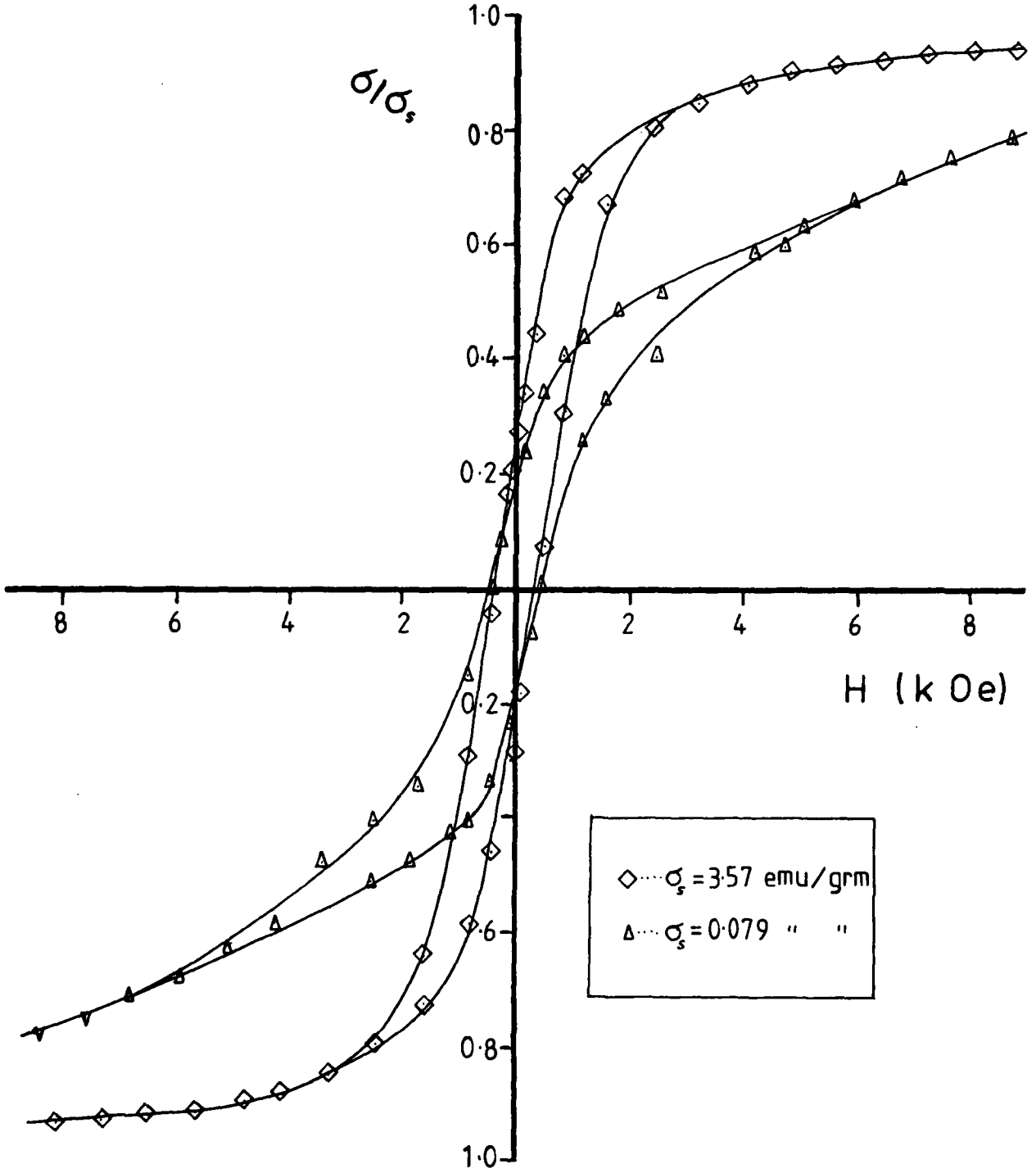

Figure (5.10.) The effect of dilution subsequent to concentration upon the magnetisation at 77K in high magnetic fields.

Sample	0	1	2	4	5
σ_s emu/grm	3.57	2.45	1.87	0.543	7.9×10^{-3}
wt % Fe	1.62	1.11	0.847	0.246	3.4×10^{-2}
ϕ_m	2.75×10^{-2}	1.90×10^{-2}	1.45×10^{-2}	4.23×10^{-3}	5.8×10^{-4}
I_R/I_s	0.250	0.250	0.250	0.215	0.180
H_c (Oe)	385	385	385	495	500

TABLE 5.4

Changes in the magnetic parameters of a fluid upon redilution with pure mercury subsequent to concentration in a magnetic field gradient, see also figures (5.9) and (5.10)

Thus it is suggested that the failure to observe any significant changes in H_c as ϕ_m is decreased imply that the nearest neighbour particle structure, perhaps imposed by the original act of magnetic concentration, was not significantly altered during the subsequent dilution with pure mercury.

5.4 Time Dependent Magnetisation

Figure (5.11) shows time dependent magnetisation measurements at room temperature for 1.47 emu/g and 0.49 emu/g tin coated iron particles in mercury. Both these fluids have viscosities similar to that of mercury.

In each case the applied magnetic field has been reduced quickly from the value H_1 to the value H_2 (these values being indicated in figure 6.1). The observed characteristic times for the magnetisation to decay are $\sim$ 30 secs. Such long time constants can only be due to large particles or aggregates whose moments are blocked within the particles, such that the magnetic moment can only relax by bulk particle rotation. For a blocked particle the energy barrier to rotation of the magnetic vector is larger than the thermal energy kT. The magnitude of the energy barrier is determined by the anisotropy K, where K may be considered to be the sum of the shape, crystal and interaction anisotropies. For unblocked particles the relaxation time would be $\sim 10^{-11}$ secs. This is about 10^{-2} times shorter than the characteristic time constant for Brownian relaxation of an individual 40A diameter particle.

Shliomis (12) has shown that the relaxation time for blocked particles in a magnetic field is given approximately by

$$\tau \sim 6\eta V/\mu H \qquad (20)$$

where τ is the time for the magnetic moment to rotate through π radians, η is the carrier viscosity, V the hydrodynamic particle volume. $\mu = \frac{4}{3} \pi a^3 I_s$ the magnetic moment, a the particle radius and H the applied field. I_s is the bulk material's saturation magnetisation.

Equation (20) can be extended to cover the case where the hydrodynamic volume is greater than the magnetic volume, i.e. the volume of the magnetic material is less than the hydrodynamic volume. In this case

$$\tau \sim \frac{6\eta}{I_s H} (1 + \delta/a)^3 \qquad (21)$$

where δ is the thickness of an adsorbed layer. For small particles where $\delta >> a$,

$$\tau_p < 48\eta/I_s H \qquad (22)$$

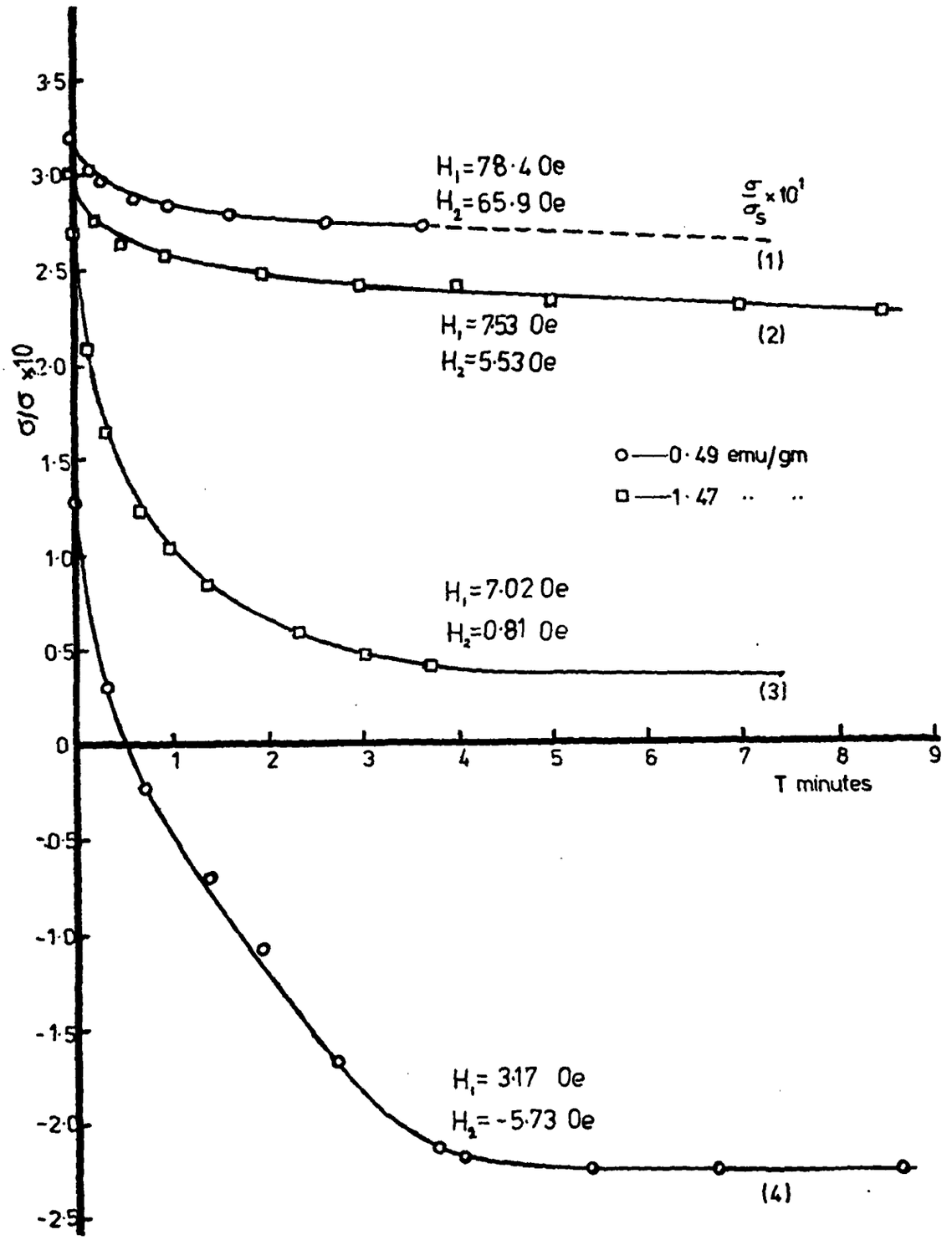

Figure (5.11) shows the time dependent magnetisation data for iron particles in mercury when the applied magnetic field is reduced from H_1 to H_2 Oe. (at room temperature)

represents the relaxation time for individual particles. For large particles or aggregates ($a > 200A$) it is reasonable to assume $\delta/a \ll 1$ and thus the relaxation time of an aggregate τ_{agg} is given by

$$\tau_{agg} \sim 6\,\eta/I_s\,H \qquad (23)$$

Application of equations (22) and (23) to the curve (iv) in figure (20) predicts $\tau_p \sim \tau_{agg} \sim 10^{-3}$ secs, where I_s has been taken as 1707 emu/cc and $H \sim 10$ Oe. In practice τ is observed to be ~ 30 secs. To obtain agreement between experiment and theory it is necessary to assume that aggregates of particles form, such that their net moment is reduced by flux closure configurations. It is possible to remove the complication that flux closure makes in interpreting the curves of figure (20) by considering the simpler case (iii), of that figure. This is because for curve (iii) the applied field has been effectively switched off at $t = 0$ and so the magnetisation decays only by Brownian diffusional rotation of the particles or aggregates.

In this case τ is given by

$$\tau_B \sim 3\,V\,\eta/k\,T \qquad (24)$$

Let the radius of a particle $a \sim \frac{1}{2}\,V^{\frac{1}{3}}$ then

$$a \sim \tfrac{1}{2}\left(\frac{\tau\,k\,T}{3\,\eta}\right)^{\frac{1}{3}} \qquad (25)$$

Then for $\eta \sim 1$p and $\tau \sim 30$ secs equation (25) yields a $\sim 10^{-4}$ cm. This value of a is in agreement with the calculated aggregate size inferred from gravitational stability experiments.

It should also be noted that equation (25) is not very sensitive to η, as for $\eta \sim 10^{-2}$p, $a \sim 2 \times 10^{-4}$ cm. For high viscosity fluids, paste-like in appearance, ie $\eta > 10^3$ p, equation (25) predicts for a $\sim 10^{-4}$ cm a value of τ of 30 hours. If a paste-like fluid is saturated in a magnetic field and then the field removed a remanence is observed which disappears in a time similar to that calculated above ie $\sim$ 24 hours.

6. Stabilisation of Particle Growth by Diffusion

In metallic ferromagnetic liquids particle growth by diffusion will always take place, causing the liquid to become unstable, unless the particles are coated. The diffusional growth occurs because of the existence of a particle size distribution in the liquid. The larger particles grow at the expense of the smaller ones by the diffusion of (iron) atoms from the surfaces of small particles, where the surface energy is large, to the surface of large particles where the surface energy is low. The surface of the iron particles may be protected with coatings of tin or sodium and in this way diffusional growth may be reduced as shown in figures (6.1) and (6.2). The experiments relating to diffusional growth have been described by Windle et al (7) and Hoon et al (6). Their results are consistent with the theory of Greenwood (8) who predicts that the particle growth rate is a maximum for particles with a radius a (a_{2m}) twice that of the mean and that $(a_{2m})^3 \alpha t$.

As can be seen from figure (6.1) for iron particles aged in mercury, particle growth is evident in the long term and stabilisation of the particle size is not obtained, whilst tin only retards the particle growth rate. However as shown in figure (6.2) long term growth is apparently prevented for particles initially coated with tin and subsequently coated with sodium.

It has been reported by Falk et al (1965) that iron particles coated with antimony dispersed in mercury are stable at high temperatures and the use of such a system as a ferromagnetic liquid for high temperature applications is therefore possible.

In the work reported here the antimony was added to the iron particles in mercury by alloying the antimony with lead to produce a eutectic alloy containing 11 % Sb and 89 % Pb which is then dissolved in mercury. This procedure is necessary since antimony is insoluble in mercury. The liquids have then been aged by heating at 420K in order to study the effect the antimony has on the particle growth rates. Simultaneous growth experiments have been carried out on uncoated iron particles and tin-coated iron particles in mercury and their relative growth rates compared.

Results show that if a quantity of antimony in excess of the amount required to form a monolayer is added to the as-prepared iron-mercury system then subsequent ageing results in a decrease in the saturation magnetisation with ageing time, as shown in Figure (6.3).

However, when sufficient antimony to form a monolayer particle coating only is added, the saturation magnetisation remains constant after ageing. The stabilisation of particle size is monitored by measuring the particle coercivity at 77K which is a function of particle size, the value remaining constant when growth is prevented. The effect of antimony and tin coatings on the coercivity is shown in figure (6.4).

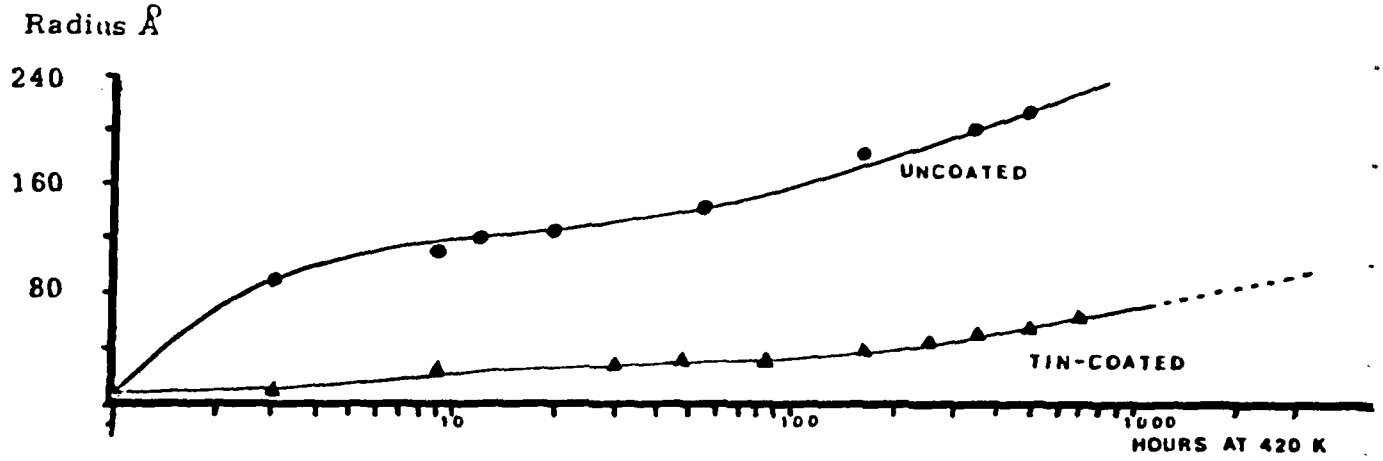

Figure(6.1) Tin stabilisation of iron particles in mercury

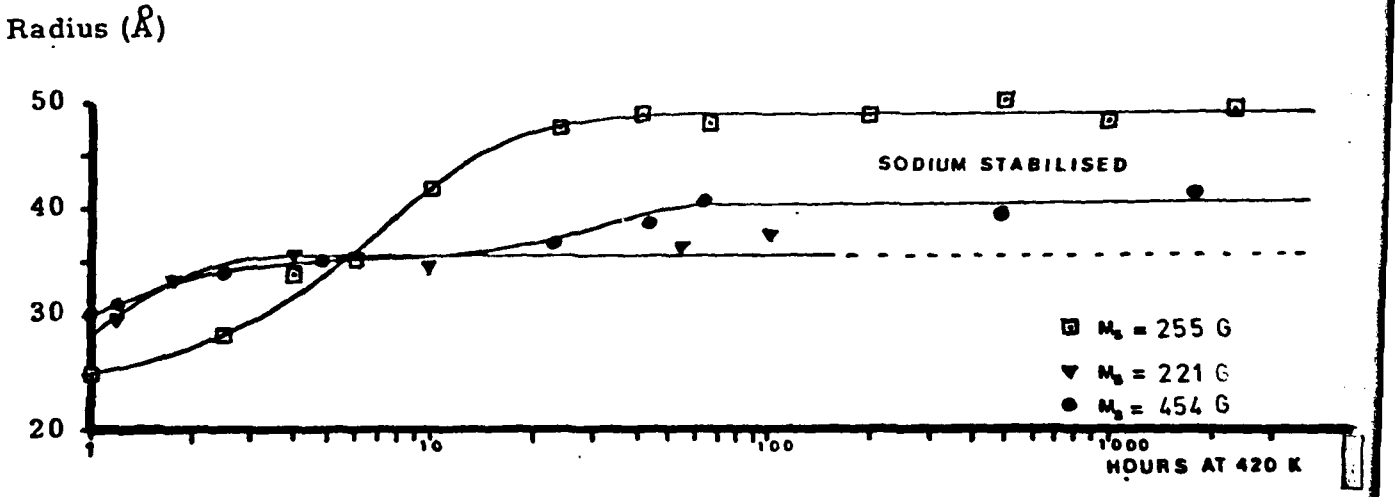

Figure(6.2) Sodium stabilisation of tin-coated iron particles in mercury

Figure(6.3)
Variation of saturation magnetisation with ageing time at 420°K for antimony coated iron particles.

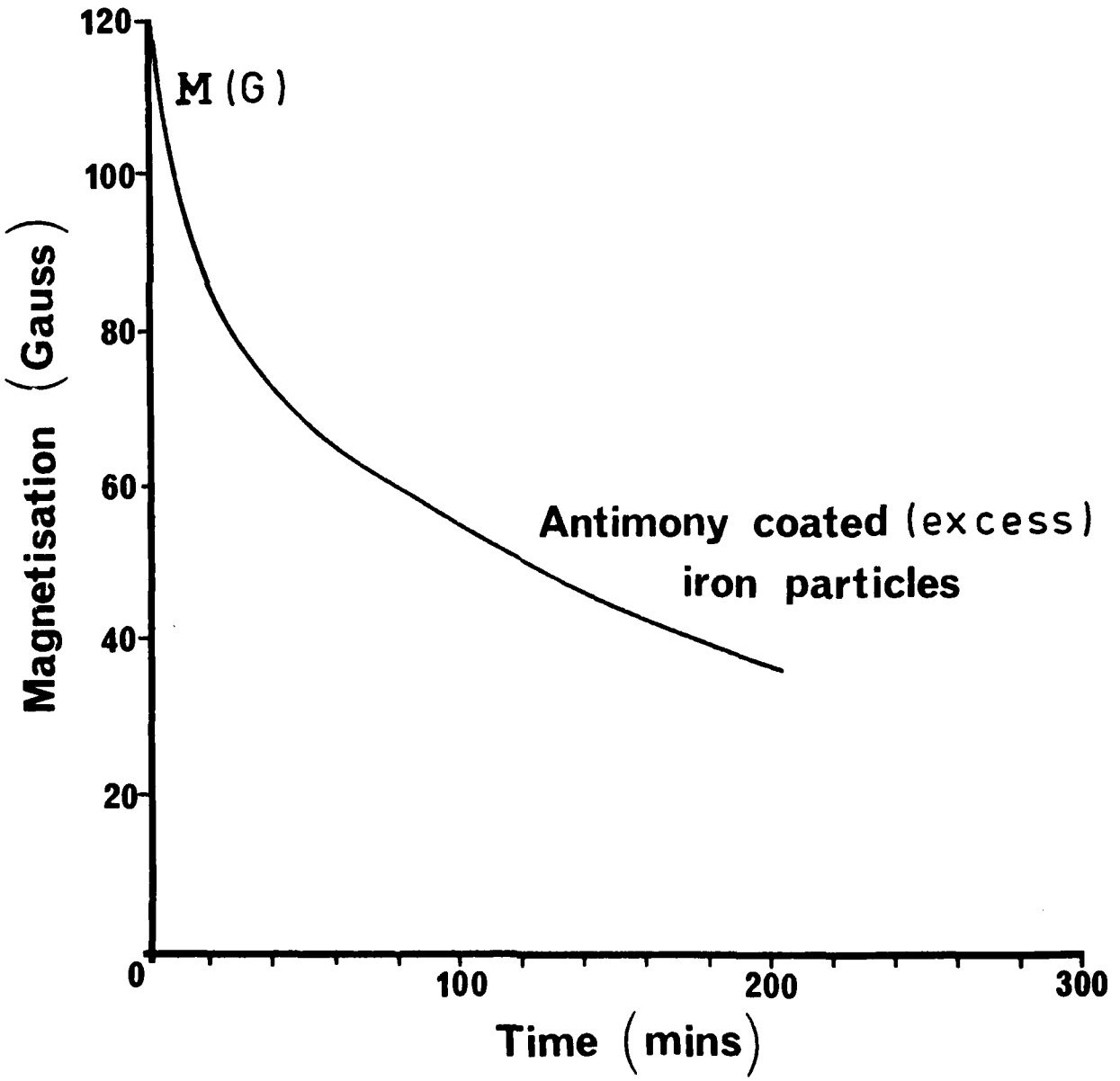

The high coercivity of the iron fluid after 10 minutes ageing indicates an initial increase in particle diameter to $\sim$ 250A, whereas the tin and antimony coated particles have not exceeded 45A diameter. The initial change in coercivity with ageing time is greater for the antimony coated particles than the tin coated ones. However, once the fluid has been aged for more than 15 hours, the antimony coated particles appear to be more stable.

Figure (6.5) shows the stabilising effect of adding different quantities of antimony to a liquid that initially contained 25A diameter particles. The quantities of antimony that were added were calculated on the basis of their being sufficient additive to stabilise 180A, 160A and 145A diameter particles. In practice it is seen that after 1000 hours of ageing at 420K the particles have diameters as inferred from the Luborsky curve of figure (5.11) of 90A, 70 and 60A respectively. Recalling that the smaller the particles the more coating material is required to stabilise them (see also equation (32)), then the disagreement between the expected and observed particle diameters, would seem to suggest that either (i) the particles have not yet reached their maximum diameter even after 1000 hours ageing, or (ii) the particles require significantly less than a monolayer coverage of antimony to stabilise them.

Resistivity and latent heat measurements have also been made on these iron-antimony-lead in mercury liquids and these confirm that whilst the antimony coats the iron particles the lead has no affinity for the particles and hence plays no stabilising role.

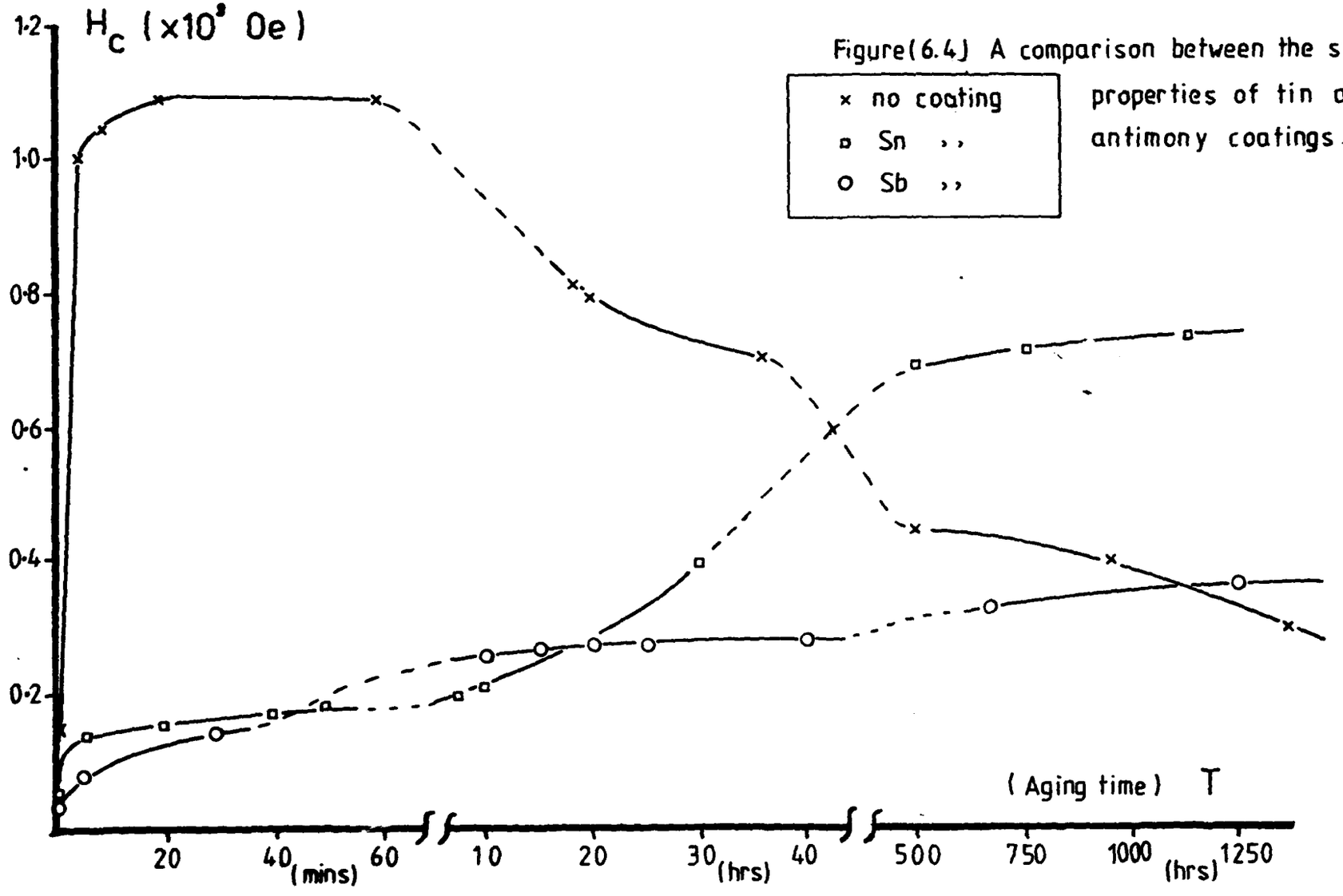

Figure(6.4) A comparison between the stablising properties of tin and antimony coatings.

Figure(6.5) The stabllisation of iron particles by antimony coatings.

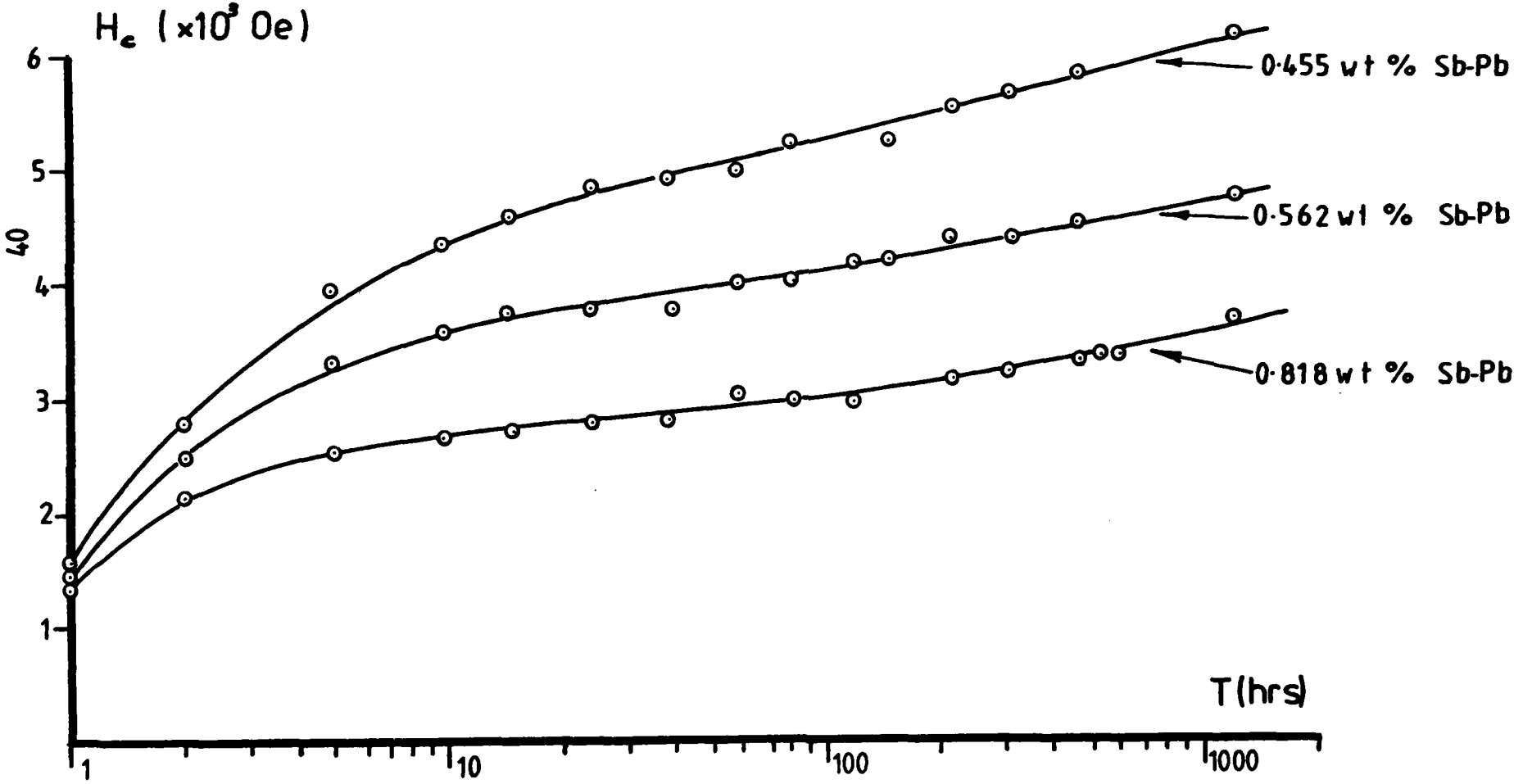

7. Stability in Fields

7.1 Gravitational Settling

The particles in a ferromagnetic liquid are not uniformly distributed in a gravitational field. At temperature T the number of particles per unit volume at a height h is given by the Boltzmann distribution

$$N = N_o \exp\left(-m^*gh/kT\right) \tag{24}$$

where $m^* = \frac{4}{3}\pi a^3 \rho^*$, $\rho^* = \rho_{Hg} - \rho_{particle}$ and a is the particle radius. The saturation magnetisation of the fluid is given by $I_s = I_s\phi$ for $\phi = N \frac{4}{3}\pi a^3$ where ϕ is the volume fraction of particles whose material has the bulk saturation value I_s.

Hence

$$I_s = I_s \tfrac{4}{3}\pi a^3 N_o \exp\left|-m^*gh/kT\right| \tag{25}$$

represents the saturation magnetisation as a function of height h for a column of single unaggregated ferromagnetic particles. This function is shown for several particle diameters in figure (7.1). However, equation (25) can never be perfectly obeyed by a concentrated ferromagnetic liquid for as $h \to 0$ finite particle packing requires that $I_s(h)/I_s < \phi_m I_s$ where ϕ_m is the maximum particle packing fraction possible, typically $\sim$0.5 for a stable fluid or $\sim$0.02 for an aggregated one. Further, no long term settling is expected if $m^*gh < kT$ and no rapid settling is expected unless $m^*gh \gg kT$, the latter corresponding to aggregates of iron particles in mercury in excess of 10^4A diameter.

Figure (7.2) shows the settling observed in a tin coated fluid which according to magnetic analysis contained 60A median diameter particles. (It should be understood that as $\rho_{Hg} > \rho_{Fe}$ "settling" represents an upward particle motion). Such rapid settling is unexpected unless particle aggregates are present. The size of these aggregates may be estimated from the velocity of the lower edge of the settling curves if it is assumed that this is determined entirely by the Stokes drag force on the aggregate. If it is also assumed that the particles are arranged as close packed spheres, that is the aggregate density is approximately equal to that of iron (i.e. there is no entrained mercury within it), then the aggregate diameter D_{agg} is given by

$$D_{agg} = \left(18\,\eta\,(dh/dt)/gp^*\right)^{\frac{1}{2}} \tag{26}$$

$$\sim 10^{-4}\text{cm}$$

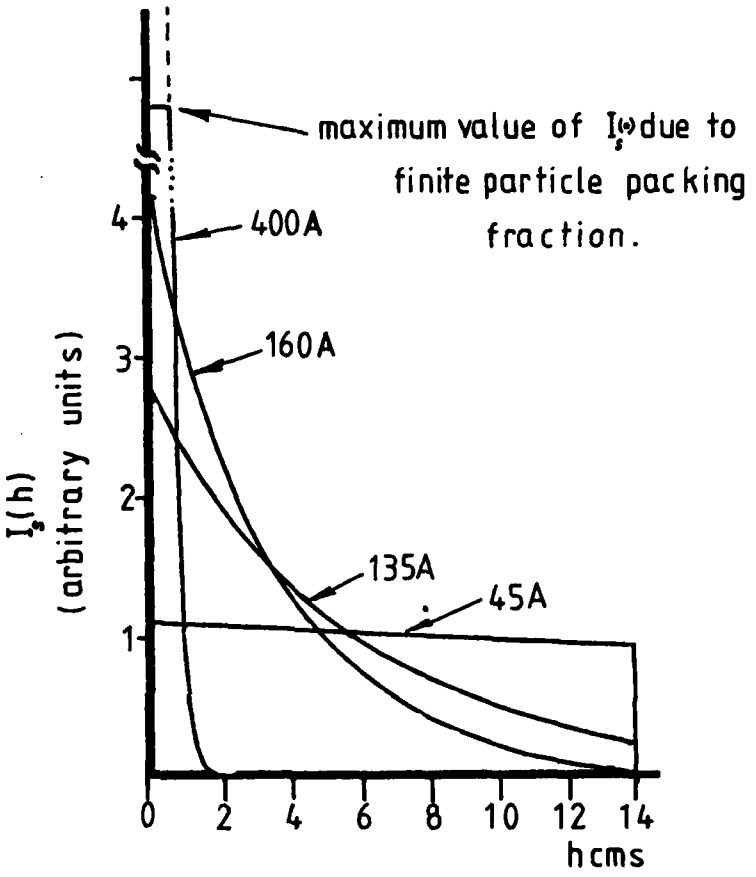

Figure (7.1)

Boltzmann distribution (normalised) of iron-particles-in-mercury, in a 14cm column.

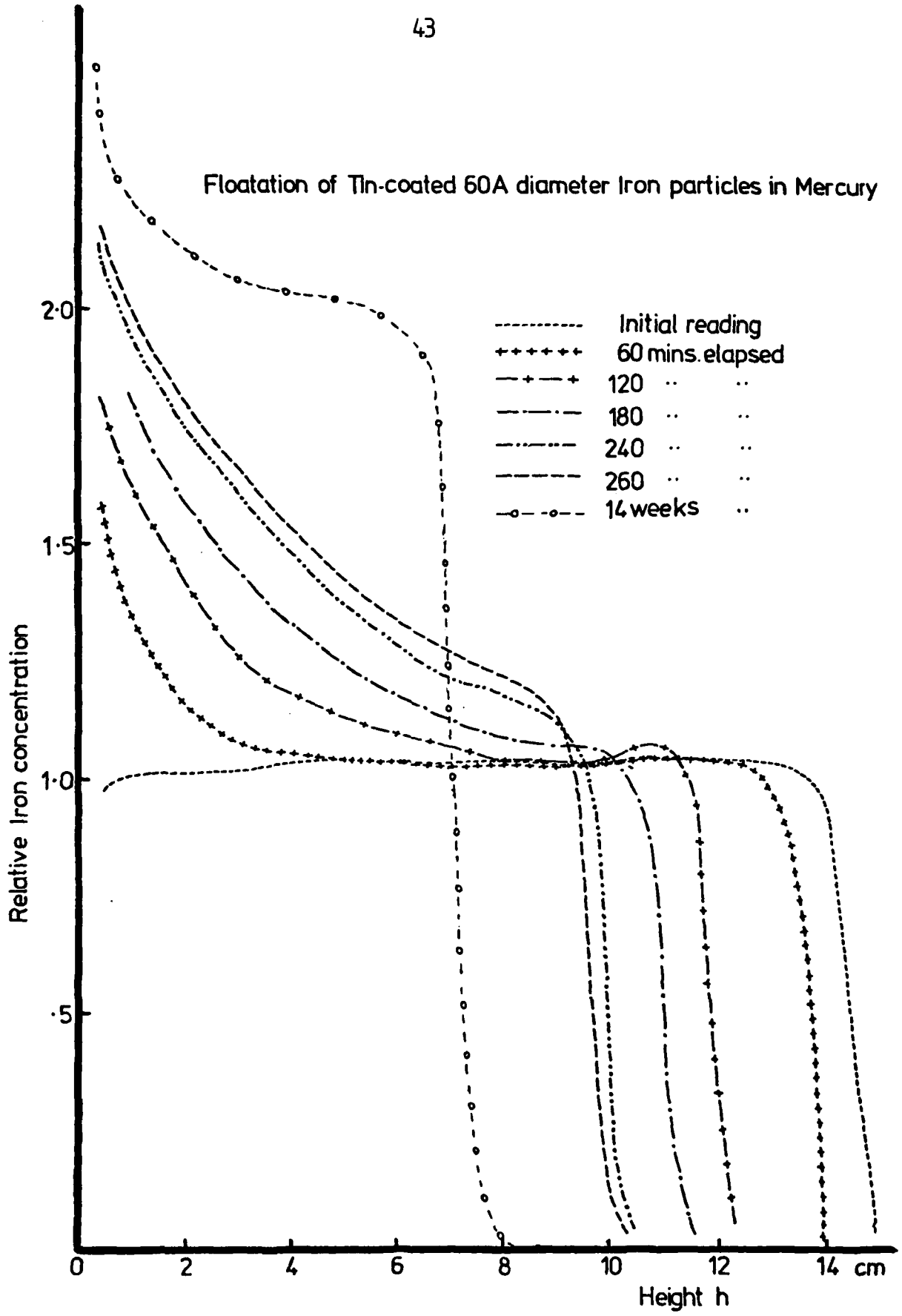

Figure (7.2) shows the relative iron particle concentration in a 15 cm column of mercury as a function of height and time.

As in practice $\rho_{Fe} < \rho_{agg} < \rho_{Hg}$ the above figure represents a lower limit for the aggregate diameter. It is possible to estimate an upper limit from the observation that it was found impossible to subsequently concentrate this fluid to more than $\sim$ 3 vol % Fe. If this concentration corresponds to cubic close packing of the aggregates (ie $\sim$ 50 vol %), then the maximum volume fraction of mercury entrained within the aggregate must be given by $(0.5 - 0.03)/0.5 \sim 0.94$. Thus as

$$\rho_{agg} = (m_{Fe} + m_{Hg})/V_{agg} \quad \text{where m and V refer to mass and volume respectively,}$$

$$= \rho_{Fe}\rho_{Fe} + \rho_{Hg}\rho_{Hg}$$

$$= \rho_{Hg} + \rho_{Fe}(\rho_{Fe} - \rho_{Hg}) \qquad (27)$$

$$\sim 13.20 \text{ grm cm}^{-3}$$

and so $D_{agg}(max) \sim 4 \times 10^{-4}$cm, from which it follows that $1 \times 10^{-4} < D_{agg} < 10^{-4}$ cm, showing that the particle settling rate is not particularly dependent upon aggregate density. If however the aggregate is permeable to the mercury a faster settling time would result as the effective density would be lower, due to the absence of entrained mercury, and the lower hydrodynamic drag. In addition any large departures of the aggregate from sphericity would also decrease the settling time and thus decrease the estimate of aggregate size.

Figures (7.3), (7.4) and (7.5) show the results of gravitational stability measurements made at room temperature for (i) iron particles in mercury, (ii) tin coated iron particles in mercury and (iii) iron particles in lead-antimony mercury alloy. These three ferromagnetic liquids were made from aliquot samples of a liquid prepared by the electrodeposition of saturated ferrous sulphate solution. The "as prepared" liquid was found to contain iron particles, of median diameter D_V = 30A and σ_{SD} = 0.6, to a concentration of 0.21 wt %. To two of these aliquot samples was added antimony in the form of antimony-lead alloy or tin metal sufficient in quantity to form only a monolayer on the iron particles. The three liquids were all observed to have a low coercivity of 250C at 77K, confirming the small particle size.

The tin-iron system is shown to be the most stable as the concentration changes little in a gravitational field even after six days. In contrast iron particles in the antimony-lead system in mercury is more seriously affected by the same gravitational field in the same period of time. The effect of a gravitational field on the concentration of uncoated iron paticles is very serious. This indicates that antimony although effectively preventing growth of the particles is not preventing aggregation as effectively as tin. From the initial sedimentation rate is appears that the aggregate diameter in the uncoated iron and

Figure(7.3) Gravitational stability of iron particles.

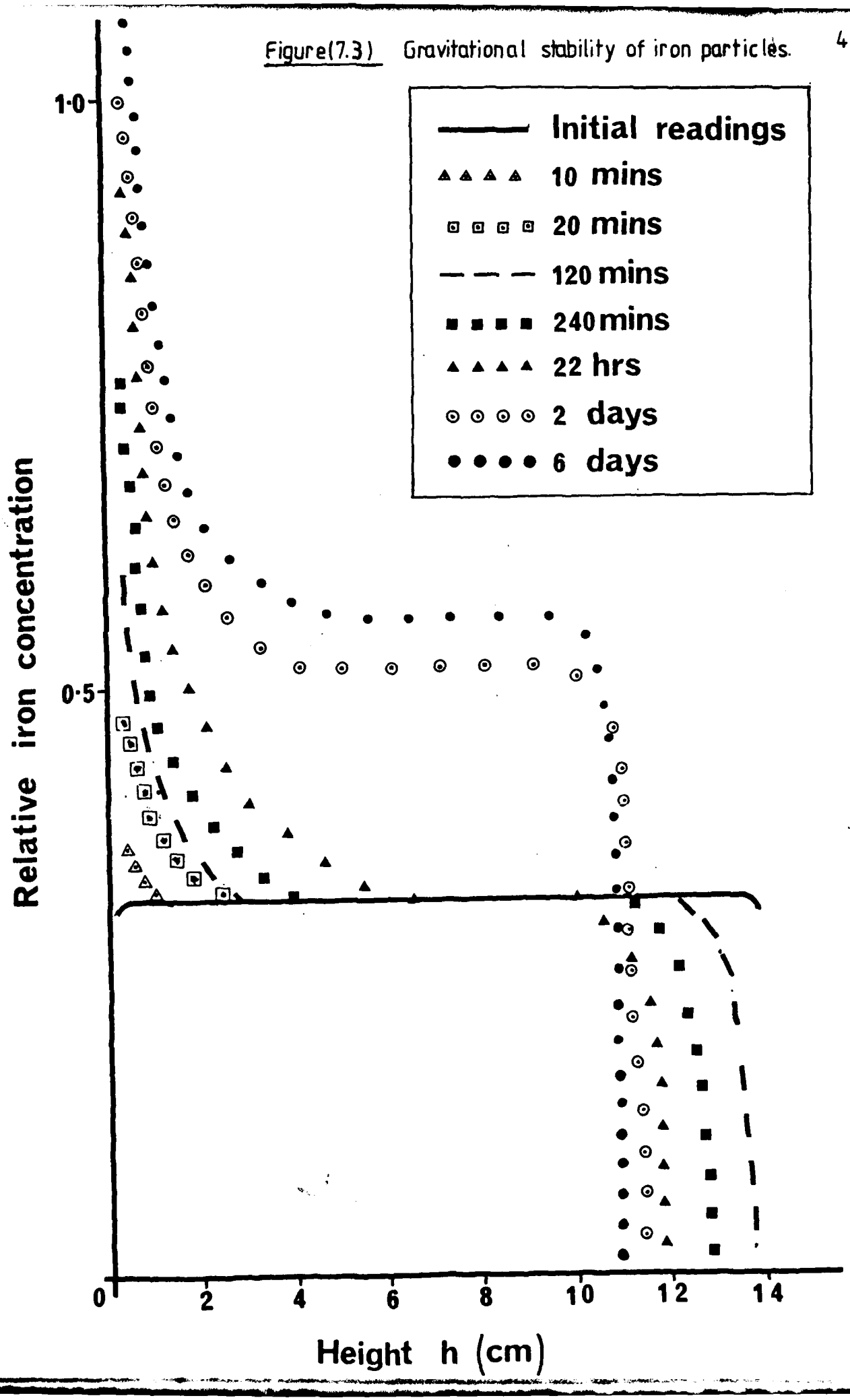

Figure (7.4)

Gravitational stability of tin coated iron particles

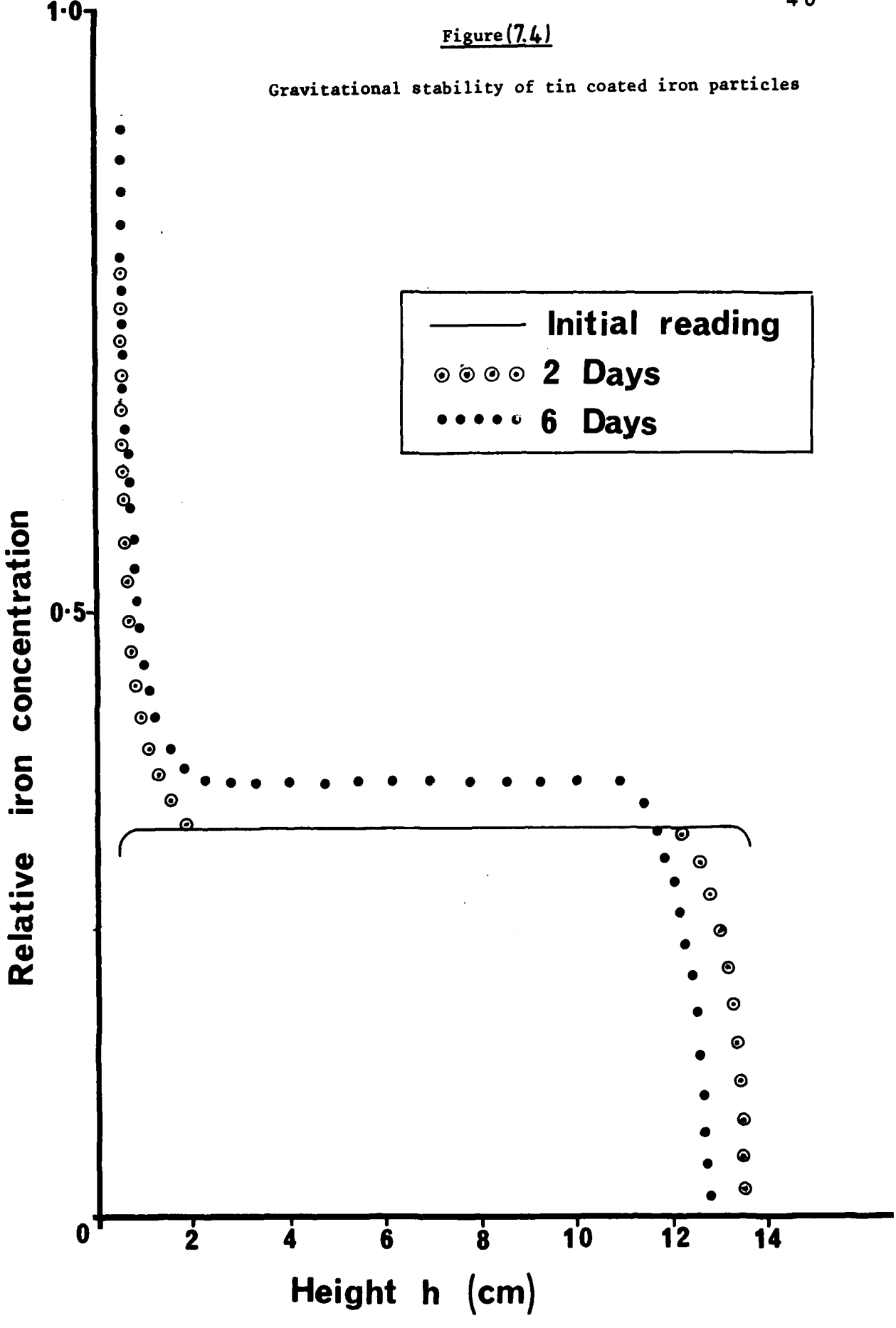

Figure (7.5)

Gravitational stability of antimony coated particles.

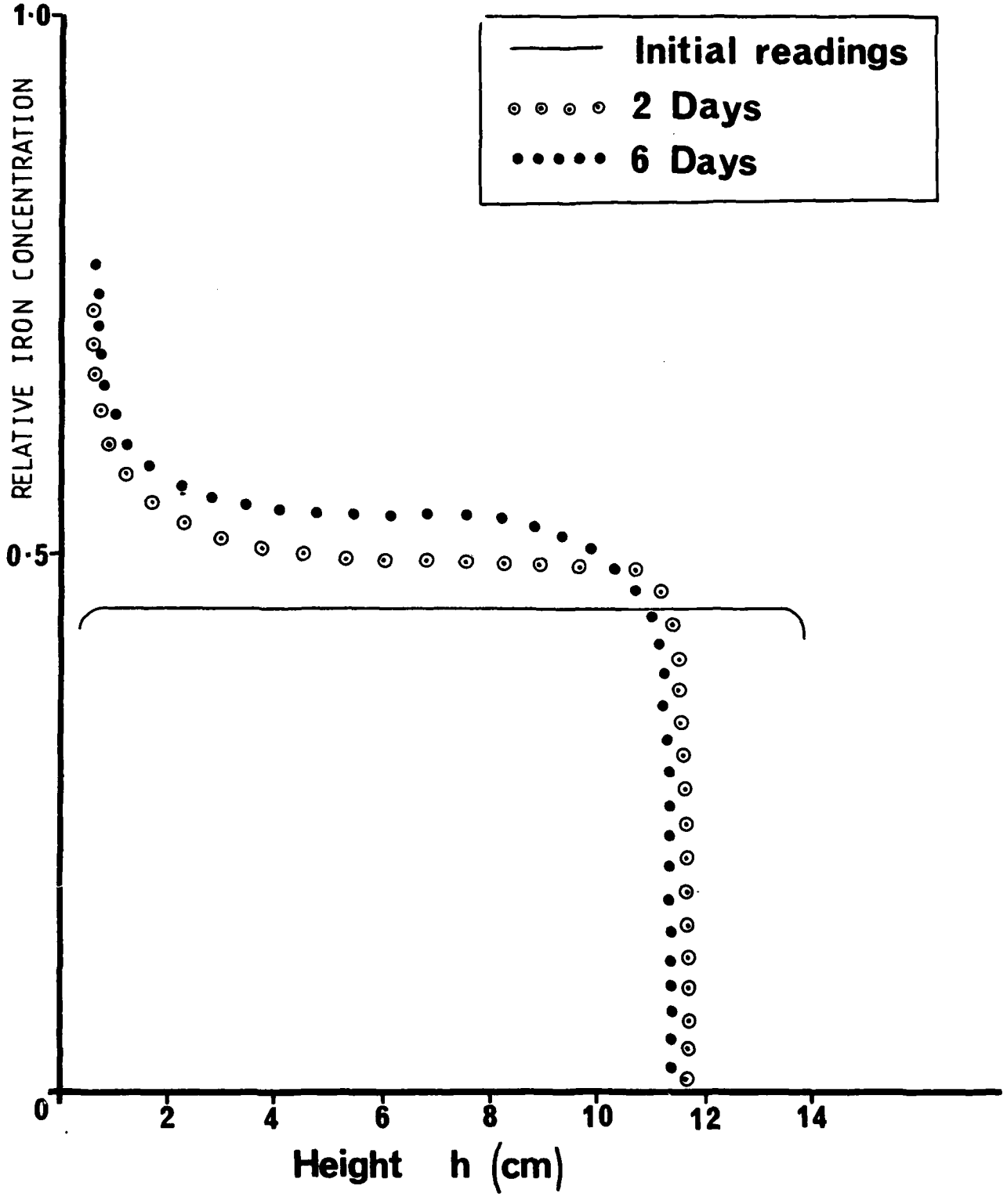

antimony coated liquids is $\sim 10^4$A whereas in the tin coated liquids it is $\sim 10^3$A. After settling has proceeded for more than one day the sedimentation rate decreases, presumably due to the increase in aggregate density causing hindering of their motion.

7.2 Stability in magnetic field gradients

The occurrence of large particle aggregates would also explain the extremely rapid motion of the magnetic fraction that is observed when mercury ferromagnetic liquids are placed in large field gradients. The fluids are observed to separate in a matter of seconds, corresponding to particle velocities of between 1 and 10 cm s^{-1}, in fields of 3.5 kG upon which is superimposed a field gradient 1.4 kG cm^{-1}.

Equation (13) which relates the terminal velocity u of a particle to its diameter D and ∇H cannot be used directly for aggregates as not all of their volume is magnetic. Thus the Stokes force must be written as

$$F_s = 3\pi D_{agg} \eta u \tag{28}$$

and the magnetic force assuming all the particles in an aggregate to be aligned in the same direction, a reasonable assumption in the 3.5 kG field used here,

$$F_m = \mu \nabla H \tag{29}$$

$$= \phi\pi/6 \; D_{agg} \; I_s \; \nabla H \tag{30}$$

Equating F_s and F_m results in

$$D_{agg} = \left(\frac{18 \eta u}{I_s \nabla H \phi} \right)^{\frac{1}{2}} \tag{31}$$

Setting I_s = 1707 emu cm^{-3}, ∇H = 1.4k G cm^{-1}, $\phi \sim 0.06$ and $\eta \sim$ 1cp implies $D_{agg} \sim 10^{-3}$ to 10^{-4}cm, for u $\sim$ 1 and 10 cm s^{-1} respectively. These values of D_{agg} are about a factor 10 higher than that estimated from the gravitational settling experiments and implies, as expected, that high magnetic field gradients promote aggregation in iron-mercury fluids.

8. The Resistivity of Iron Particle in Mercury Liquids

The fluids described in this section have all been prepared in the usual manner by electrodeposition, and their electrical resistivity measured between 77K and 300K using a conventional four probe method with current reversal.

The lower curve of figure (8.1) shows the effect on the resistivity of adding free tin to pure mercury, at room temperature. A simple linear depression of the fluid resistivity with tin concentration is observed provided that the tin concentration remains less than 0.6 wt % (the saturation limit). Above this concentration there is a sharp increase in the resistivity.

The upper curve of figure (8.1) shows a similar resistivity plot for a fluid containing 0.1 wt % iron particles coated with tin. The solubility of iron in mercury is negligible ($< 10^{-7}$ wt % at room temperature); the iron being present as 40A diameter particles. The initial preparation contained sufficient tin to form a monolayer coating around the iron particles (0.04 wt % Sn). Tin added in excess of this forms a solution with the mercury, reducing the resistivity until the excess solubility limit is reached.

In figure (8.2) the resistivity of a 0.8 wt % iron in mercury fluid is shown. This fluid contains more iron particles than the 0.1 wt % Fe fluid and thus explains how it is possible to add 1.2 wt % tin before saturating the fluid. By comparison with figure 8.1 it is obvious that 0.6 wt % of this tin is residing on the particles and in addition the characteristic behaviour of the 0.6 wt % Sn in pure Hg system is here observed displaced by approximately 0.6 wt %. The maximum and point of inflection in the resistivity occurs at tin concentrations consistent with the adsorption of one and two monolayers respectively. This may be shown by considering an equation adapted from one given by Luborsky (15) equating the mass of tin m_{Sn} adsorbed in the form of monolayers by iron particles and mass m_{Fe} and radius a such that

$$m_{Sn} = m_{Fe} \sqrt{3}\, A_{Sn}^{\frac{1}{3}} (2\, w_{Sn})^{\frac{2}{3}} (N^{\frac{1}{3}}\, w_{Fe}\, a)^{-1} \qquad (32)$$

where w_{Sn} and w_{Fe} represent the densities of tin and iron respectively and A denotes the atomic weight and N is Avogadro's number.

A value of m_{Sn}, obtained from the resistivity maxima in figure (8.2), is substituted into equation (8.1). This yields a value of 40A for the particle diameter as compared with 35A determined from measurements of the coercivity at 77K on the same sample. This agreement lends support to assumptions that the resistivity maxima corresponds to the adsorption of a monolayer of tin.

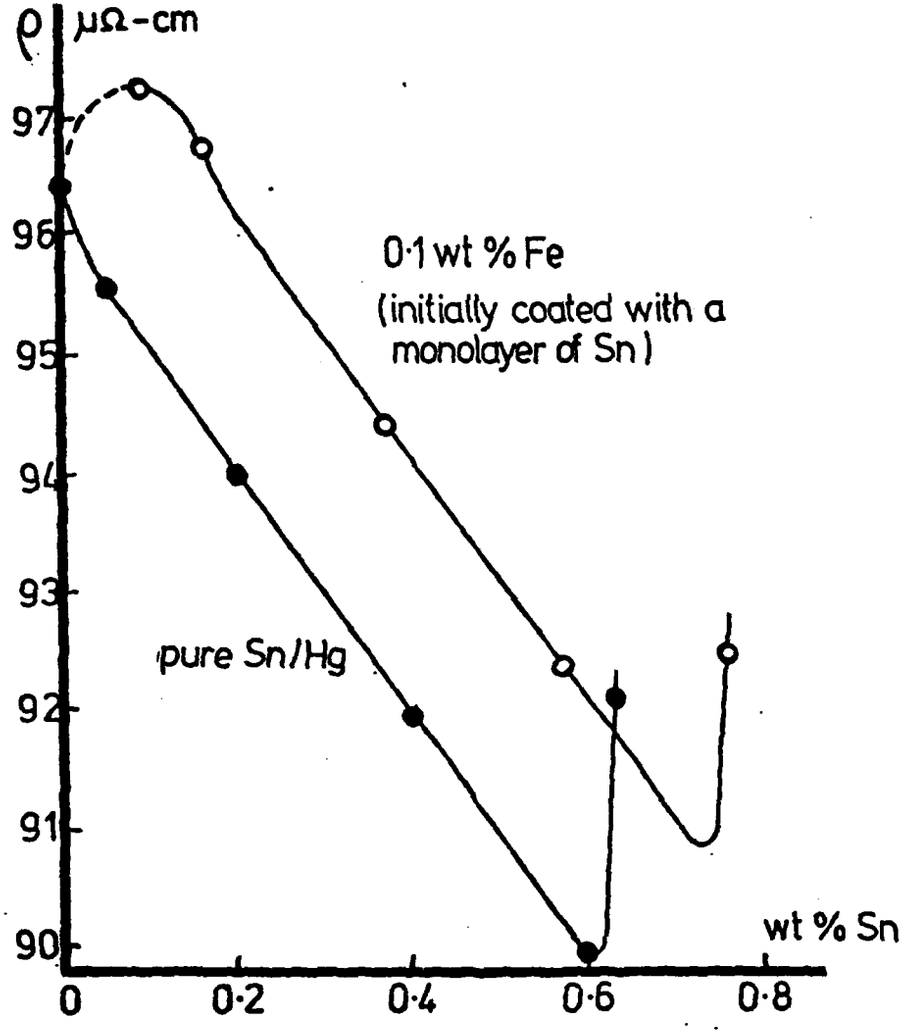

Figure (8.1) shows the depression in the resistivity of pure mercury and of a fluid initially coated with a monolayer of tin, when excess tin has been added.

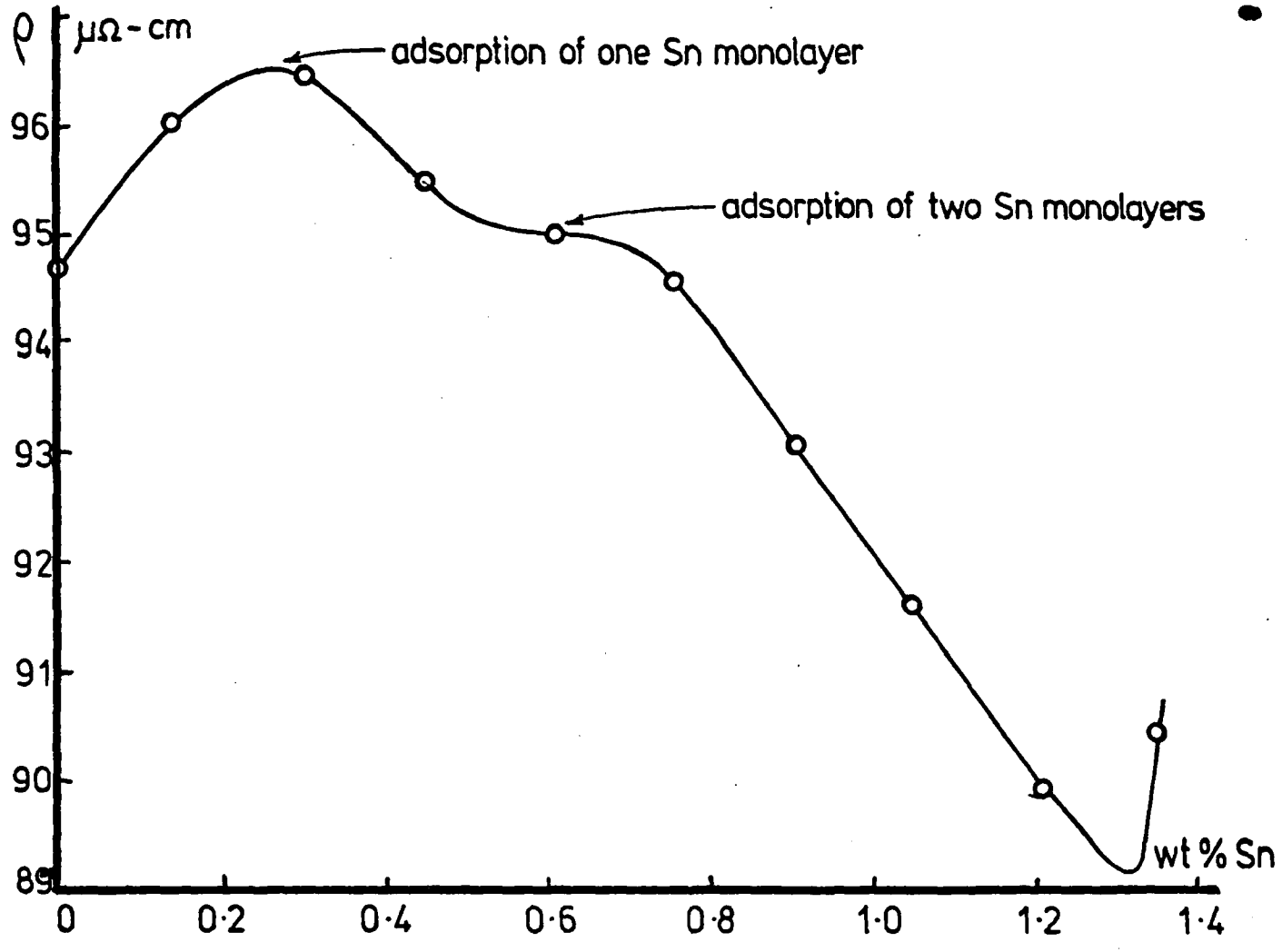

Figure (8.2) shows the variation in resistivity of an initially uncoated iron particle in mercury fluid, as tin has been added.

When a quantity of tin sufficient to exceed monolayer saturation is added to an iron-mercury system, tim dependent resistivity is observed. Initially upon addition of the excess tin, the resistivity is depressed, as the tin remains free in the mercury. But as time progresses the tin precipitates out onto the iron particles and multilayers of tin will form. The characteristic time constant for this reaction depends upon (i) the difference between the heat of solution of tin in mercury and the heat of formation of a tin multilayer (ii) the ratio of the total quantity of excess tin added to the total particles surface area of the system, and (iii) the distance across which the tin atoms must diffuse; i.e. the inter-particle distance. Such behaviour is shown in figure (8.4) for a variety of iron particle and tin concentrations.

Figure (8.5) shows a similar plot for a tin coated system to which sodium has been added to improve the long-term stability of the fluid (see Popplewell et al (1)). Again association of the sodium to the tin coated iron surface is inferred from the behaviour of the resistivity. Small quantities of sodium added to mercury increase its resistivity, but not by as much as when similar quantities are added to mercury containing tin coated iron particles.

It is pertinent to discuss here some magnetic concentration experiments. Iron particle fluids to which sufficient tin has been added to form a monolayer have been magnetically concentrated. The residual non-magnetic phase has been shown to consist entirely of mercury, by measurements of its resistivity and chemical analysis. The same experiment performed with sodium in place of tin does not show similar results. The sodium resides on both the particle surface and in the mercury. This is inferred from chemical analysis, since if a quantity of sodium is added to iron in mercury then the quantity added in excess of that required to form a monolayer may be extracted by shaking with dilute hydrochloric acid.

That there should exist an equilibrium between iron coverage and sodium in solution may be understood from the heats of formation of iron-sodium inter-metallic compounds and mercury-sodium alloys; the heats of formation being almost identical and strongly exothermic. In comparison the tin-iron reaction is exothermic, and the mercury-tin endothermic. Thus the former is energetically preferred (see Smithells (17)). The direct interpretation of the resistivity of systems containing sodium is complicated because of the sodium's spacial distribution.

Figure (8.6) shows the typical plot of change in the resistivity upon dilution for (a) an as-prepared fluid, and (b) the same fluid after reconcentration in a magnetic field gradient of 1.5 kG. No satisfactory explanation for the shape of these curves has been proposed. However, as it was demonstrated in section (5.3) that the exposure of an iron-mercury liquid to a high magnetic field gradient causes irreversible changes in the magnetic properties then it is likely that the change in resistivity is related to irreversible particle chaining of aggregation. Indeed subsequent reconcentration in the same field gradient imparts no further resistivity changes to the fluid.

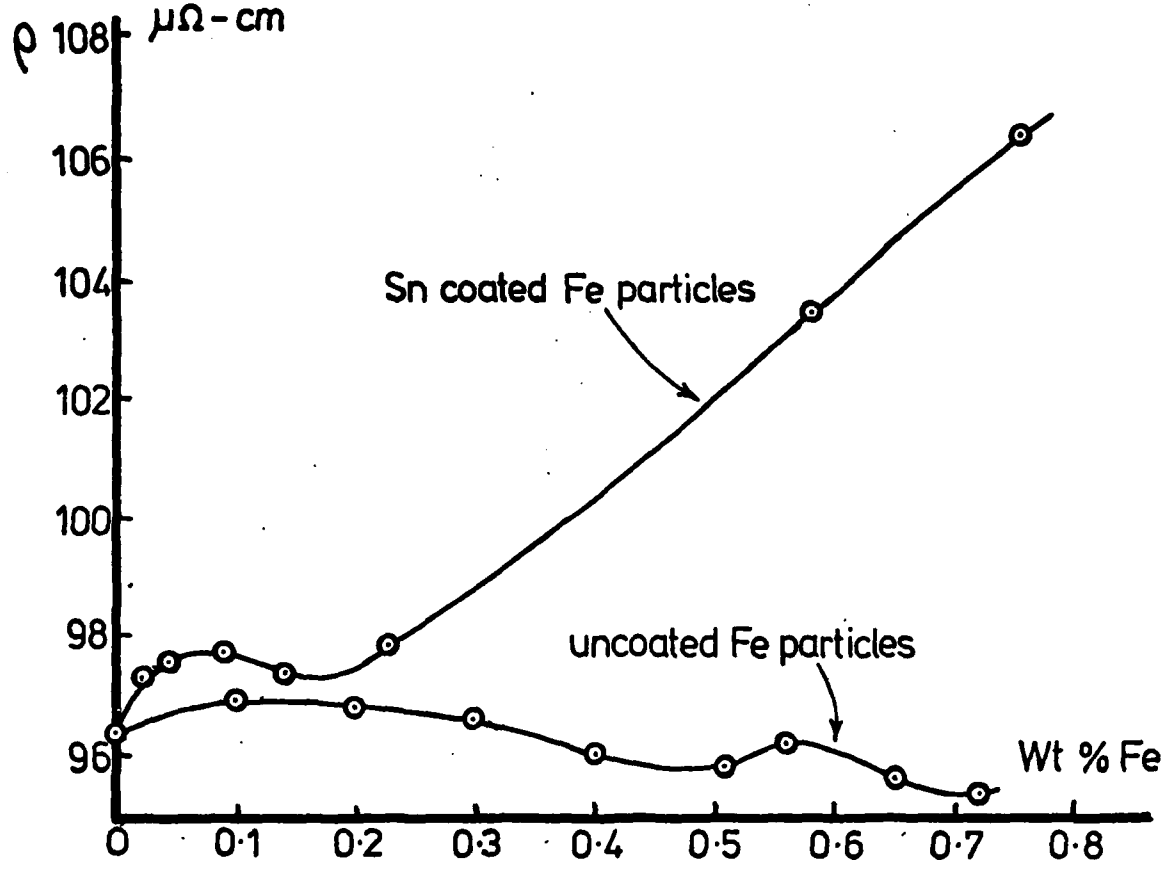

Figure (8.3) shows the variation of the resistivity for uncoated and tin-coated iron particles as the iron particle concentration is increased.

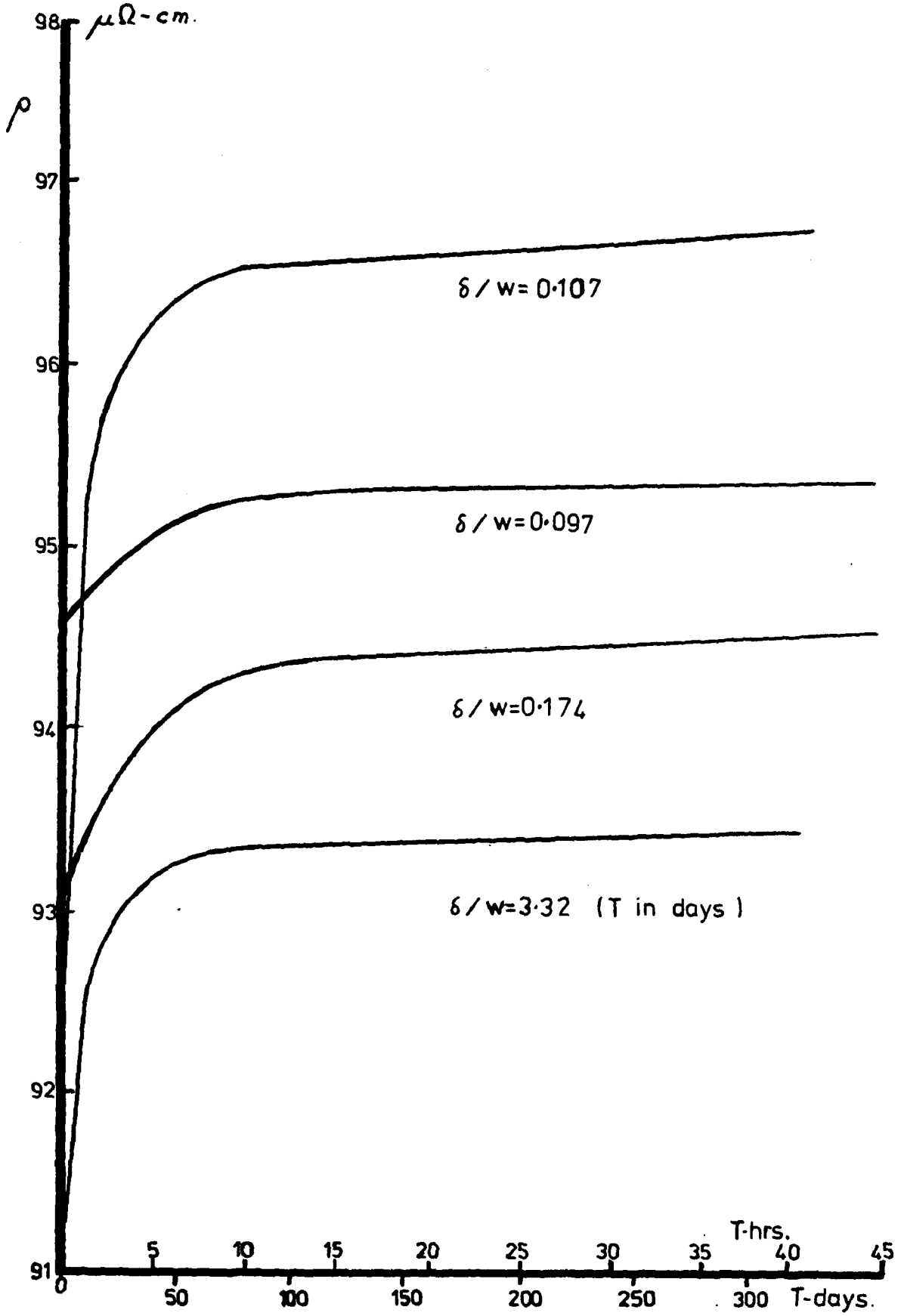

Figure (8.4) shows the time dependent resistivity observed for tin-coated iron particles, of weight % w; where excess tin, of weight % δ, has been added to the fluids at t = 0.

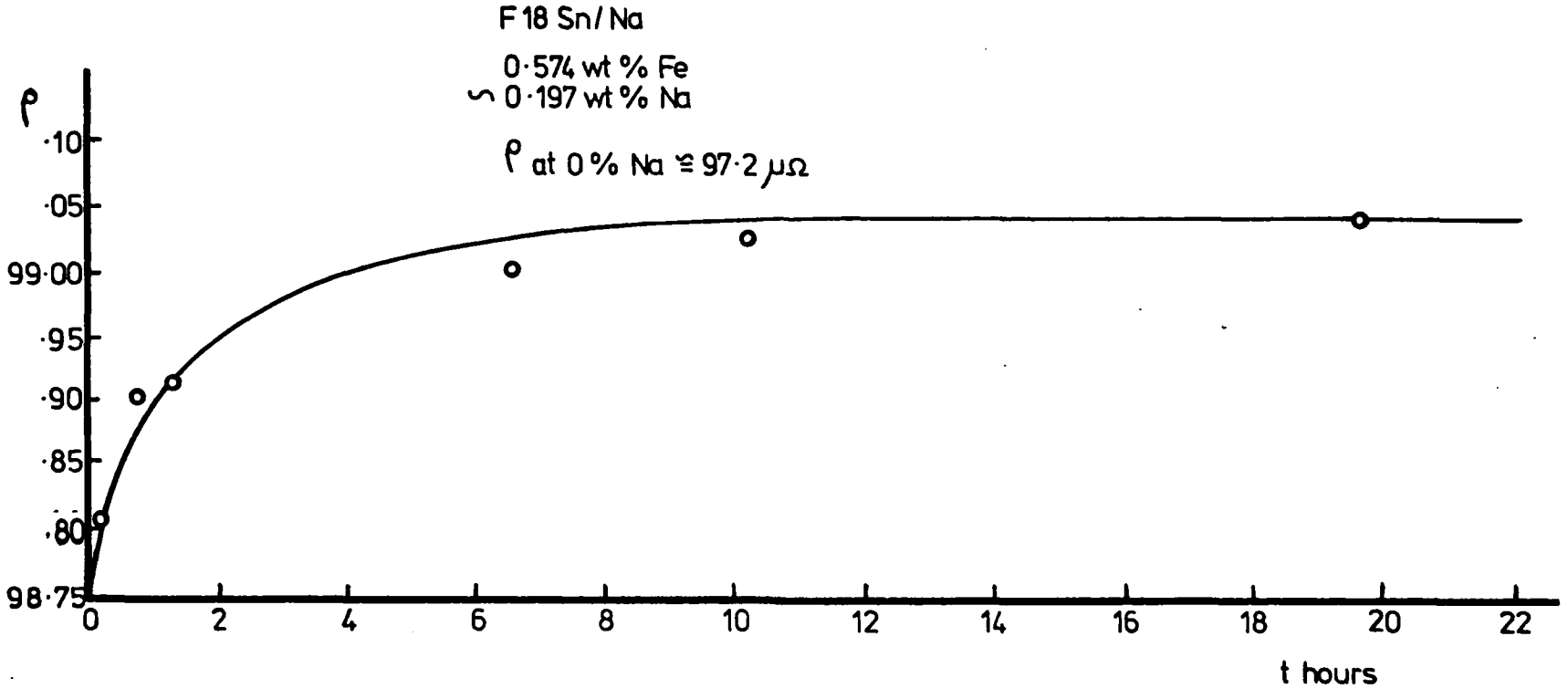

Figure (8.5) shows the time dependent variation in the resistivity of a tin coated iron particle fluid to which sodium has been added at t = 0.

Resistivity of 30A diameter particles of Iron in Mercury

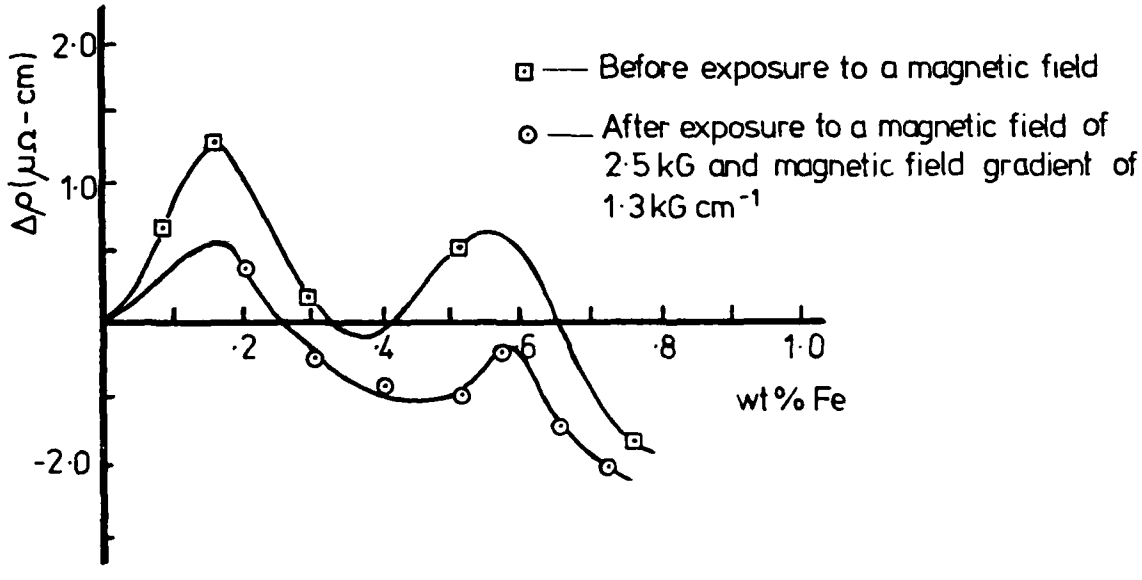

Figure (8.6) shows the variation in the resistivity for an iron particle in mercury fluid as the concentration is decreased (i) before exposure to a magnetic field and (ii) after reconcentration in a magnetic field gradient.

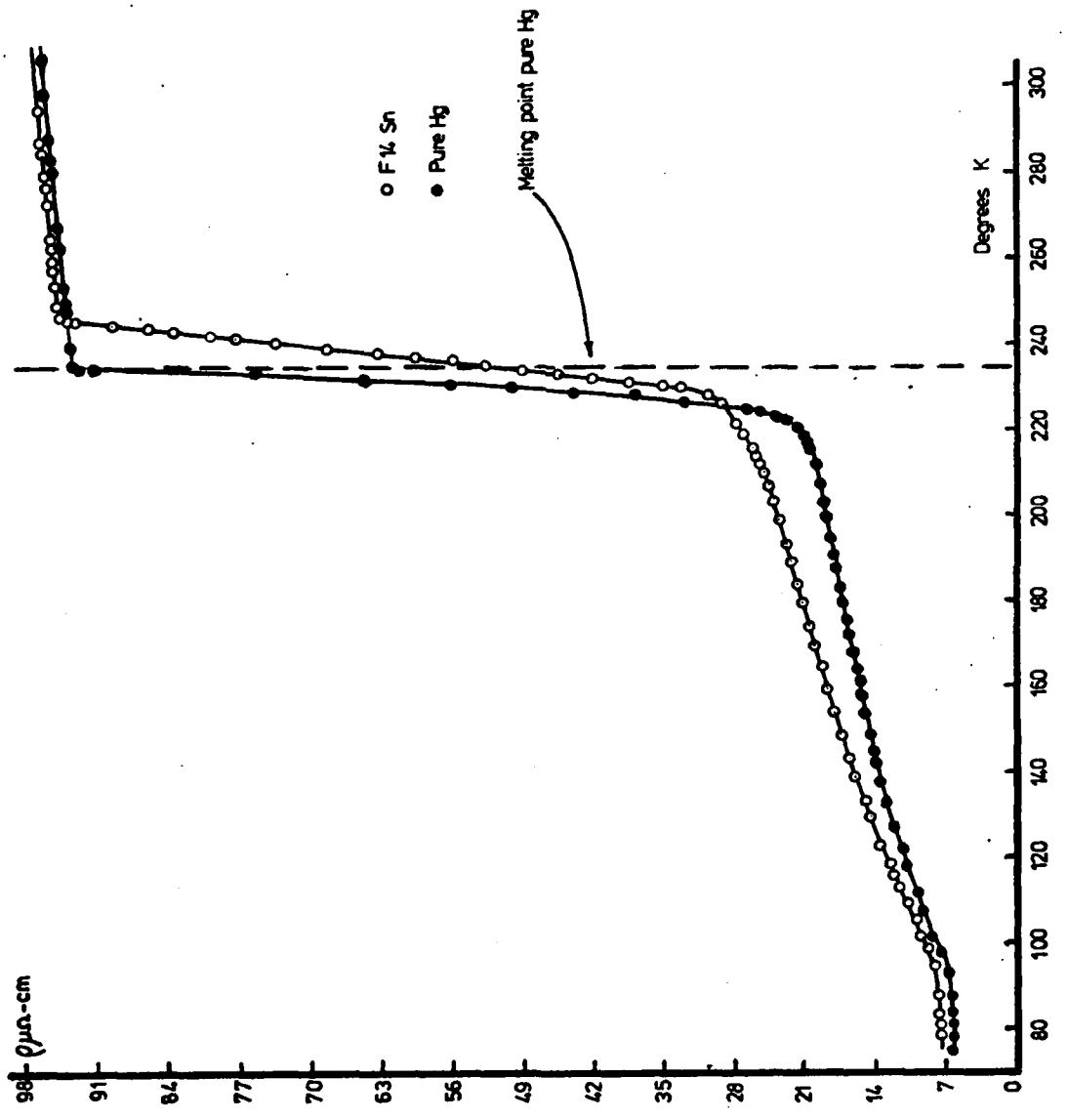

Figure (8.7) shows the variation in the resistivity of a tin-coated iron particle fluid in mercury and pure mercury as a function of temperature.

Figure (8.7) shows the resistivity behaviour of a tin coated iron fluid and pure mercury under identical experimental conditions as a function of temperature. Figure (8.8) shows the difference in the resistivities of the two samples as a function of temperature. The presence of impurities, in the form of iron particles, in the solid crystalline mercury is expected to have a greater influence upon the resistivity than the same concentration of iron particles would have on the resistivity of the less ordered liquid mercury. The approach to the melting point in mercury is accompanied by a rapid change in the resistivity. The resistivity of the iron-tin mercury system as it approaches the melting point is accompanied by a more gradual change in ρ. This is most probably due to a combination of pre-melting (see latent heat results) and effects associated with bound mercury.

Figure (8.9) shows the results of a comparative study of the resistivity of lead-mercury (Pb-Hg) antimony-lead-mercury (Sb-Pb-Hg), iron-lead-mercury (Fe-Pb-Hg) and iron-antimony-lead-mercury (Fe-Sb-Pb-Hg) systems carried out to determine whether or not antimony and lead coat the iron particles.

It is seen that Pb in Hg (curve (i)) depresses the resistivity up to the point where the solubility limit of Pb $\sim$ 1.3 wt % is exceeded in a similar manner to that of tin in mercury in figure (8.1). If Pb is added to a fluid already containing iron in mercury (0.58 wt % 23A particles), for which it is seen $\rho_{Fe-Hg} < \rho_{Hg}$, then the behaviour of curve (ii) is very similar to that of curve (i), demonstrating that the lead resides in solution rather than coats the particles. When the eutectic Sb-Pb is dispersed in mercury, curve (iii), the lead goes in to solution depressing the resistivity but the insoluble antimony exists as fine particles which increase the electron scattering in a manner similar to excess tin and lead in mercury. If however the Sb-Pb alloy is added to an iron-mercury fluid (curve (iv)) of the same concentration as in the iron-mercury fluid depicted in curve (ii), the behaviour of the resistivity is the same as if only the lead was in solution and thus the antimony must form a coating on the particles.

Figure (8.10) shows the variation in fluid resistivity for antimony coated and uncoated iron particles of 30A diameter in the concentration range 0 to 1.36 wt % iron. Because lead is also present in the antimony coated system the resistivity is depressed below that of the iron-mercury fluid. The upper curve shows an interpolated plot where the effect of the lead in solution has been substracted off.

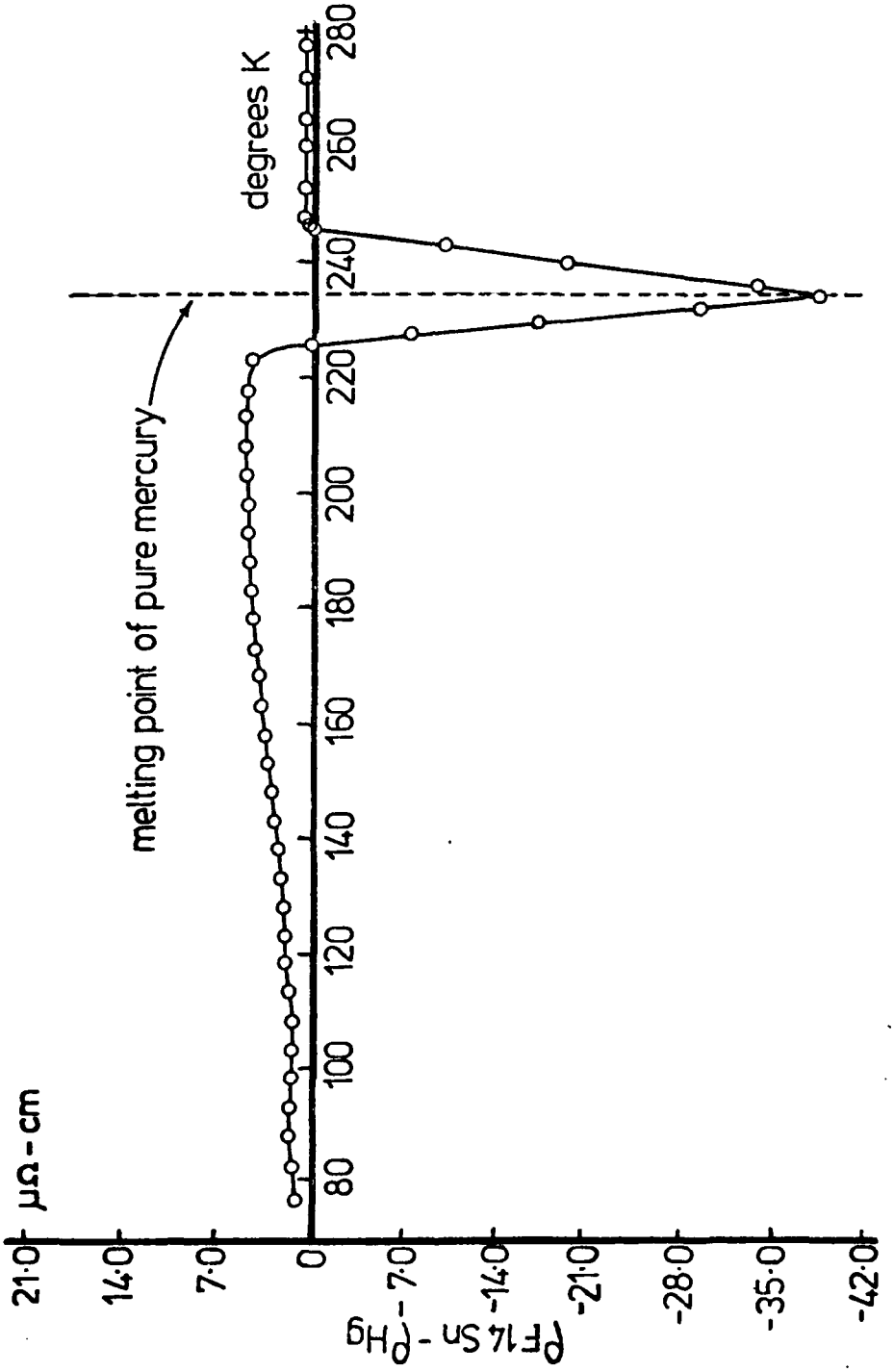

Figure (8.8) shows the difference in the resistivities of a tin-coated iron particle in mercury fluid and pure mercury at the same temperature.

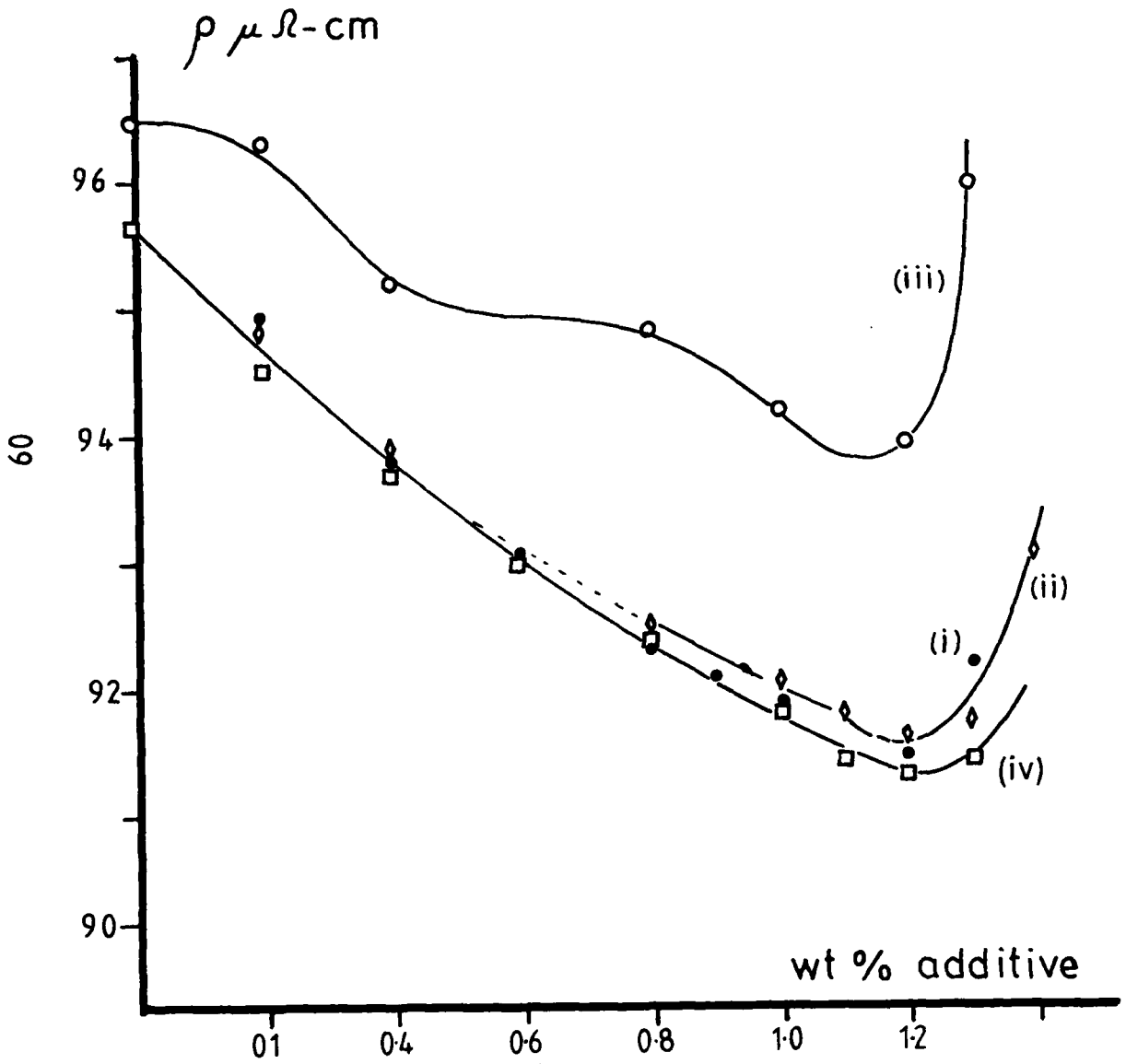

Figure (8.9)

- ● Hg-Pb
- ○ Hg-Pb-Sb
- ◊ (0·58 wt % Fe)+ Hg-Pb
- □ (,, ,, ,,)+ Hg-Pb-Sb

The variation in the resistivity of antimony-lead additive liquids.

Figure (8.10) The resistivity of uncoated and antimony coated iron particles in mercury.

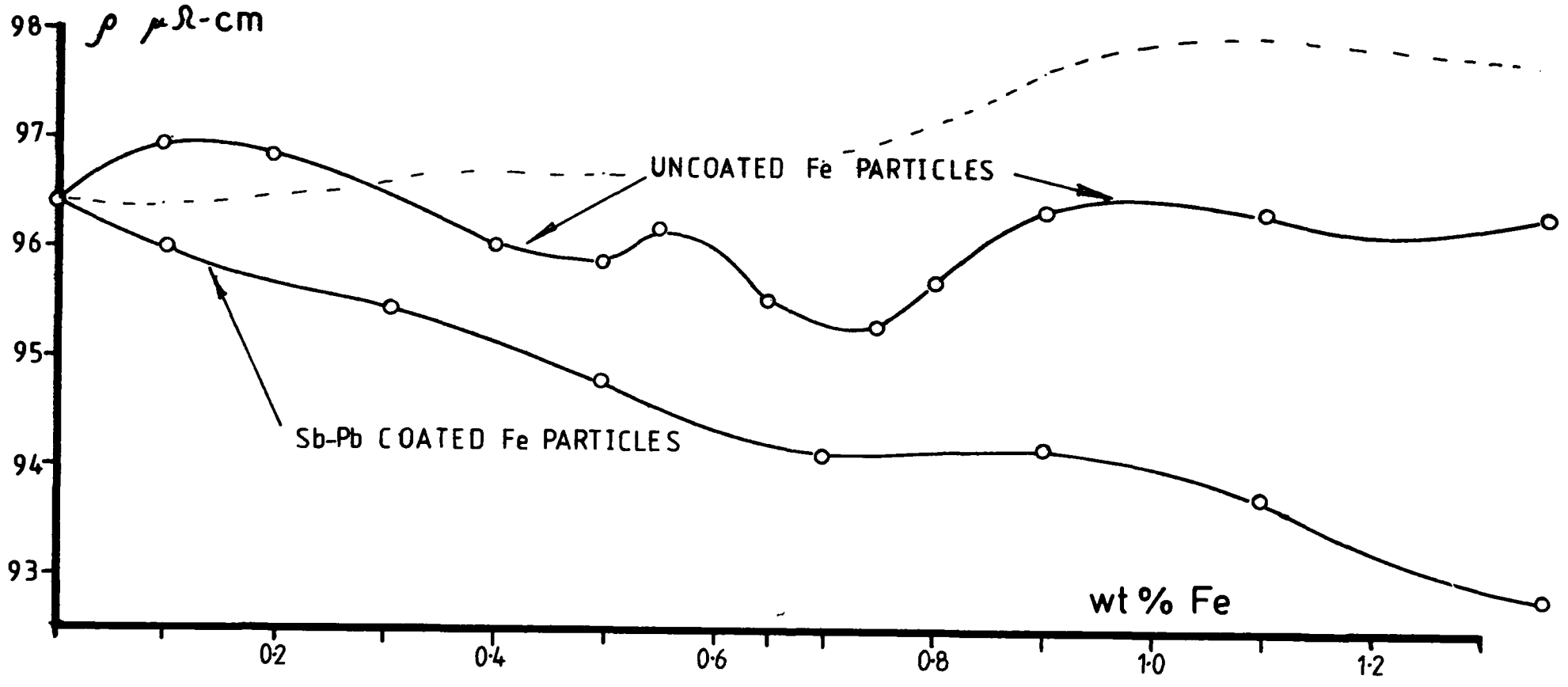

9. Viscosity Measurements

The most striking feature of the viscosity of ferromagnetic liquids containing iron particles is the transition from a viscosity (η), characteristic of a liquid, to a paste like high viscosity as the concentration is increased beyond a critical value. This behaviour is indicated in figure (9.1). In the limit as the shear rate tends to zero, the liquid-paste transition occurs around 1 wt % iron for $D_{H_c} \sim 40A$. This is equivalent to a particle volume fraction ϕ of ~ 0.02. This transition is not expected at such low concentrations if the iron particles are unaggregated. Figures (9.2) and (9.3) show that the liquids exhibit only thinning. A characteristic yield stress, S_B below which elastic deformation occurs is clearly seen for the concentrated 1.16 wt% liquid of figure (9.3). For larger values of shear stress the increase in shear rate is in direct proportion to the shear stress. This region is then described by an apparent or pseudo-viscosity η_B. This behaviour is characteristic of a gell or paste. The flow of gells and pastes may thus be characterised by a coefficient of internal friction η_B, formally analagous to viscosity in a normal fluid. The value of η_B in figure (9.3) is 4.45p in comparison with the viscosity of pure mercury of 1.5×10^{-2}p.

The flow behaviour of gells and pastes is explainable in terms of a coherent structure and/or high particle anisotropy caused by particle interactions which may be overcome by a shear stress field of magnitude S_B, such that

$$(S - S_B) = \eta_B \sigma \qquad (33)$$

where S is the applied shear stress and σ the shear rate.

The recovery time of such a system is the time taken τ^1 for the viscosity to return to the original zero shear value when the stress is removed. Any energy barriers in the particle interaction curve determine this time τ^1, but in their absence recovery is practically instantaneous ($\tau^1 \sim 10^{-6}$s) and comparable to the rapid coagulation time Θ^*. If the experimental time is less than τ^1, then thixotropy is observed.

Goodeve (18) has pointed out that at every point on the shear-stress curve, the stress required to obtain the given shear consists of the sum of a constant shear independent part, equal to S_B and a part proportional to the rate of shear; the bond breaking and viscous contributions respectively.

Figure(9.1) Viscosity vs wt % Fe 45 Å particles uncoated
(at given shear rates in cm/sec/cm)

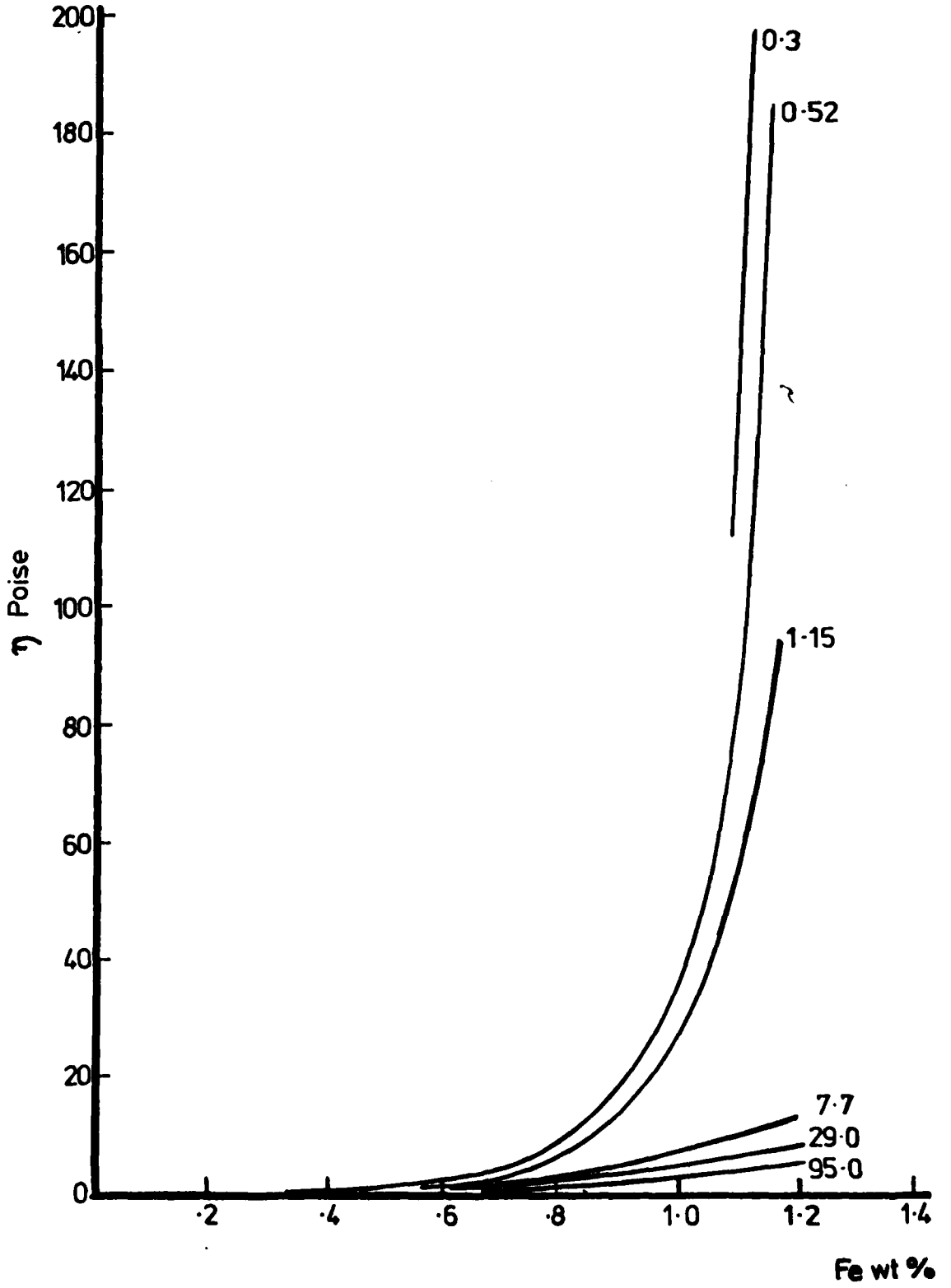

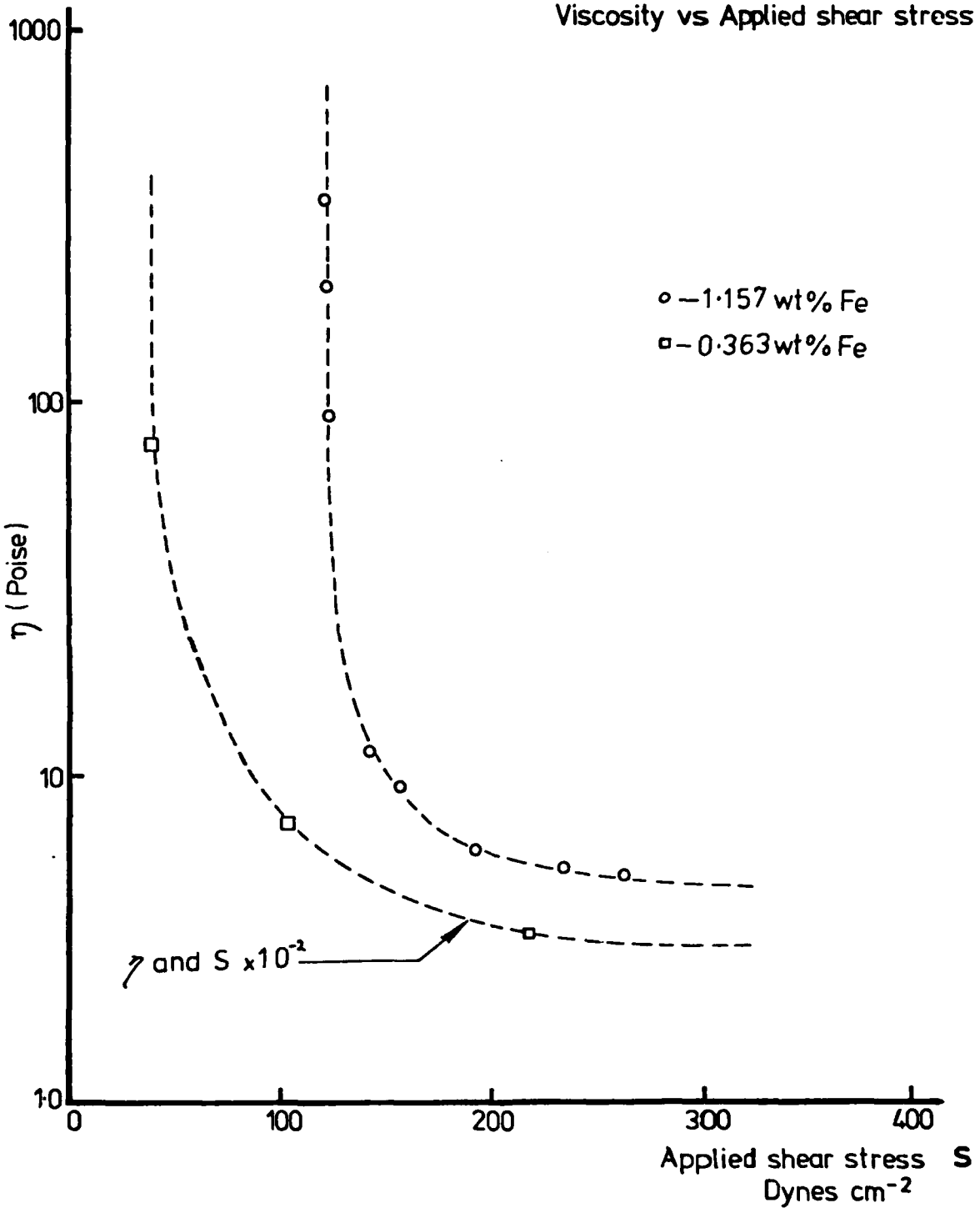

Figure (9.2) shows shear thinning behaviour for two iron particle in mercury fluids.

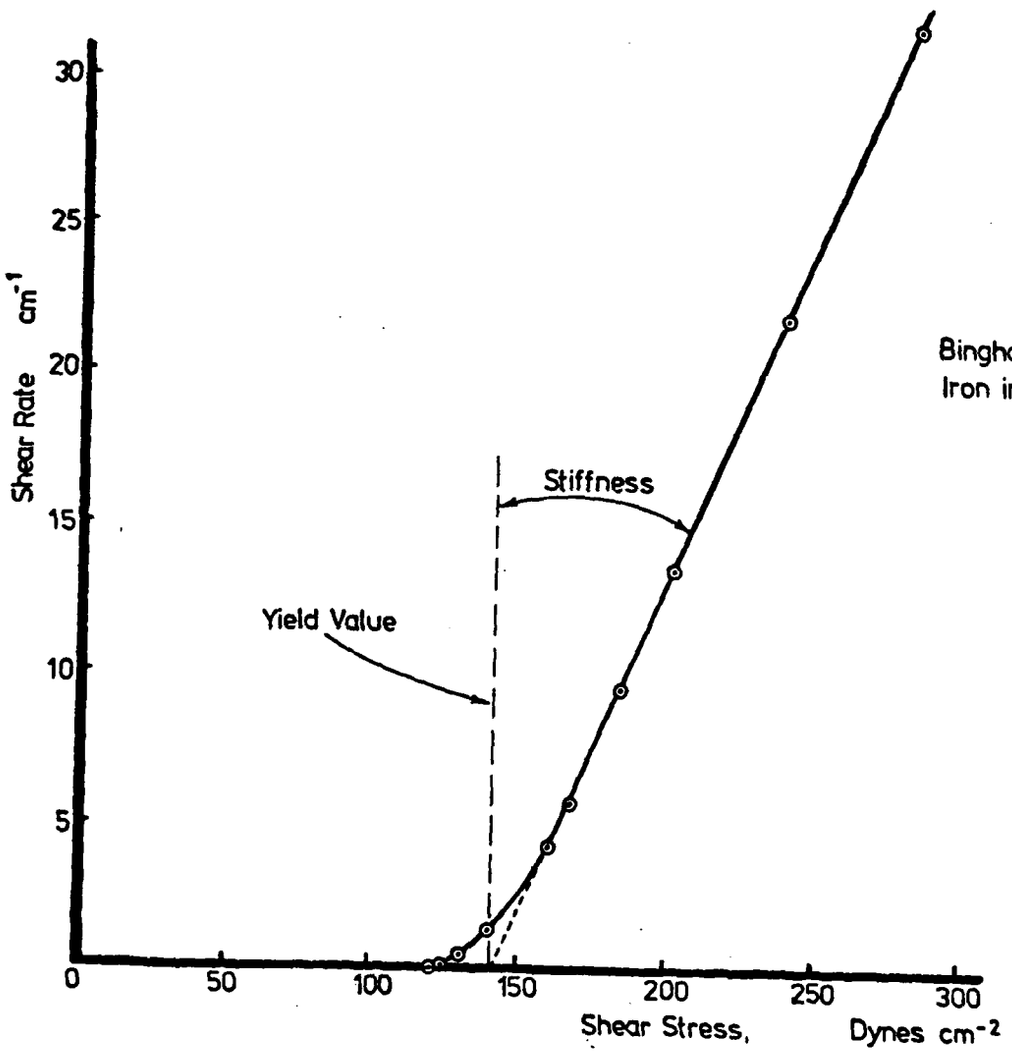

Bingham Plot for concentrated Iron in Mercury fluid (1·157 wt % Fe)

Figure (9.3) shows the 'Bingham fluid' behaviour for a 1.157 wt% iron particle in mercury fluid.

Thus from equation (35)

$$S = \eta_B \sigma + S_B \tag{34}$$

$$\text{as} \quad \eta = \eta_B + S_B/\sigma \quad \text{where } \eta \equiv S/\sigma \tag{35}$$

and η_B and S_B are constants that may be determined from experiment, ie from figure (9.3.).

De Gennes (30) has used percolation theory to describe the viscosity in the region of a sol-gel transition, as seen in figure (8.1), such that for low shear rates

$$\eta = \text{const } (\phi_c - \phi)^{-\alpha} \tag{36}$$

where ϕ_c corresponds to the gellation or percolation point and the value of X which depends upon the dimensionality of the system, lies in the range $0.7 < \alpha < 1.7$. For three dimensional contact between particles $\alpha \sim 1.2$. Equation (41) may be fitted to the low shear rate data of figure (9.1) by plotting $\ln(\eta)$ versus $\ln(\Delta\phi)$ for $\Delta\phi = \phi_c - \phi$, then $\alpha \sim 1.6$ and 0.84 for shear rates of 3 and 0.5 s^{-1} respectively, suggesting that equation (41) is a valid description. However, percolation theory also predicts that $\phi_c \sim 0.3$ for random particles or ~ 0.27 and 0.156 for chainlike and spherelike aggregates respectively (see Granqvist and Hunderi (32)). These figures are much higher than the observed value of $\sim$0.02. However, if large aggregates containing entrapped mercury occur, as suggested by the sedimentation experiments then the aggregate volume fraction being much higher would be consistent with an effective volume fraction of $\sim$0.3 to 0.5.

Rosensweig et al (3) have shown that a rigid surfactant layer of thickness δ will increase the fluids viscosity in the manner described by equations (2) and (3). These equations predict a linear relationship between $(\eta-\eta_o)/\phi\,\eta_o$ and ϕ_o. This is plotted in figure (9.4). However, the observed experimental relationship is only linear in the region $\eta_s \gg \eta_o$ such that $(\eta-\eta_o)/\eta\,\phi \to \phi^{-1}$. The differing gradients also predict different values of δ for the same fluid, depending upon the shear rate.

An extremely important qualitative observation has been made regarding the effect upon the viscosity of iron-mercury liquids when tin or antimony is added. This is that a fluid containing sufficient iron to form a paste becomes liquid on the addition of tin or antimony. It is known that the tin and antimony coats the particles and thus upon their addition the closest approach of the particles must increase. It is also generally observed that coated particles may be concentrated to a greater extent than uncoated particles of the same magnetic diameter. This suggests that the magnetic dipole interactions between particles are a major factor in determining a fluid's viscosity.

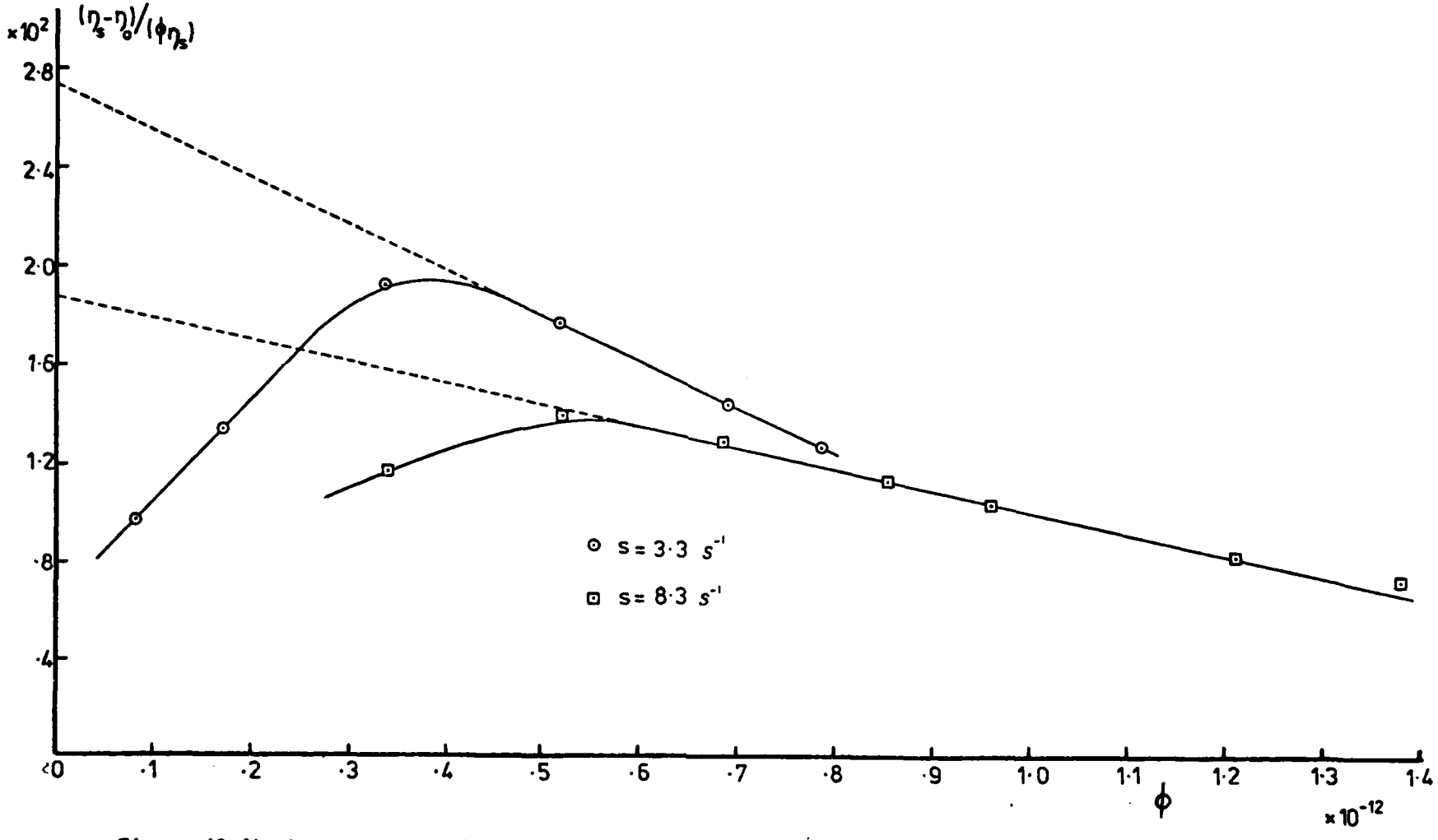

Figure (9.4) shows the very limited validity of the equations (2) and (3) in explaining the observed viscosity of iron particles in mercury.

To test this hypothesis further a series of copper-mercury liquids were prepared by electrodeposition and their concentration at the fluid-paste threshold determined. It was found that the threshold occurred at $\phi \sim 30$ vol % Cu almost exactly the value of ϕ_c expected from E.M.T. theory. Also at 2 vol %, the concentration at which iron particles become paste-like, the viscosity of the liquid was only $\sim 6\%$ higher than that of pure mercury. Thus it seems reasonable to conclude that the high viscosity of the iron-mercury liquids owes much to the magnetic dipole interactions, especially as ferromagnetic cobalt-mercury liquids are also observed to have high viscosities.

10. Surface Tension Measurements

Mercury, like all liquid metals, has a high surface tension and large contact angle. With regard to the possible use of mercury based ferromagnetic liquids in magnetic devices it is of interest to know whether the surface tension of the fluid is significantly different from that of pure mercury. A lower surface tension would normally be desirable. Mercury will act on any metal with which it also readily forms alloys, such as Au, Sn, Pb, Cu, Al etc., by disolving the metal until the mercury becomes saturated. Mercury will also remove the oxide surfaces of those metals with which it forms alloys, notably aluminium. These oxides then rise to the surface expelled because of their lower density and the fact that they are not readily wetted by the mercury. These oxides then form a surface scum a situation which represents the minimum surface free energy configuration for the oxide and alloy. Although these scums appear to wet glass and metal surfaces they are not representative of the bulk fluid.

For mercury alloys small quantities of solute generally depress the surface tension. This is observed in figure (10.1) in which data is presented for the interfacial surface tension and contact angle between mercury-tin alloys and a glass plate, determined by Quincke's method. The surface tension becomes increasingly depressed as more tin solute is added until the solubility limit is reached. After this point excess tin appears in the surface as a scum and although the 'surface' interfacial tension falls dramatically, as previously mentioned this is not typical of the bulk fluid.

Figure (10.2) shows measurements of the air-liquid interfacial tension for an iron-mercury fluid using Jaeger's method in addition to some using Quincke's method for the liquid-solid interfacial tension. It is seen that in both cases the surface tension decreases as the iron particle concentration increases, suggesting that the iron particles act in a similar way to tin metal impurities in the mercury. At high iron concentrations the fluid becomes so viscous that it will not flow under its own weight and thus no further data may be obtained. It was also noted that if tin was added to the iron fluid, the surface tension was not further depressed, indicating that the tin resides on the particles. When excess tin was added, the surface tension was depressed, as shown in figure (10.2) as tin oxide had now formed on the surface.

The surface tension of paste like fluids can appear to be very low, in as far as the fluid appears to wet glass or metal surfaces. However, the determination of the surface tension in figure (10.2) demonstrates this observation to be misleading as it is only because of the increased viscosity (see also figure (9.1)) that the fluid cannot flow to take up its minimum energy surface. Further if these 'pasty' liquids are examined under the microscope, a finite convex radius of curvature between the fluid and plate may be observed indicating that the contact angle is greater than 90^{o} and thus wetting does not occur.

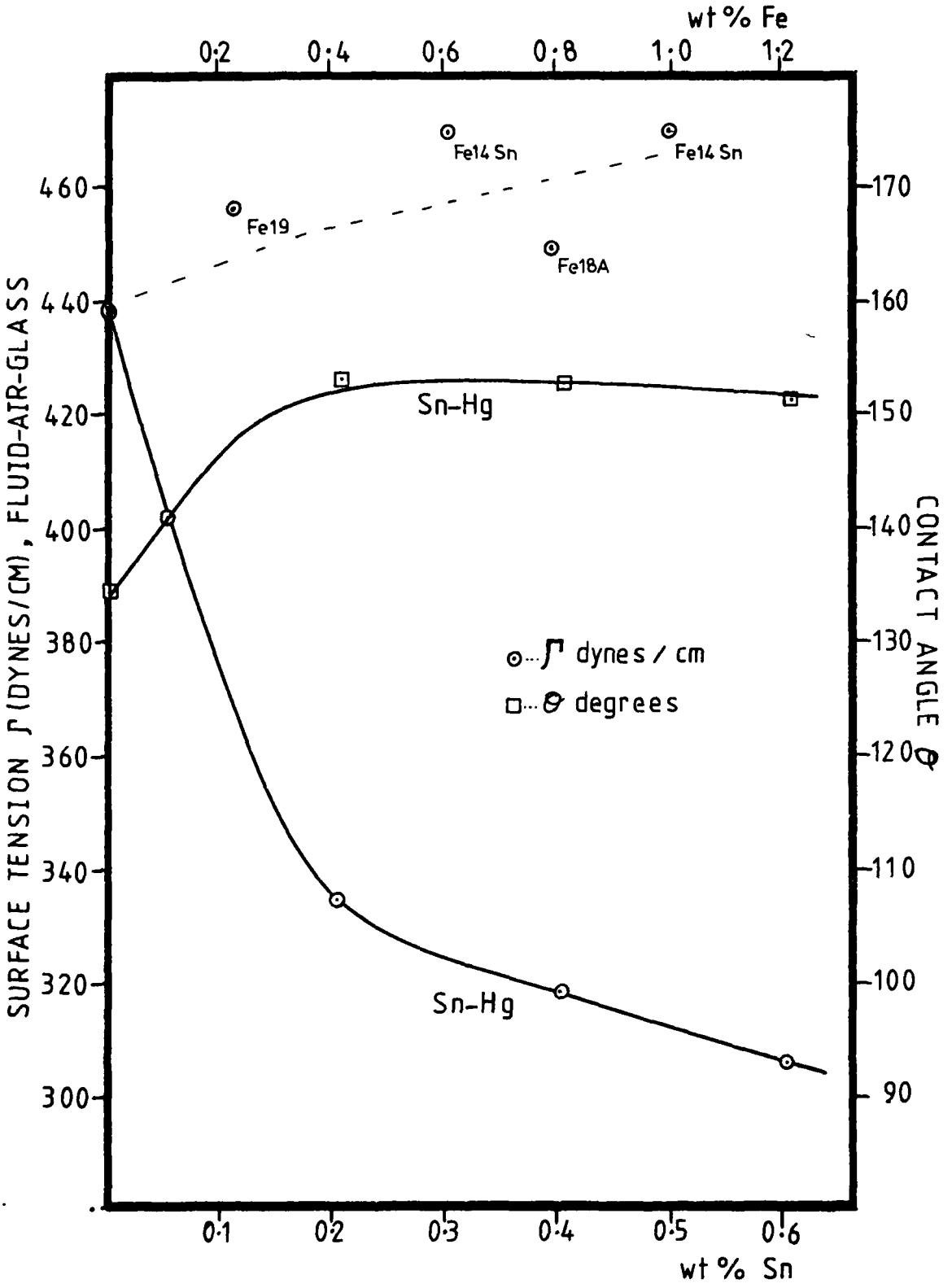

Figure (10.1) The surface tension and contact angle between tin mercury alloys and iron mercury fluids and a glass plate in air.

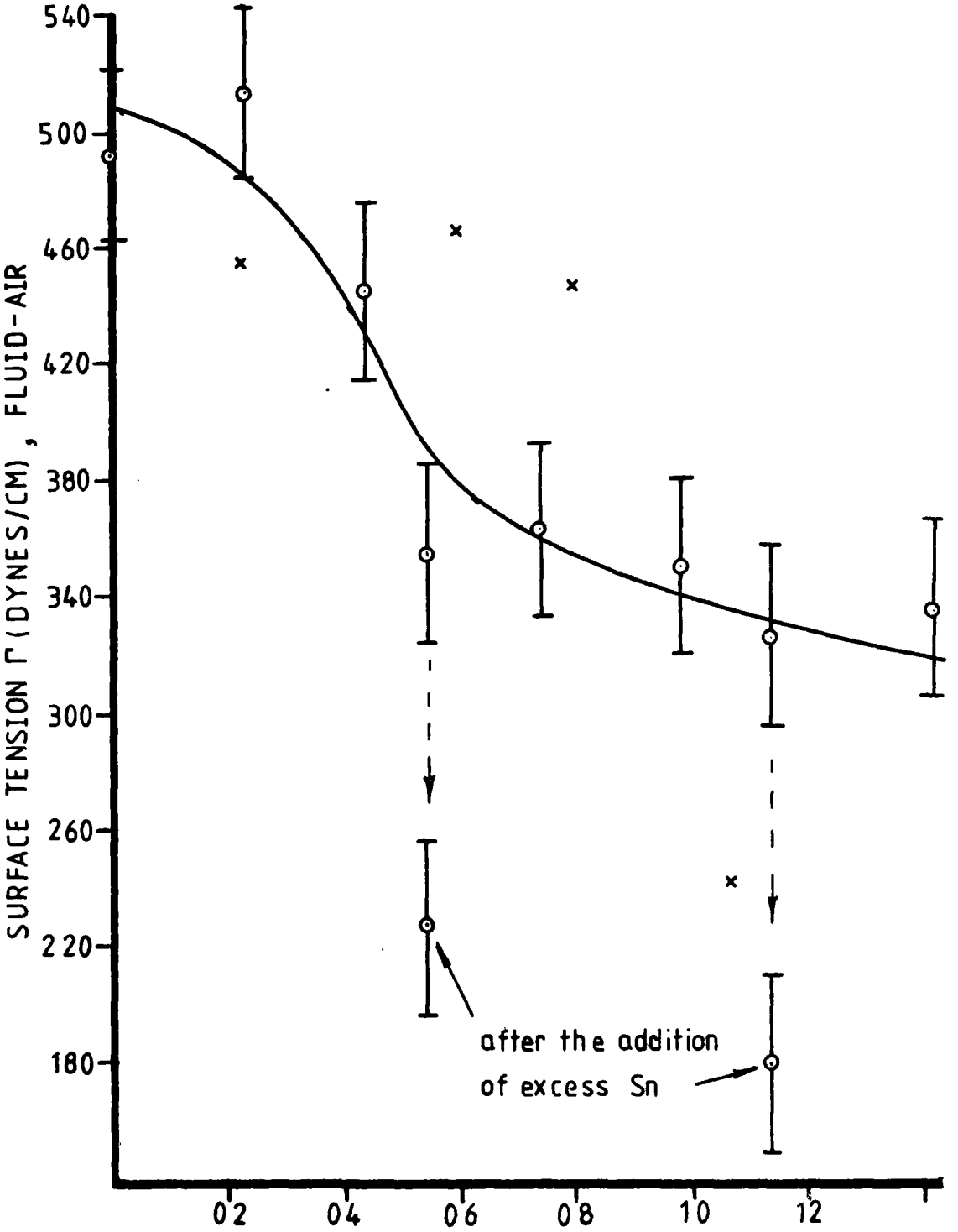

Figure (10·2)

Surface tension of 40A diameter iron particles in mercury at 288K, determined by Jaegers method.

11. Phase Changes at the Melting Point

The solid-liquid transition has been investigated using a differential scanning calorimeter (D.S.C.). This particular investigation arose as a result of observations of temperature dependent magnetic measurements where the analysis of data required that the melting point of the iron-mercury system be established.

The principal results are summarised in figures (11.1) and (11.2). These figures show the line shapes produced by the D.S.C. when scanning from low to high temperatures. Isothermal lines are inclined at an angle θ to the line shape base line. θ is the angle defined by the leading edge for the melting transition of pure mercury at 234K as shown in figure (11.1.1). The total area of the curve represents the latent heat of fusion.

Figure (11.1.2) shows the line shape for 0.75 wt % iron in mercury. Note that significant premelting extends over some ten degrees. No premelting is observed, as would be expected for 99.999% pure mercury (see figure (10.1.1)). The area of the premelted region, ie the area to the left of the dotted line in figures (11.1.2) and (11.1.3), is normally a measure of the impurity of the system and is designated by Qp.

Figure (11.1.3) shows the results for a fluid containing tin coated iron particles with an identical particle concentration to the fluid studied in figure (11.1.2). The premelting curve shows a bump which is characteristic of all tin coated iron fluids. The cause is unknown but likely to be associated with the affinity of the tin coating for the mercury, possible evidence for a monolayer of bound mercury.

In marked contrast is the line shape for figure (11.1.4) for free tin in mercury of the same concentration as that present in figure (11.1.3). Here structure appears to the right of the melting point and represents the heat of transition from β tin in mercury to tin in solution in liquid mercury. This structure, consistent with the known Sn-Hg phase diagram (see reference (11)), always exists when free tin is present but never if iron particles are also present. This would seem to indicate that tin is not in solution in the fluids containing iron particles but is associated with the particles as a coating. This result is also consistent with the measurements of resistivity of these fluids described in section (8).

Figure (11.2) shows a series of line shapes produced for antimony additive liquids. Figure (11.2.1) shows that below the solubility limit of lead, Hg-Pb gives an almost identical line shape to pure mercury, consistent with the Hg-Pb phase diagram (see Smithells (17)).

Figure (11.2.2) shows the result for the control 1.6 wt % iron-mercury sample which is similar to the 1.6 wt % iron-lead-mercury liquid of Figure (11.2.3) except that the premelting is slightly greater, because of the excess lead that is in solution, consistent with the resistivity results of section (8).

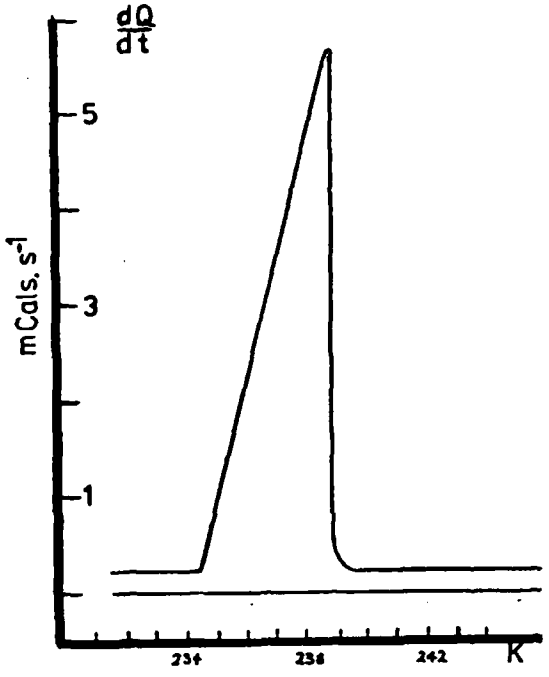

(1.) PURE Hg

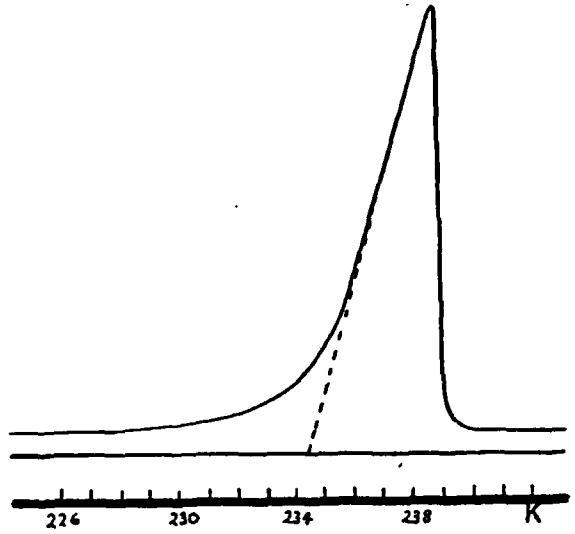

(2.) Fe PARTICLES (0·75wt%) IN Hg

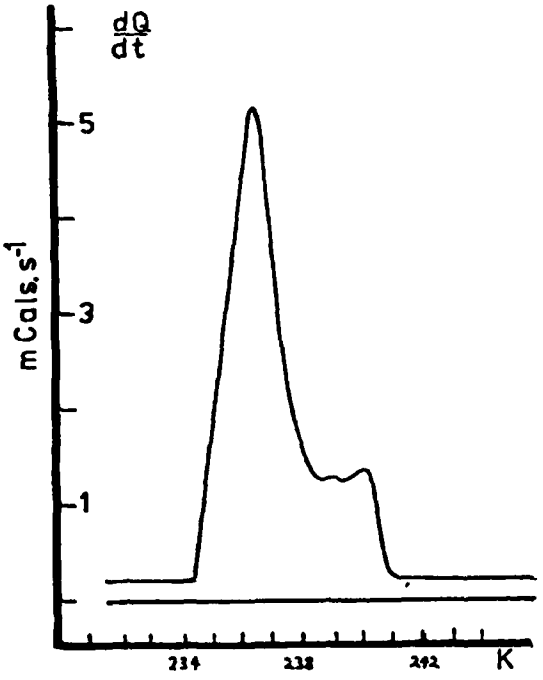

(3.) 0·4wt% Sn IN Hg

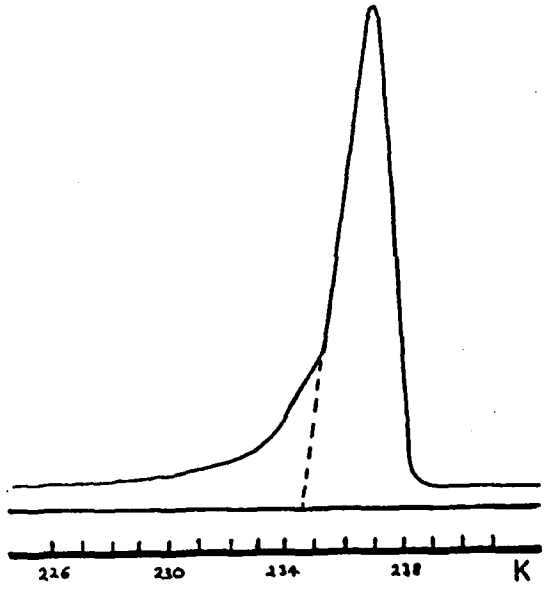

(4.) Sn COATED Fe PARTICLES IN Hg
(0·4wt% Sn , 0·75wt% Fe)

Figure (11.1) shows the line shapes for various samples produced by the D.S.C. as the samples are melted.

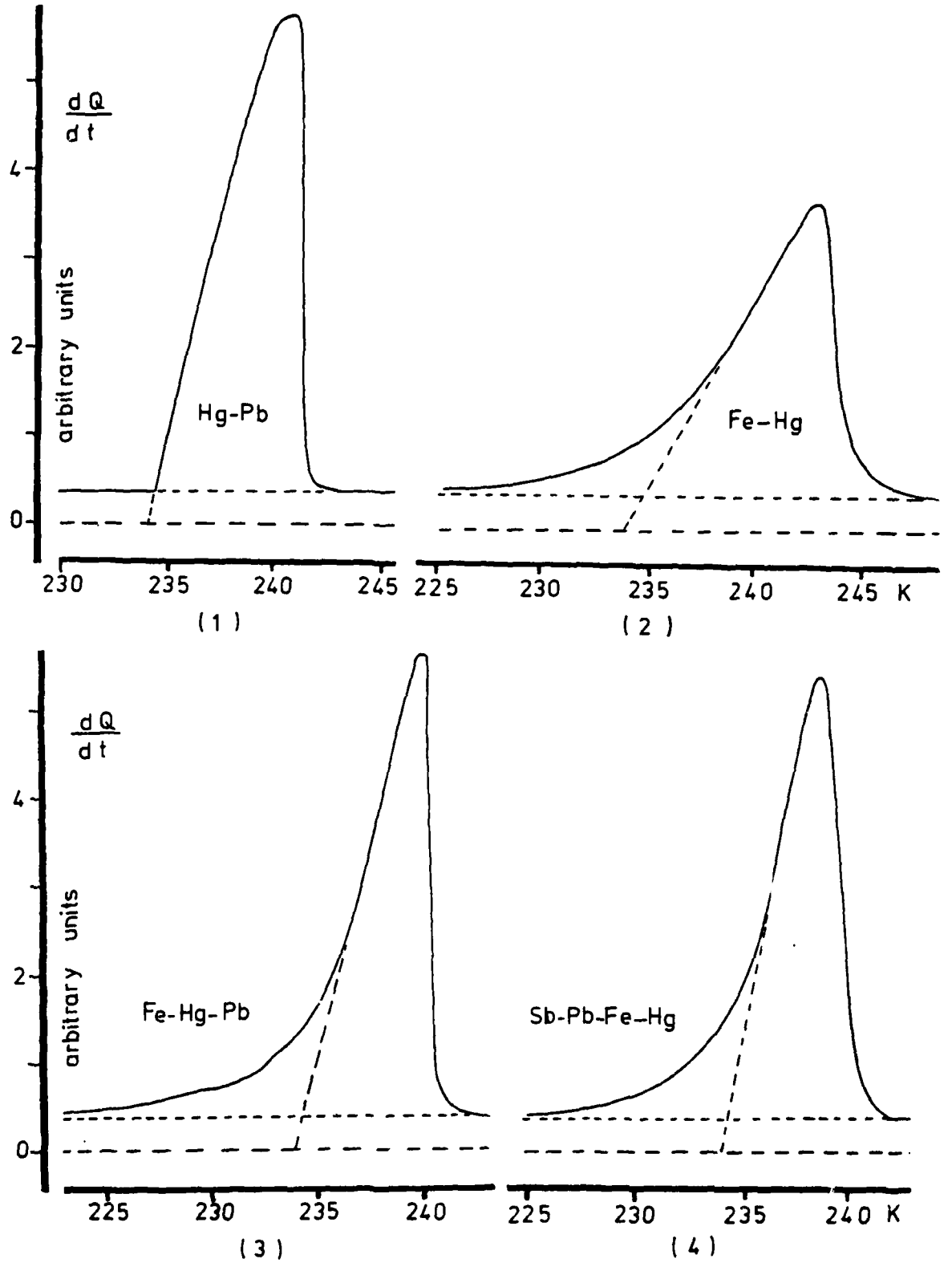

Figure(11.2) the line shapes for various samples produced by the D.S.C. as the samples are melted

Figure (11.2.4), the line shape for the antimony-lead-iron-mercury liquid, is almost identical to that of the lead-iron-mercury liquid of figure (11.2.3). This is indicative of the fact that the antimony is not in solution but resides on the iron particles. If this were not the case the insoluble antimony would reside as particles in the mercury and significantly enhance the premelting of the system.

Figures (11.3) and (11.4) show the ratio of Qp to Q the total latent heat of transition for the tin and antimony additive series respectively. It is seen in figure (11.3) that at the region where the liquid's viscosity becomes paste like, at approximately 1 wt % tin coated iron, there is an accompanying sharp increase in Qp, even though Q is approximately constant for all concentrations of iron (see figure (11.3)). One explanation of this is that the amount of free mercury, in the thermodynamic sense, is decreasing as it is gradually used to form bound mercury layers, implying further the mercury's affinity for the tin coated iron particles.

However if this were the sole cause of the behaviour of Qp it might be expected that the total latent heat Q of the sample would also change with change of iron concentration. Figure (10.3) shows that this is not the case. Particle interactions are most likely to be important in determining the behaviour of Qp. It should be noted that because of premelting, there exists no single melting point characteristic of a given fluid.

The variation of Qp and Q for the antimony lead systems is not as marked as for the tin additive systems. However it is seen from figure (11.6) that the antimony must coat the iron particles as the Qp/Q behaviour for the antimony-lead-iron liquid is identical within experimental error to that of the lead-iron-liquid.

Comparison of figure (11.6) with (11.5) reveals that no sharp rise in Qp/Q is observed as the antimony fluid becomes paste-like, as is seen for the tin coated fluid. The exact reason for this is unknown but it may be that this is evidence that mercury bound layers do not form on antimony coated particle. This would be consistent with the fact that due to antimony's insolubility, mercury has little affinity for the antimony coating. In contrast, because of the high solubility of tin in mercury, the latter has a high affinity for tin coated particles.

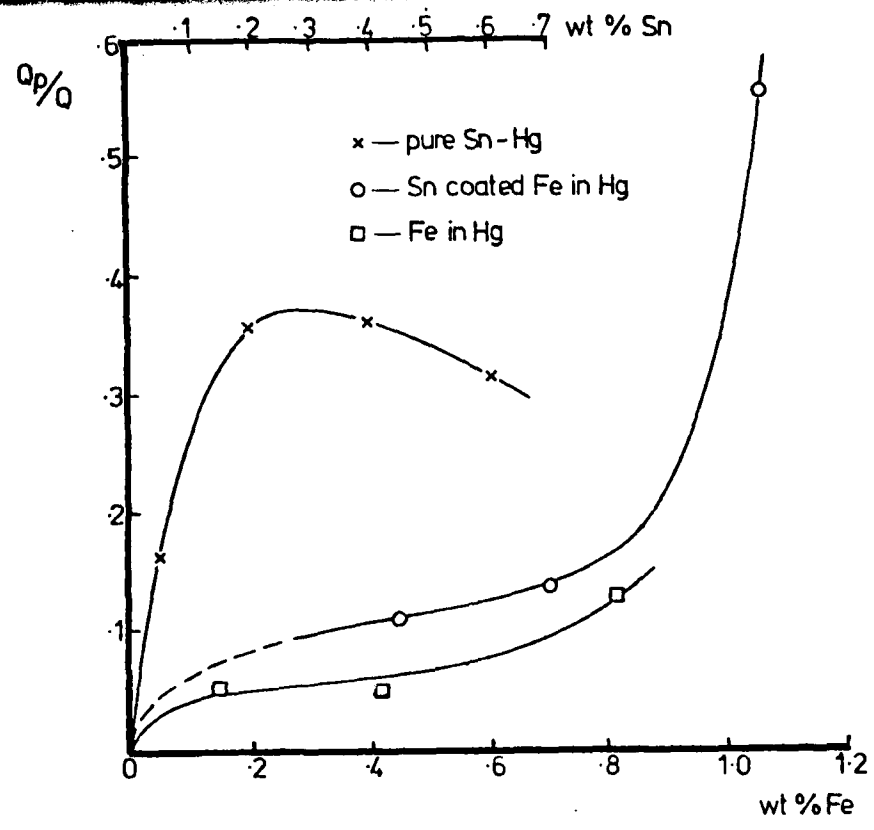

Figure (11.3) shows the ratio of premelting heat to total heat of transition as a function of iron and tin concentration.

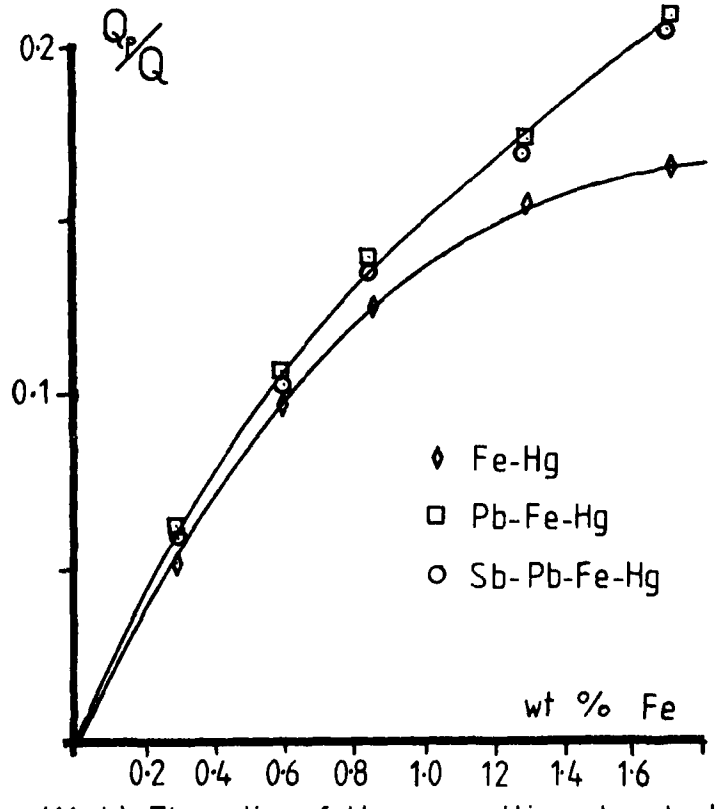

Figure(11. 4) The ratio of the premelting heat to the total heat of transition as a function of iron, lead and antimony concentration.

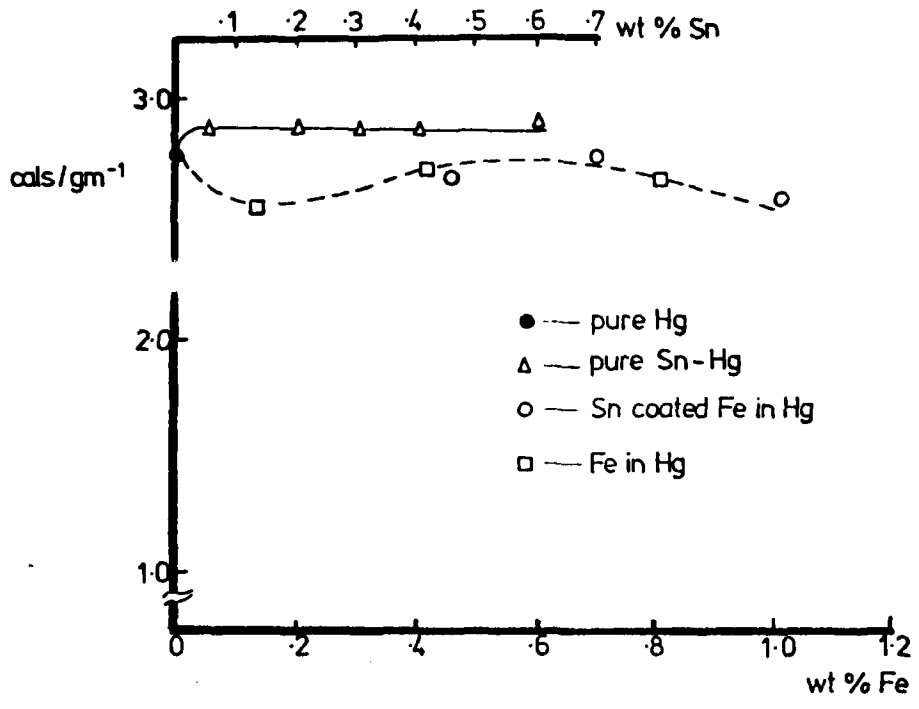

Figure (11.5) shows the total heats of transitions as a function of iron and tin concentration.

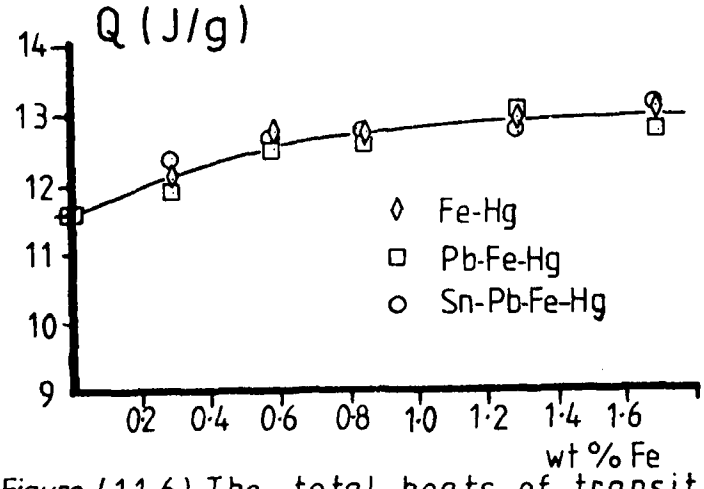

Figure (11.6) The total heats of transition as a function of iron and lead-antimony concentration.

12. Aggregation in iron-mercury ferromagnetic liquids

It has become apparent during the period covered by this report that the aggregation of iron particles in mercury ferromagnetic liquids determines many of these physical and magnetic properties. Thus in this section some of the possible aggregating forces are discussed in order that future experimental work and liquid development may be directed in such a manner as to reduce these forces.

Aggregation in the liquid occurs when particle collisions are perfectly inelastic. Such inelastic collisions result when, for some finite particle separation there exists in the inter-particle (energy) potential, a "well" of greater depth than kT. This statement defines fluid stability in a completely general generic way. It may be written as

$$E_T(r) + kT \geq 0 \tag{44}$$

where $$E_T(r) = E_m(r) + E_v(r) + E_E(r) + E_s(r) \tag{45}$$

The terms in equation (45) represent the total, magnetic, van der Waals' electrostatic and steric terms respectively. These terms are now discussed individually.

12.1 The magnetic interaction $E_m(r)$

For two particles

For two spherical particles of magnetic moments μ_1 and μ_2 and diameter D_1 and D_2 separated by a centre to centre distance r, the magnetic interaction may be written as

$$E_m(r) = \bar{\mu}_1.\bar{\mu}_2/r^3 - 3(\bar{\mu}_1.\bar{r})(\bar{\mu}_2.\bar{r})/r^5 \tag{46}$$

where $\mu_1 = \frac{\pi}{6} D_1^3 I_s$ and $\mu_2 = \frac{\pi}{6} D_2^3 I_s$.

If the dipoles are co-linear, then $E_m(r)$ reduces to the form of the maximum magnetic interaction,

$$E_m(r) = -2\mu^2/r^3 \tag{47}$$

Further if the particles are allowed to core into content, then r = D and thus

$$E_m(r)\ (\text{maximum}) = -\frac{1}{18}\ (\pi I_s)^2 D^3 \qquad (48)$$

Thus if the ferromagnetic liquid is to be stable to magnetic interactions then it follows

$$kT > \frac{1}{18}\ (\pi I_s)^2 D^3$$

and hence

$$D_m < \left(\frac{18kT}{\pi^2 I_s{}^2}\right)^{\frac{1}{3}} \qquad (49)$$

For iron particles in mercury at room temperature this implies that $D_m < 30A$.

In a real fluid however a particle size distribution exists, and thus the net attraction between a large particle and a small one, may exceed kT although the liquid's median particle diameter is less than 30A. In this case, for two co-linear dipoles equation (48) becomes

$$E_m(r)(\text{maximum}) = -2\left(\frac{\pi I_s}{6}\right)^2 \frac{8D_1^3 D_2^3}{(D_1+D_2)^3} \qquad (50)$$

and thus the condition for stability becomes

$$\frac{1}{D_1} + \frac{1}{D_2} = \left(\frac{4\pi^2 I_s{}^2}{9kT}\right)^{\frac{1}{3}} \qquad (51)$$

Equation (51) is plotted for T = 297 and 420K and $E_m(r)$ in figure (12.1). In addition, if a particle is coated with a non-magnetic coating, such as tin or antimony or even an organic surfactant, of thickness δ then the magnetic interaction is further reduced by effectively increasing the distance of closest approach. It is also important to note that even if the particles were to be coated with a non-magnetic surfactant of 10A diameter, the liquid would still be only meta-stable if some particles of 50A diameter were present.

It is apparent from figure (12.1) that if a liquid is to be stable against magnetic interactions, then all possible combinations of particle pairs must lie below the appropriate curve. It is seen that a liquid is only stable at room temperature if the total particle size distribution lies below 30A. As the particles are generally distributed with a log normal volume distribution, this means in practice that 4 times the standard deviation (σ) from the median particle diameter, must be less than 30A.

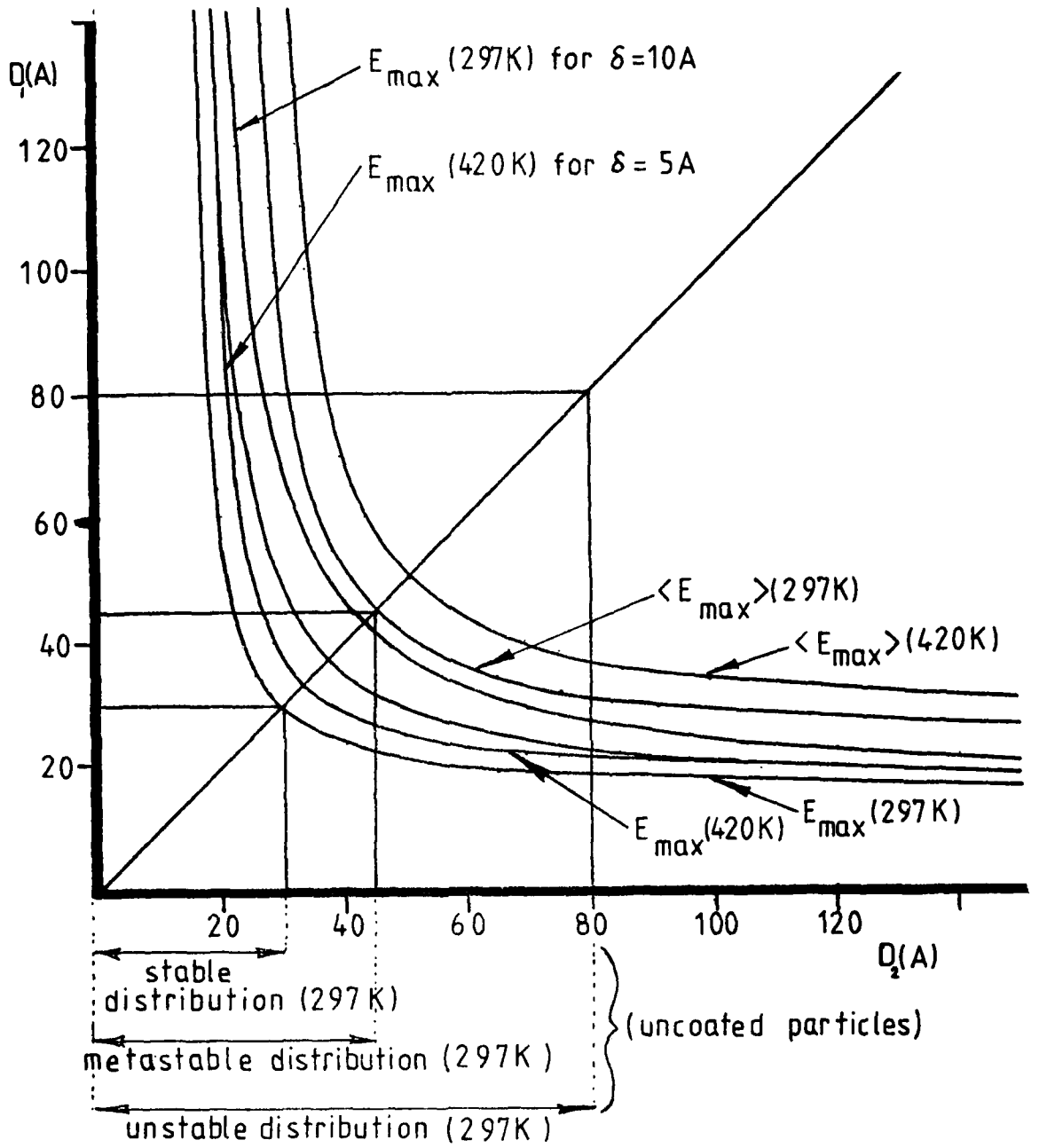

Figure(12.1) Stable binary combinations of coated and uncoated iron particles.

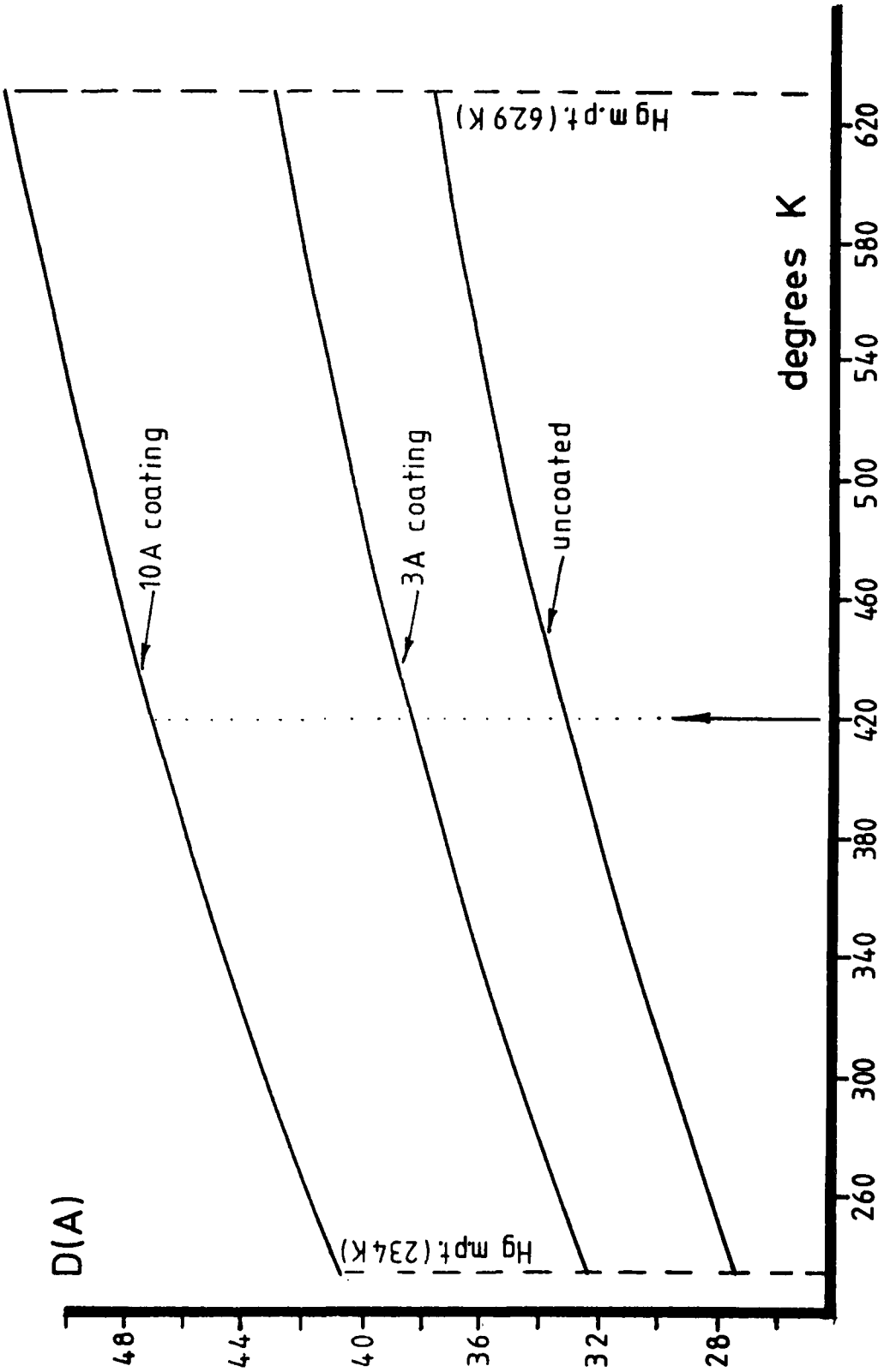

Figure(12.2) Maximum iron particle diameter thermally stable to magnetic aggregation.

That this is a reasonable criterion for fluid stability is readily shown as for a normalised Gaussian distribution the total number of particles of greater diameter than $4\sigma_s$ from the mean, is less than 0.003% of the total distribution, or 0.135% for $3\sigma_s$ from the mean. Thus if a liquid is to be stable against magnetic aggregation, then D_m, as defined by equation (49) must be at least $4\sigma_s$ from D_V. Recalling that for the log normal distribution, the log of D_V is a Gaussian, then it immediately follows that for stability against magnetic dipole forces,

$$D_m > D_V \exp 4\sigma_{s_o} \qquad (52)$$

where σ_{s_o} is the normalised standard deviation as given from magnetic data by equation (19). For uncoated particles $D_m \sim 30A$, and thus for $\sigma_{s_o} \sim 0.1\ D_V$ must be $\sim 20A$. It is seen from equation (52) that the liquids stability is critically dependent upon σ as

$$\sigma_{s_o} = \tfrac{1}{4} \ell n(Dm/Dv)$$

This in turn implies that in the future liquids must be prepared with particles of as small a standard deviation as possible.

Figure (12.2) shows the dependence of the maximum stable particle size upon temperature. The figure shows that whilst a liquid containing for example uncoated 30A diameter particles may be aggregated at room temperature, it may be unaggregated at $\sim$ 550K. If such a transition between an aggregated and unaggregated system occurred, then the viscosity should also decrease. Thus the present "thick" paste-like liquids, may well show a significant decrease in viscosity if sufficiently heated. Further, and perhaps more important, the observation that particle coatings decrease the liquid viscosity may be understood from figure (12.2), as a tin layer of 3A thickness could well arise as a result of the addition of excess tin, and this would "unaggregate" 30A particles at room temperature.

12.2 The van der Waals interaction $E_V(r)$

The van der Waals interaction between two identical spherical particles of material (1) dispersed in a media of material (2) may be written as

$$E_V(r) = - \frac{A_{121}\ D}{24(r-D)} \qquad \text{for } r << D \qquad (55)$$

where A_{121} is the Hamaker constant applicable to the van der Waals interaction between two bodies of material 1 transmitted across the medium 2.

For a dielectric material such as ferrite $A_{11} \sim 10^{-13}$ ergs, but for a metal $A_{11} \sim 10^{-12}$ ergs principally because of the high free electron density, where A represents the Hamaker constant appropriate for the van der Waals attraction between identical bodies across a vacuum space. Thus the van der Waals attraction between metallic iron particles is expected to be larger than for ferrite particles in a commercial fluid. However, it is also expected that the metallic mercury will screen out some of the low frequency components of the van der Waals attraction, effective reducing A_{121} below that of A_{11}.

It has been shown by Israelachvilli and Tabor (33) that for a metal A is principally characterised by its plasma frequency ω_p, such that

$$A_{11} = \frac{3\hbar}{16\sqrt{2}} \omega_p \tag{56}$$

$$\text{for } \omega_p = \left(\frac{4\pi n e^2}{m}\right)^2 \quad \text{(c.gs units)} \tag{57}$$

where e is the charge on the electron, m its mass and n the number of free electrons per cm^3.

Further it can be shown that the combining law

$$A_{121} \simeq \left(A_{131}^{\frac{1}{2}} - A_{232}^{\frac{1}{2}}\right)^2 \tag{58}$$

may be used to determine A_{121} in terms of two other known Hamaker constant A_{131} and A_{232}. Thus if the medium 3 corresponds to vacuo, then equation (80) becomes

$$A_{121} \simeq \left(A_{11}^{\frac{1}{2}} - A_{22}^{\frac{1}{2}}\right)^2 \tag{59}$$

and so by substituting into equation (81) equations (78) and (79)

$$A_{121} \simeq \frac{3\hbar}{16\sqrt{2}} \left(\frac{4\pi e^2}{m}\right)^2 \left(n_1^{\frac{1}{2}} - n_2^{\frac{1}{2}}\right)^2 \tag{60}$$

The values of n_1 and n_2 must be chosen with care, as their experiment values depend upon the actual experimental technique involved. It would seem that optically determined values of n_1 and n_2 would be the most appropriate, as ω_p is characterised by an ultra violet frequency for metals. Values of $n_{eff} = 0.22$ and 1.98 would seem appropriate (see Mott and Jones (34)) where n_{eff}, the effective number of free electrons per atom consistent with high frequency optical data, is related to n by

$$n_1 = n_{eff} \, N/A\rho_g \tag{61}$$

where A and ρ_g refer to the metals atomic weight and density respectively and N to the Avogadro number.

Thus for iron particles in mercury a value of A_{121} of 2.1×10^{-13} is deduced from the above analysis. It is seen that this is lower than is normally expected for A for metals in accord with the simple ideas of screening. However, this value must be treated only as a guide to the probable value of A_{121}. This is because the mercury only becomes

optically transparent at frequencies > ωp. Below ωp the effective dielectric constant of the free electron gas is complex and causes significant damping of any optical frequencies. As $\omega p(Hg) > \omega p(Fe)$ it is expected that the mercury will not be fully transparent to $\omega p(Fe)$ and so $A_{121} < 2.1 \times 10^{-13}$ ergs, see figure (12.3). However as the distances between particles are very small, the attenuation that $\omega p(Fe)$ suffers is also likely to be small.

In principle the true value of A_{121} for iron in mercury can be constructed by evaluating the dielectric constant of the mercury free electron gas from $0 < \omega < \infty$, and summing the contributions that each frequency makes, weighted according to its spectral intensity, to A_{121}. This represents however a mamoth undertaking and presupposes the existence of the relevant optical data.

A more important statement that may be made concerning A_{121} is that if $\omega p(Fe) = \omega p(H_g)$ then $A_{121} \rightarrow 0$, and no van der Waals attraction between particles occurs. As ωp is related to n_{eff}, and n_{eff} to the metal's resistivity ρ_e, it is seen that any decrease in ρ_e due to alloying of the mercury could reduce A_{121}. Although metals such as lead, tin and aluminium are known to decrease $\rho_e(Hg)$ this decrease is only of $\sim$ 1% and so could not reduce $n_{eff}(Hg)$ to that of iron. This problem is receiving further considerations.

12.3 The steric and electrostatic interaction $E_s(r)$ and $E_E(r)$

The steric and electrostatic terms represent particle repulsive energies and so if

$$kT + E_s(r) + E_E(r) = E_m(r) + E_v(r) \qquad (62)$$

The term $E_E(r)$ represents the charge layers repulsion due to charge transfer. It has been found that whilst the repulsion that this affords is theoretically very large at particle separations of a few Angstromns, the van der Waals attraction is far greater at about 5 to 10 angstromns. Thus there exists in $E_T(r)$ a minimum >> kT and particle aggregation must occur. The form in three dimensions of the charge density distribution $\rho(r)$ at a spherical iron particle-mercury interface has been discussed by Hoon (5) who shows that $\rho(r)$ is given approximately by

$$\rho(r) \sim \tfrac{2}{3} e C \phi_{Hg} \phi \qquad (63)$$

where ϕ_{Hg} is the work function of mercury, and ρ a particle of diameter D.

$$\phi = \left(\frac{D}{2} + \delta\right) \frac{\phi'}{r} (\exp - \beta_1 r)/(\exp - \beta_2(\tfrac{D}{2} + \delta)) \qquad (64)$$

$$\text{and} \quad \beta_1^2 = 4\pi e C \phi_{Fe} \phi^{\frac{1}{2}} \quad \beta_2^2 = 4\pi e C \phi_{Hg}^{\frac{1}{2}} \qquad (65)$$

SCHEMATIC FREE-ELECTRON ABSORPTION SPECTRUM

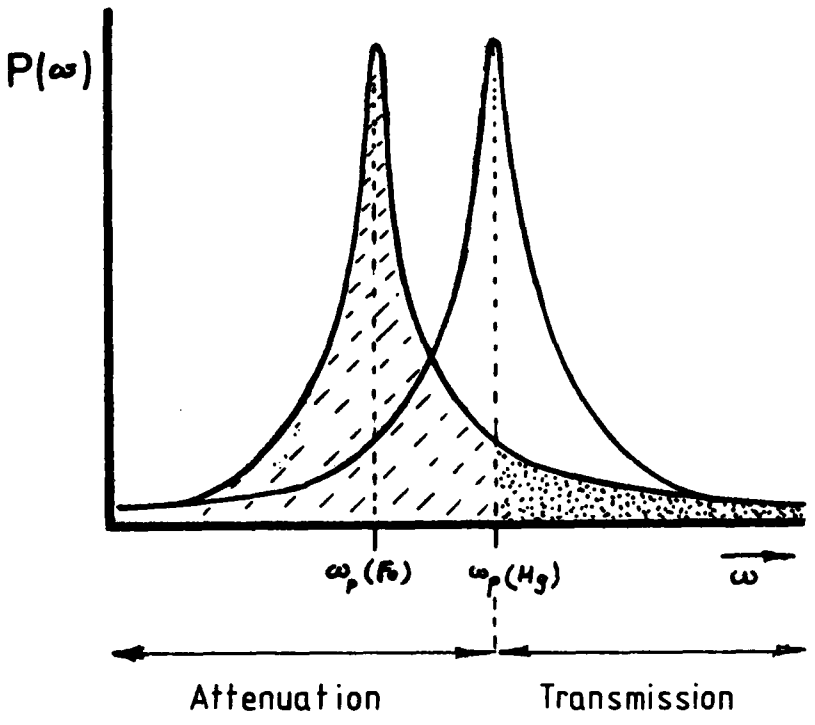

Figure (12.3) Schematic representation of screening by the liquid mercury fluid matrix, consequently reducing the dispersion force between iron particles in the fluid.

$$C = \frac{4\pi}{h^3}(2m)^{3/2} \tag{66}$$

$$\text{where} \quad = (\phi_{Fe} - \phi_{Hg})(\delta\phi - \phi\gamma^{-1} - 1)^{-1} \tag{67}$$

and ϕ_{Fe} and ϕ_{Hg} refer to the work functions of Fe and Hg respectively and δ is a dimension identified with an atomic diameter. The constant ϕ and γ are given by

$$\gamma = \frac{\beta_1}{\text{Tanh}(\beta_1 D/2)} - \frac{2}{D} \tag{68}$$

$$\phi = \beta_2 + \frac{2}{(D + 2\delta)} \tag{69}$$

For iron particles in mercury β_1 and β_2 are $\sim 1.4 \times 10^8$ and 1.8×10^8 respectively and thus the exponential dependent of $\rho(r)$ assures that the charge layer width, which supplies the particle repulsion, is only of a few Angstromn's. In comparison, the van der Waals force has a $1/r$ dependence and thus dominates at distances > than the charge layer width.

The functions $E_m(r)$, $E_V(r)$ and $E_E(r)$ are plotted for comparison in figure (12.4). The abscissae is given in reduced units of (r/D), and so as $E_V(r)$ is α $1/r$, it is $E_V(\bar{r})$ is a constant for all particles. Note the dominance of $E_m(r)$ over all other interactions for D = 60A.

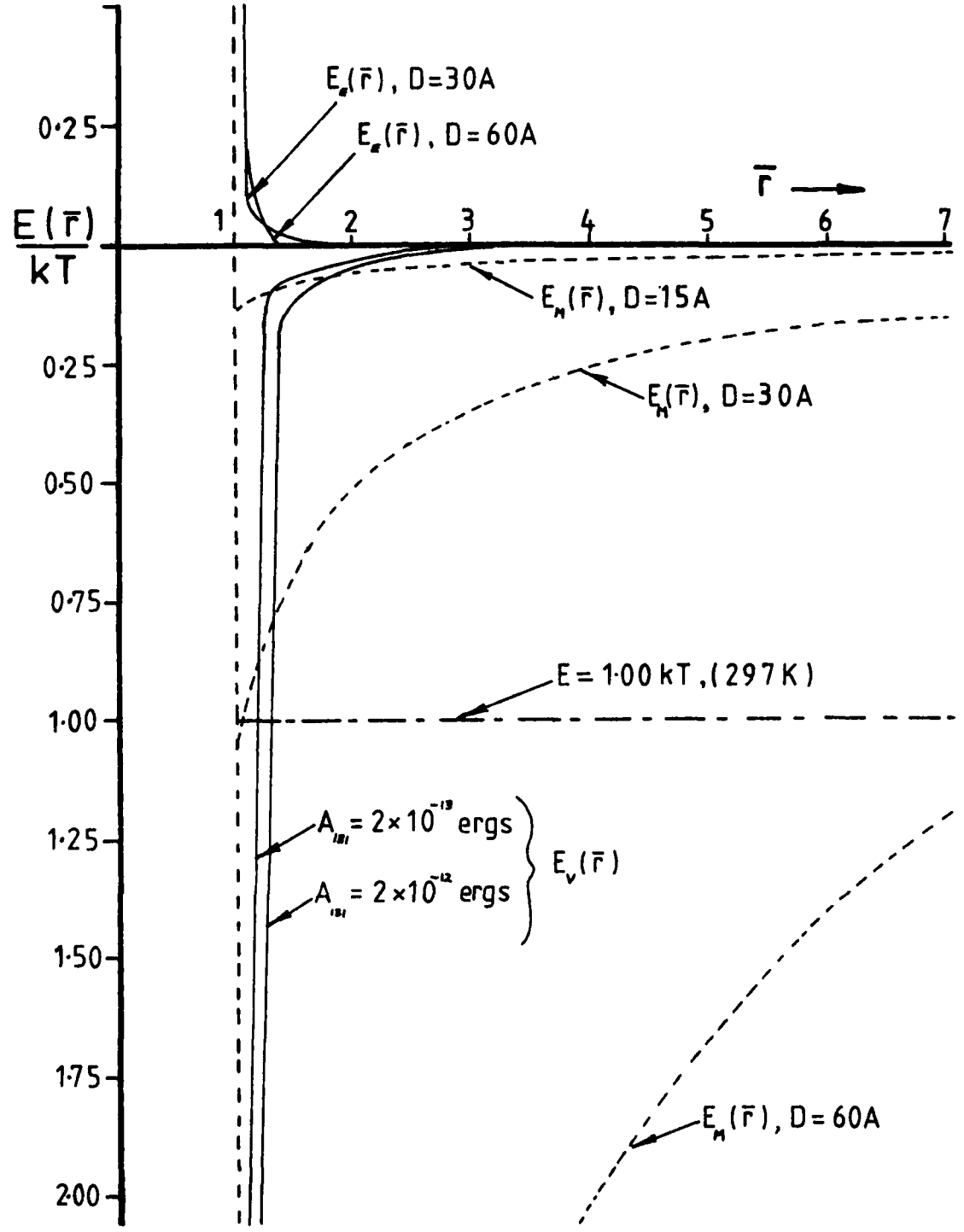

Figure (12.4) The magnetic E_M, van der Waals E_v, and electric E_e interaction energies between iron particles in mercury, as a function of separation distance $\bar{r} = r/D$, at 297 K.

13. Concluding Remarks

The resistivity data, presented in section 8, has enabled the spatial location of the metallic additives; tin, antimony, lead and sodium to be determined. The data has shown differences in the behaviour of uncoated iron, tin-coated iron and antimony coated iron systems which have been attributed to either the existence of charge layers or high resistance intermetallic coatings or both. There is also evidence that the state of agglomeration modifies the resistivity behaviour of these fluids.

The presence of tin and antimony coatings has also been strikingly corroborated by latent heat measurements. From these measurements there also appears evidence for the existence of mercury bound layers, although not of large spatial extent. The existence of such layers would not be inconsistent with the reported temperature dependence of resistivity of iron particles in mercury.

It has been possible to study systematically some of the conditions that determine I_S, I_R, H_C and χ_i for a given sample, where I_S is the sample's saturation magnetisation, I_R the remanence, H_C the coercivity and χ_i the initial susceptibility. Each of these parameters is strongly affected by particle size distributions and interactions, crystal, shape and structural anisotropies. The conditions for particle chaining in zero field have also been theoretically investigated. From this analysis it is clear that if an iron-mercury liquid is to have a low viscosity, that is no chains or ringsmust be present, then the median particle size must be much less than 25A so that no particles in the liquid have a diameter greater than 25A. This requires that the standard deviation be small such that $25A > D_v \exp 4\sigma_{SD}$, that is the requirement that less than 0.1% of the particles in a log normal distribution are greater than 25A in diameter, if the particles are uncoated and distributed according to the log normal distribution function.

It is also likely that, due to aggregation in these liquids, the hydrodynamic and magnetic particle sizes will differ widely. The presence of aggregates in these liquids has been confirmed and their size determined from measurements of the fluid stability in a gravitational field (see section 7). The dilution and demagnetising field experiments of section 5 imply that the magnetic behaviour of the aggregates is affected appreciably by nearest neighbour interactions. The time dependent magnetic data of section 5.4 can only be understood in terms of the existence of large aggregates. This implies strong nearest neighbour interactions, since for the fluids at room temperature, it is easier to rotate the aggregate than the individual particle moments.

It should be noted that the viscosity data presented in section 9 cannot be explained by theories which assume that the iron particles are hydrodynamically separate or loosely interacting entities. The viscosity behaviour may, however, be explained in terms of aggregates, especially open structured aggregates (ie flocs). It is then unnecessary to talk of bound mercury layers of the order of 50A thickness on the iron particles

AD-A084 447 UNIVERSITY COLL OF NORTH WALES BANGOR SCHOOL OF PHYS--ETC F/G 20/3
PREPARATION AND PROPERTIES OF A STABLE METALLIC FERROFLUID.(U)
FEB 80 S R HOON, S W CHARLES, J POPPLEWELL DA-ERO-77-G-037

UNCLASSIFIED NL

2 OF 2
AD
A084447

END
DATE FILMED
6 80
DTIC

surface in order to explain the paste-like nature of the fluids which contain 1 wt %, 40A diameter iron particles in mercury.

Open aggregates would also explain the magnetic field gradient instability, where the observed particle transport rate is orders of magnitude faster than that predicted from the iron particle diameters obtained from coercivity measurements.

It has also been observed that the addition of tin or antimony reduces the viscosity of the fluid, a fact which must be related to the coating ability of these additives. This reduction in the liquid's viscosity is believed to be principally due to the decrease in the magnetic interaction between particles. This then suggests that low viscosity high iron concentration liquids may be produced if the particles are both coated and of small diameter and if the particle size distribution is narrow.

A theoretical investigation of van der Waals forces between iron particles in mercury has also been undertaken in which the possible screening role of the mercury has been investigated. This has enabled limits to be placed upon the size of these van der Waals forces. It would appear that they dominate over all other forces at very close range (< 4A) but that for larger particle separations magnetic dipole forces dominate.

The possible magnitude of particle repulsive forces due to the occurrance of charge transfer at the iron particle mercury boundary has also been investigated theoretically. It is seen that although a particle repulsive force does occur, it is not sufficient to overcome both the van der Waals and magnetic dipole forces between particles.

In summary, it may be said that the magnetic, resistivity, latent heat, viscosity and gravitational stability experiments have enabled the iron particle interactions in mercury to be investigated. It is now apparent that the existence of aggregates determines many of the properties of the fluids. The forces determining the formation of the aggregates may be considered to be (i) short range van der Waals' forces and (ii) longer range magnetic forces.

As a result of these studies a more realistic model of the iron-mercury fluids has evolved; a development fundamental to the progress of further work if low viscosity, high iron concentration stable liquids are to be produced.

14. Future Work

Evidence has been presented that the viscosity of iron in mercury fluids is related to the existence of aggregates. These aggregates are caused by the existence of both magnetic dipole and van der Waals forces between particles. It is believed (see sections 9 and 12) that the magnetic forces may be significantly reduced by making the particles and particle standard deviation smaller and also by the further addition of particle coatings. Thus in future work a reduction in particle size and standard deviation will be attempted by investigating new methods of liquid preparation, and a continuation of the investigation of coating materials. As the latter will, by increasing the particle separation, reduce the magneto static interactions and thus the liquid viscosity. At present fluids of $\sim$ 1000 Gauss have been prepared although these are paste-like. It is likely that coatings could reduce the viscosity of these fluids by several orders of magnitude, or for the same viscosity increase the strength of the fluid to 10,000 Gauss. This figure of 10,000 Gauss is an order of magnitude higher than any known non-metallic commercial liquid.

It is felt that the current understanding of the physical properties of mercury-iron ferromagnetic liquids is sufficient to enable a specially designed seal to be constructed. It is believed, as a result of the surface tension measurements of section (10), that this seal may have to incorporate novel copper flashings to ensure that the liquid wets the seal. Further, it is hoped that copper flashing of a cone and plate viscometer may facilitate the use of this instrument, previously not possible because the liquids did not wet the cone or plate, to measure smaller quantities of liquid in order that a more extensive analysis of the liquids viscosity may be made. (At present the Poiseuille viscometer requires over 30cc's of fluid for a complete viscosity analysis).

Future work will still, however, concern itself with elucidating further the van der Waals interaction between iron-particles in mercury, as although coatings may significantly reduce magnetostatic interactions, the ultimate fluid stability will still rely on counteracting the particle-particle van der Waals interaction. In this respect the study in section (10) of van der Waals forces implies that more specific ultra-violet optical data is required for all the metallic components of these metallic ferromagnetic liquids.

15. References

1. J. Popplewell, S.W. Charles and S.R. Hoon, 2nd Conference on 'Advances in Magnetic Materials and their Applications' IEE p.13-16 (Sept 1976).

2. H. De Bruyn (i) Proc. of Int. Congress on Rheology, Holland, 1948, Amsterdam 1949, p.1195
(ii) Rec. Trav. Chim., 61 (1942) 863.

3. R.E. Rosensweig, J.W. Nestor and R.S. Timins: A.I.Ch.E.-I.Chem.E. Symposium Series No.5, p.5:104 (1965).

4. M. von Smolochowski (i) Physik Z., 17, p.557-585, (1916)
(ii) Z.Physik Chem., 92, p.129 (1917).

5. S.R. Hoon, Thesis, U.C.N.W., Bangor, Wales, U.K.

6. S.R. Hoon, J. Popplewell and S.W. Charles IEE Transactions on Magnetics, Vol. Mag. 14. No.5 981-983 (1978)

7. P.L. Windle, J. Popplewell and S.W. Charles, IEEE Transactions on Magnetics, Vol. 11, 1367-1369 (1975).

8. G.W. Greenwood, Acta Met., 4, p.243 (1956).

9. R.W. Chantrell, J. Popplewell, S.W. Charles, Physica, 86-88B, p.1421 (1977).

10. E. Kondorski (i) C.R. Acad.Sci., URSS, 80, p.197 (1951).
(ii) Bull.Acad.Sci., URSS, (Phys), 16, p.398 (1952).

11. F.E. Luborsky, J.A.P. Suppl., 32, p.1715 (1961).

12. M.I. Shliomis, Sov.Phys., USP, 17, 2, 153 (1974).

13. T.B. Jones and D.A. Kruger, Office of Naval Research Report, AD/A-001 107, September 1974.

14. E.A. Peterson, D.A. Kruger, M.P. Perry and T.B. Jones, AIP Conf. Proc., No. 24 p.560-561 (1975).

15. F.E. Luborsky, J. App. Phys., 33, p.2385 (1962).

16. N.D. Lang, Phys. Rev., 4, No. 12, 4234 (1971).

17. C.J. Smithells, Metals Reference Book, Butterworths (1949).

18. C.F. Goodeve, Trans. Farad. Soc., 35, p.342-358 (1939).

19. V. Novotny and p.P. Meinke, Phys. Rev., 138, 4186 (1973).

20. F.D. Rossini, "Chemical Thermodynamics" p.294, John Wiley and Sons, N.Y. (1950).

21. M. Flindt, U.S. Patent 3 130 004/1964.

22. C.P. Bean and J.D. Livingstone, J. Appl. Phys. Suppl 30, p.1205 (1959).

23. C.P. Bean and I.S. Jacobs, J. Appl. Phys. 27, 1448 (1956).

24. R.M. Asimow, Trans Mettl. Soc., AIME, 233, p.401 (1965).

25. R.W. Chantrell, J. Popplewell and S.W. Charles, IEE Transactions on Magnetics, Vol. Mag. 14, No.5 p (1978).

26. P.L. Windle, J. Popplewell and S.W. Charles, 'Preparation and properties of a stable metallic ferrofluid', Annual Technical Report (September 1975), DAERO-75-G-025.

27. E.P. Wohlfarth, Proc. Roy. Soc. A232, p.208 (1955).

28. R.B. Falk and G.D. Hooper, J. Appl.Phys. 32, Suppl. 1905 (1961).

29. R.W.L. Landauer, AIP Conf. Proc. (USA) Vol. 40 p.2, (1978).

30. P.G. De Gennes, C.R. Acad. Sci. (Paris) B286, p.131 (1978).

31. (a) S. Kirkpatrick, Phys. Rev. Lett. 27, 1722 (1971).
(b) S. Kirkpatrick, Revs. Mod. Phys. 45, 574 (1973).

32. G.G. Granqvist and O. Hunderi, Phys. Rev. B18, 1554 (1978).

33. J.N. Israelachvilli and D. Tabor, Progress in Surface and Membrane Sci. Acad. Press. 17, 1, (1973).

34. N.F. Mott and H. Jones, The theory of the properties of metals and alloys. Oxf. Univ. Press (1936).

35. R.W. Chantrell, J. Popplewell and S.W. Charles, ICM Munich September (1979).

Publications arising from the work sponsored by the US Army

1. 'The Long Term Stability of Mercury Based Ferromagnetic Liquids', P.L. Windle, J. Popplewell and S.W. Charles, IEE Transactions on Magnetics, Vol. 11, 1367-1369, 1975.

2. 'The Long Term Stability of Magnetic Properties of Ferromagnetic Liquids Containing Iron Particles in Mercury', J. Popplewell and S.W. Charles. A paper presented at the Joint MMM-Intermag Conference, June 1976 and to be published 1977.

3. 'The Long Term Stability of Metallic Ferromagnetic Liquids', J. Popplewell, S.W. Charles and S.R. Hoon. A paper published September 1976 by the IEE and delivered at the 2nd Conference on 'Advances in Magnetic Materials and their Applications'.

4. 'The Effect of a Particle Size Distribution on the Coercivity and Remanence of a Fine Particle System', R.W. Chantrell, J. Popplewell and S.W. Charles, a paper published in Physica 86-88B, p.1421, 1977, and delivered at the International Conference on Magnetism in Amsterdam, September 1976.

5. 'The Resistivity of Conducting Ferromagnetic Liquids Containing Iron Particles in Mercury', S.R. Hoon, J. Popplewell, S.W. Charles, a paper published in the IEE Transactions on Magnetics Vol Mag-14, No. 5, p.981, (1978) and delivered at the Intermag Conference, Florence, May 1978.

6. 'The Preparation and Properties of a Stable Metallic Ferrofluid' S.W. Charles and J. Popplewell. Report on the Workshop on the Thermomechanics of Magnetic Fluids, Hemisphere Pub. Corp., Washington D.C.

7. 'Time dependent Magnetisation of Iron Particles in Mercury Ferromagnetic Liquids', S.R. Hoon, J. Popplewell and S.W. Charles, Intermag Conference, New York, July 1979.

8. 'Aggregation in Iron-Mercury Ferromagnetic Liquids', Second International Conference on Ferromagnetic Liquids, Florida, March 1980.